The Effects of Trimethylamine-N-Oxide and Guanidinium Chloride on Aqueous Hydrophobic Contact-Pair Interactions

by

Ryan Macdonald

A Thesis submitted to the Faculty of Graduate Studies of

The University of Manitoba

in partial fulfilment of the requirements of the degree of

MASTER OF SCIENCE

Department of Chemistry

University of Manitoba

Winnipeg

Table of Contents

Abstract

Trimethylamine-N-oxide (TMAO) and guanidinium chloride (GdmCl) are both highly studied molecules in the field of protein folding/unfolding. Thermodynamic studies have shown that TMAO, an organic osmolyte, is a strong stabilizer of the protein folded state, while GdmCl is known to be one of the most effective protein denaturants. Although TMAO and GdmCl are well studied the mechanism by which they stabilize and denature proteins, respectively, is not well understood. In fact there are few studies looking at their effects on hydrophobic interactions. In this work we determine the effect of TMAO and GdmCl on hydrophobic interactions, by looking at the model system of phenyl and alkyl hydrophobic contact pairs. Contact pair formation is monitored through the use of fluorescence spectroscopy, i.e., measuring the intrinsic phenol fluorescence being quenched by carboxylate ions. Hydrophobic interactions are isolated from other interactions through a developed methodology. The results show that TMAO addition to the aqueous solvent destabilizes hydrophobic contact-pairs formed between phenol and carboxylate ions. The TMAO acts as a "denaturant" for hydrophobic interactions. For GdmCl the data shows that for small alkyl groups, acetate and propionate, hydrophobic contact-pairs are slightly stabilized or are not affected, respectively. For the larger alkyl groups GdmCl disrupts contact pair formation and destabilizes them. GdmCl's effect on hydrophobic interactions shows a size dependence on carboxylate ion size, i.e., as carboxylate ion tail length increases the contact pair formed with phenol is destabilized to a greater degree.

Acknowledgements

I would like to thank Dr. Khajehpour for all of his guidance and advice throughout the two years that I have done this work. I would also like to thank my parents Jim and Carol Macdonald for supporting me while attending school.

List of Tables

Chapter 3

List of Figures

Chapter 1

Chapter 3

Chapter 4

Chapter 1

Introduction

1.1 Protein Structure

Proteins play a vital part in our everyday lives [1]. Proteins have many roles in living and even nonliving (viruses) organisms [2], such as helping maintain structure of cells [3], acting as pores in cellular membranes for easy passage of particles across [4], they act as enzymes to catalyze biochemical reactions [5], and can also act as signaling molecules, such as hormones [6]. The basis of a protein's function lies in its three dimensional structure, i.e. its folded state, which is dependent on its amino acid sequence [7]. Proteins have four levels of structure, which are primary, secondary, tertiary, and quaternary [8].

Protein primary structure is determined by the linear order of amino acid residues, linked together by peptide bonds [9]. As each amino acid contains both an amine and a carboxyl functional group, every single amino acid can therefore participate in at least two peptide bonds. This nature of amino acid structure allows for long chains of amino acids to be linked together, by peptide bonds, to form a polypeptide chain or protein. As an example, Figure 1-1 shows the peptide bonds formed within a tripeptide; one of them is highlighted by a red box. Polypeptides are formed by the translation of mRNA, which is transcribed from DNA, by ribosomes and it is the chemical makeup of DNA/RNA base pairs which gives rise to the specific amino acid sequence of the polypeptide, known as the genetic code. Through molecular biological techniques, DNA base pairs can be altered by insertion or deletion of nucleotide bases, or by a processes known as DNA recombination, which allows us to make specific changes to protein primary structure quite easily. Thus, these techniques allows us to study the importance of specific amino acid residues with respect to a protein's function and or structure.

A protein's secondary structure is more complicated than its primary amino acid sequence. The peptide bond undergoes a resonance stabilization [10], which leads to the peptide bond having double bond characteristics. The double bond characteristic prevents free rotation around the peptide bond (ω), and only allows specific geometric conformations (cis and trans). The rotation of the other two bonds (ψ and φ) results in the two forms of secondary structure present in most proteins, which are the α-helix and the β-sheet. These two forms of secondary structure are held together mostly by hydrogen bonding interactions [11, 12]. For the α-helix hydrogen bonds are formed between the carbonyl oxygen of one amino acid (position i) and the amide hydrogen of another amino acid (position i+4). This repeating pattern of hydrogen bonding leads to the helix shape [12].

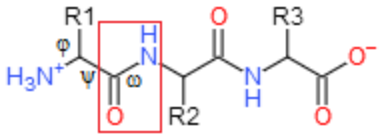

Figure 1-1. Model tripeptide formed between any three amino acids, except proline. Where R1/2/3 represents the functional side chain group of the specific amino acid. The peptide bond between amino acid 1 carboxyl and amino acid 2 amine occurs within the highlighted box.

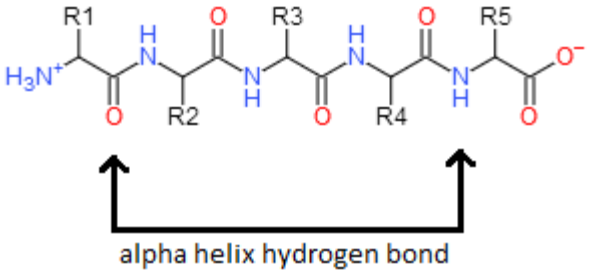

Figure 1-2. Representation of the α-helix hydrogen bonded formed between amino acid at position i and amino acid at position i+4.

On the other hand, β-sheets are formed when carbonyl oxygens/amide hydrogens of one peptide chain hydrogen bond with amide hydrogens/carbonyl oxygens of a parallel or anti-parallel chain [11].

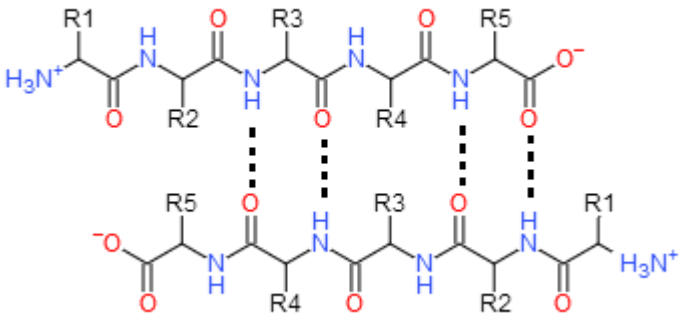

Figure 1-3. Representation of β-sheet hydrogen bonds (dashed lines) formed between two anti-parallel peptide chains.

Although it is known how hydrogen bonds are oriented in secondary structure and even which amino acids tend are prevalent in each type of secondary structure, it is still incredibly hard to predict the overall fold of a protein. This is mostly due to the complicated tertiary structure interactions that drive the secondary structure to adopt specific three dimensional conformations. Many of these interactions are long range with respect to the linear protein chain, so it is difficult for computer simulations to predict how some of these interactions will occur. Tertiary structure interactions involve electrostatic interactions, covalent bonds, van der Waal's interactions, and hydrophobic interactions driven by the hydrophobic effect [13]. Quaternary structure is the conformation of multiple subunits or monomers interacting with each other to form a higher order protein. The interactions holding the structure together are the same ones as those involved in tertiary structure.

There are four main interactions holding proteins together to keep their overall fold; covalent bonds, electrostatic interactions, van der Waal's interactions, and hydrophobic interactions. Other than the peptide bond, the main covalent bond formed within a folded protein is the disulfide bond. Disulfide bonds are formed when the amino acid cysteine's thiol group covalently bonds with another cysteine's thiol group [14]. The two residues do not have to be in close proximity with regards to primary structure, but just have to be close to each other in three dimensional space in the overall fold of the protein. These interactions are quite strong due to their covalent nature, but they can be broken easily when subjected to reducing conditions and or reducing agents, such as dithiothreitol (DTT), to form two S-H groups [15].

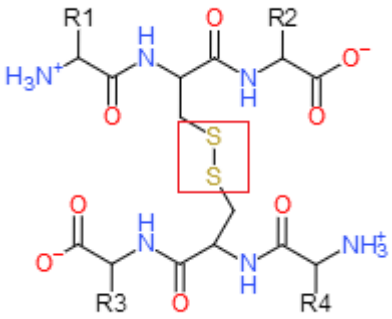

Figure 1-4. Representation of a disulfide bond, formed between two cysteine residues.

In the case of electrostatic interactions there are a few sub types, such as hydrogen bonding, dipole interactions, and ionic interactions [16]. Although hydrogen bonding is mostly encountered in the formation of α-helix and β-sheet secondary structure, however some amino acid side chains such as serine are able to partake in hydrogen bonding as well [17]. On the same note, dipole interactions are those formed between polar side chains, which are not quite as strong as the hydrogen bond. A dipole is formed in a molecule when there is a large difference in electronegativities of the elements that make up the molecule. This creates a positive pole and a

negative pole in a molecule, which allows for electrostatic interactions to occur between molecules that contain dipoles. On a macromolecule level dipoles can exist due to the additive nature of individual dipoles. This allows for secondary structures to have an overall dipole. Most notably is the dipole present in the α-helix, where one end of the helix has a partial positive charge and the other end has a partial negative charge [18]. This phenomenon allows for multiple helices to attract to each other through dipole interactions. Ionic interactions, sometimes called salt bridges, are those formed between the basic residues (histidine, arginine, and lysine) and acidic residues (glutamic acid and aspartic acid) [19]. The strength of electrostatic interactions, especially ionic interactions, are largely dependent on the protein's environmental factors, which include pH and salt concentrations [20].

Hydrophobic interactions are those between the non-polar amino acids. Although a single hydrophobic interaction is not very strong, it is the multitude of them within most proteins that contribute to an overall strong interaction. Most globular proteins are made up of a hydrophobic core, isolated from the aqueous solvent, which is covered by a hydrophilic shell that is exposed to the aqueous solvent [19]. It is hydrophobic interactions that force non-polar residues to reside in the core. This globular protein structure is driven by the hydrophobic effect, which will be discussed in more detail later. Hydrophobic interactions in proteins can be disrupted by the presence of certain chemicals, such as detergents or denaturants like guanidinium chloride or urea.

1.2 The Hydrophobic Effect

The hydrophobic effect is a very important phenomenon, as it is one of the major interactions stabilizing biological macromolecules (proteins, nucleic acids, lipid bilayers,

micelles) [21-23]. The hydrophobic effect is the tendency of non-polar molecules, introduced to an aqueous environment, to preferentially interact with each rather than with water molecules [24]. This intriguing phenomenon has been observed for many years and has prompted researchers to extensively study this effect over the years to gain a better understanding of thermodynamics behind such processes [25-29]. The underlying interactions involved in the hydrophobic effect are hydrophobic interactions, which have been broadly categorized as the preference of non-polar molecules to prefer non-polar or non-aqueous solvents [24]. Interestingly, the hydrophobic effect is specific to water only, as the hydrogen bond network and structure of water causes unique changes in the thermodynamics of the solvent when a hydrophobic molecule is introduced.

The basis of hydrophobic interactions are the measure of the standard free energy of transfer ΔG_{tr}° of a non-polar molecule, H, from its pure organic phase to water [30-33], following the equation:

$$H_{organic} \leftrightarrow H_{water} \tag{1-1}$$

Where, $H_{organic}$ is a hydrophobe in an organic phase and H_{water} is the same hydrophobe in water. The standard free energy of transfer of a non-polar molecule to water is positive, which means that an aqueous environment is not favourable for the solubilization of non-polar molecules. The standard free energy of transfer is made up of two components, which can be viewed in the following equation:

$$\Delta G_{tr}^{\circ} = \Delta H_{tr}^{\circ} - T\Delta S_{tr}^{\circ} \tag{1-2}$$

Where, ΔH_{tr}° is the standard enthalpy of transfer, T is temperature, and ΔS_{tr}° is standard entropy of transfer. The enthalpy is a measure of the change of non-covalent interactions when a hydrophobe is transferred to water from an organic phase; these include, water-water interactions, water-solute interactions, and solute-solute interactions within its organic phase. The entropy term represents the disorder/order of the system, in this case the reorganization of the water hydrogen bond network [24, 34] when a hydrophobe is introduced to the water solvent. The thermodynamics of transferring a non-polar molecule into water describes the total process, which involves the formation of a cavity in the solvent, the transfer of the solute into said cavity, and the rearrangement of solute and solvent molecules to obtain the best favourable interactions between them possible [24, 35, 36].

Originally, it was assumed that the unfavourable transfer free energies of hydrocarbons into water, at room temperature, was due to large positive enthalpy of transfer terms. This reasoning was based on Regular Solution Theory [37], which showed that unfavourable mixing of liquids was usually due to a large positive enthalpy. Surprisingly however, it was found that enthalpies for specific hydrocarbons were measured to be small and some even negative [38, 39]. One important discovery in support of these finding was that the solubility of many alkanes is at a minimum around room temperature [40], which corresponds to an enthalpy term of zero; the temperature at which enthalpy contribution to the transfer free energy is zero is known as T_H, and for most linear alkanes that temperature is just above room temperature [24, 30-33]. Therefore, at room temperature, these results support the idea that the unfavourable transfer of a non-polar molecule in water must be due to a large drop in entropy. Haymet, Dill, and Southall's results are in agreement, indicating that at temperatures around T_H hydrophobic interactions are driven by entropy [36].

Traditionally, the explanation for this large drop in entropy has been based on the clathrate cage model (or iceberg model) [33, 41]. In this model when a hydrophobic solute is transferred from an organic phase to water, water has to reorganize its hydrogen bond network to accommodate the solute molecule. For instance, if a non-polar molecule, represented by a hard sphere, is introduced to an aqueous solution the local water hydrogen bond structure changes, which leads to a "cage" of water molecules around the hydrophobic oil molecule [41]. The hydrophobe in this situation has caused water to become more ordered, which is indicative of a decrease in entropy; this gives rise to the unfavourable ΔG_{tr}° of non-polar molecules. If many more non-polar molecules were added to the water, then there would be a decrease in entropy for

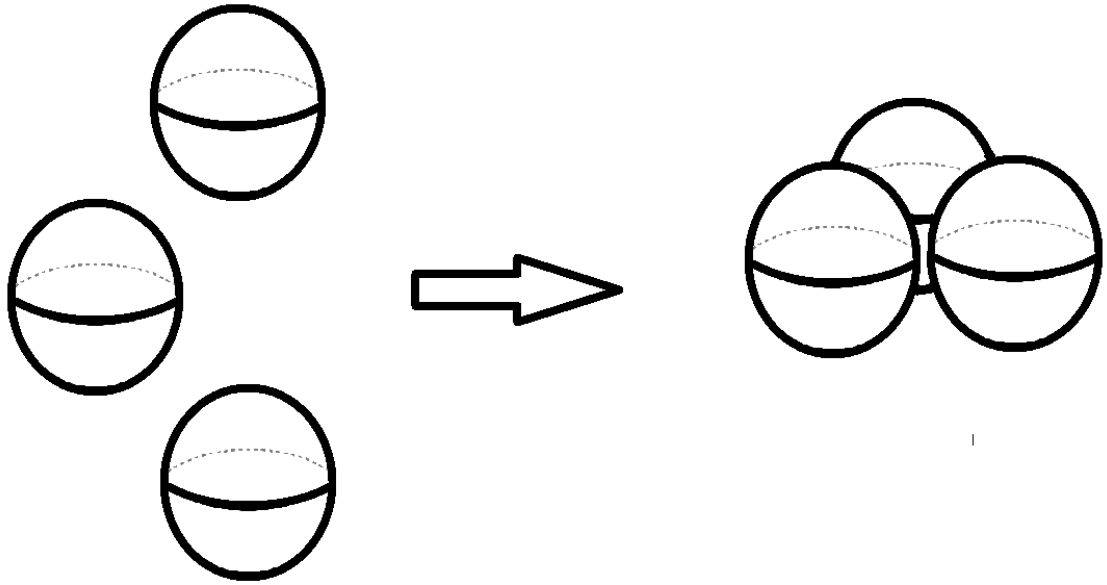

Figure 1-5. Visualization of surface area reduction by hydrophobic molecules in aqueous solution

each molecule introduced. The overall entropy of the solution is dependent on the ordering of the water structure around the non-polar molecules; as more hydrophobes are added the total surface area of them is increased proportionally by how many molecules are present, and therefore more ordered water structure is needed [42]. Thus, the amount of ordered water structure is dependent

on the accessible surface area of the hydrophobic molecules and if accessible surface area was minimized there would be an increase in entropy due to the presence of less ordered water. To accomplish the task of minimizing the total exposed surface area, hydrophobes simply aggregate together and only the outside surface of the hydrophobic globule is exposed to water [31, 42, 43]. For example, if each hydrophobe was represented by a hard sphere, as in Figure 1-5, with each sphere having 1 unit of surface area (SA), then the total surface area of three spheres would be 3 units of SA. However, if all the spheres aggregated together, then the total exposed surface area would be reduced by some amount and would therefore be less than 3 units of SA. Overall, this vast reduction in total exposed surface area leads to less ordered water structure (than in the case of all non-polar molecules separately in the solution), which means less of a decrease in entropy and leads to a relatively more negative ΔG, i.e., a more favourable energy of aggregation.

The ordering of water itself was first thought to be the explanation for the low solubility of hydrocarbons in water [24]. However, expressing hydrophobicity of hydrophobes in terms of solubility is not adequate for a proper explanation. This is due to the fact that measurements of solubility, using T_H as a reference, do not allow for proper measures of the thermodynamic parameters involved in the complex water reordering process when a hydrophobe is transferred to water [30]. The standard free energy of transfer may also be defines using solubility:

$$\Delta G_{tr} = -RT \ln \frac{X_{water}}{X_{organic}} \tag{1-3}$$

Where, R is the gas constant, T is the temperature, X_{water} is the mole fraction of the solute in the water phase, and $X_{organic}$ is the mole fraction of the solute in its pure liquid phase. Since the solute is in its pure liquid state before being transferred to water, it is considered to be in its standard state where the free energy is equal to zero; and this applied to all temperatures. In other

words, the pure liquid phase free energy is kept constant even as temperature is increased. This can be seen in Figure 1-6, where O_1 and O_2 would be considered at the same state. However, in

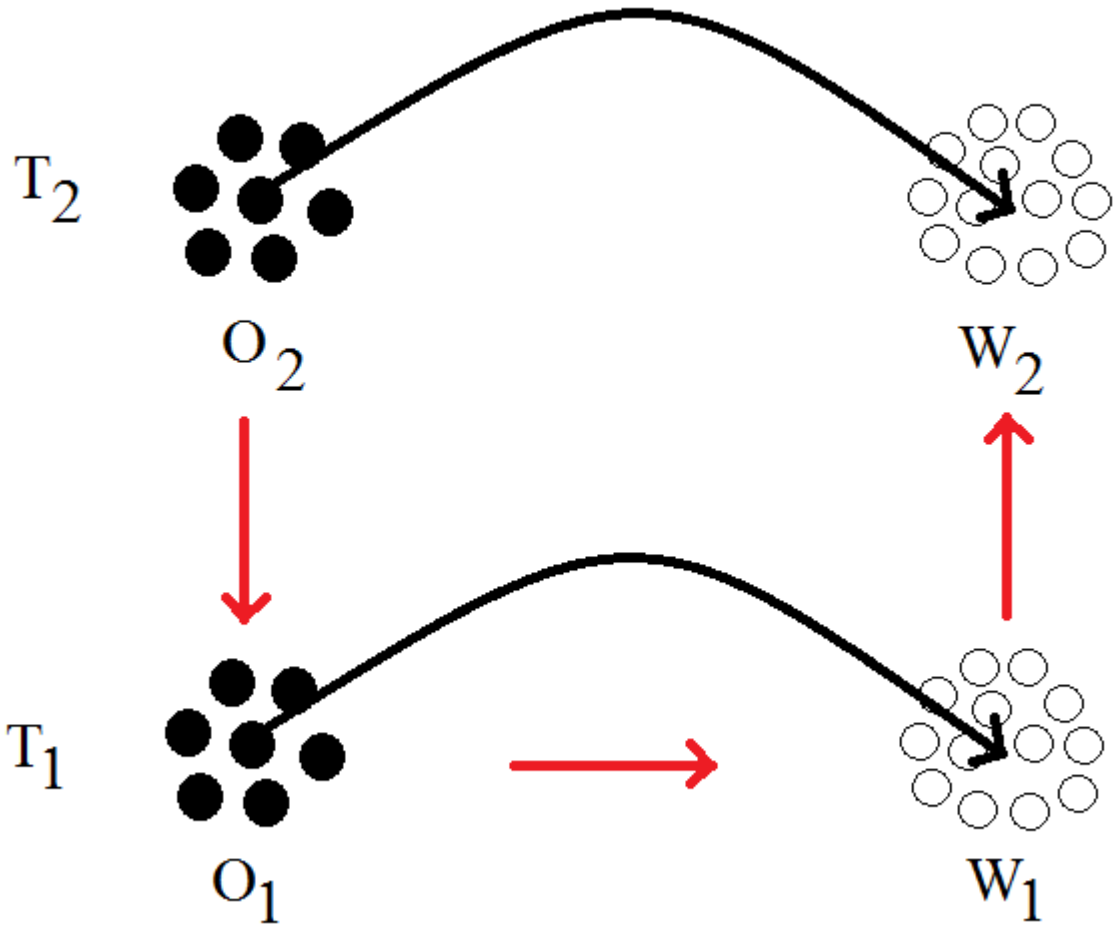

Figure 1-6. Visualization of the transfer of a hydrophobe in its pure liquid phase to water. Where, T_1 and T_2 are two different temperatures, O_1 and O_2 are the organic phases at their respective temperatures, and W_1 and W_2 are the water phases at their respective temperatures.

reality the pure liquid phase is different at every temperature, and therefore does not fully describe the transfer of a hydrophobe in its pure liquid state to a water phase. To fully compare transfer free energies at different temperatures O_1 and O_2 must be considered to have different

free energies, and the difference between T_2 and T_1 transfer free energies would be the transition through the following states: $T_2 \rightarrow T_1 \rightarrow W_1 \rightarrow W_2$ (red arrows).

Thermodynamic analyses show that hydrophobic interactions are very temperature dependent; as temperature increases, the ordered structure of water around the hydrophobe melts out, which represents the bulk water [24]. The re-organization of water structure produces a large heat capacity change, ΔC_P, which is typical for the transfer of a hydrophobe to water [30-32]. As temperature increases the ΔC_P is reduced, corresponding to the loss of ordered water structure. The large heat capacity change of the solution is the reason why hydrophobic interactions are dependent on the temperature. The heat capacity represents the temperature dependence of the entropy term and the enthalpy term [24]. When entropy contributions to the transfer free energies are at zero, the temperature is known as T_S, which interestingly also seems to be a constant for the hydrocarbons measured [30]. At this temperature the water can be said to have no ordered structure. However, at T_S the transfer free energies are actually at a maximum (the transfer of a hydrophobe to water is most unfavourable here), which indicates that as temperature increases the contribution of enthalpy to transfer free energies increases as well. Therefore, the enthalpy term is dependent on the re-ordering of water structure along with the entropy term. It can be seen from Figure 1-7 that as temperature is lowered there is a drop in both enthalpy and entropy, which corresponds to the amount of ordered water structure (increases) present around a hydrophobe [24, 30-33, 36]. If the reordering of water is minimizing unfavourable interactions between solvent and solute molecules (enthalpy) then that must mean that this reorganization is actually improving the solubility of hydrocarbons in water. These findings are in agreement with results from Shinoda and Fujihira, who showed through the use of hypothetical solubility curves and other thermodynamic analyses that the re-ordering of water increases the solubility of

hydrocarbons by a specific factor [33, 44]. Therefore, using solubilities as a measure of hydrophobicity is not in good practice to represent the underlying processes of the hydrophobic

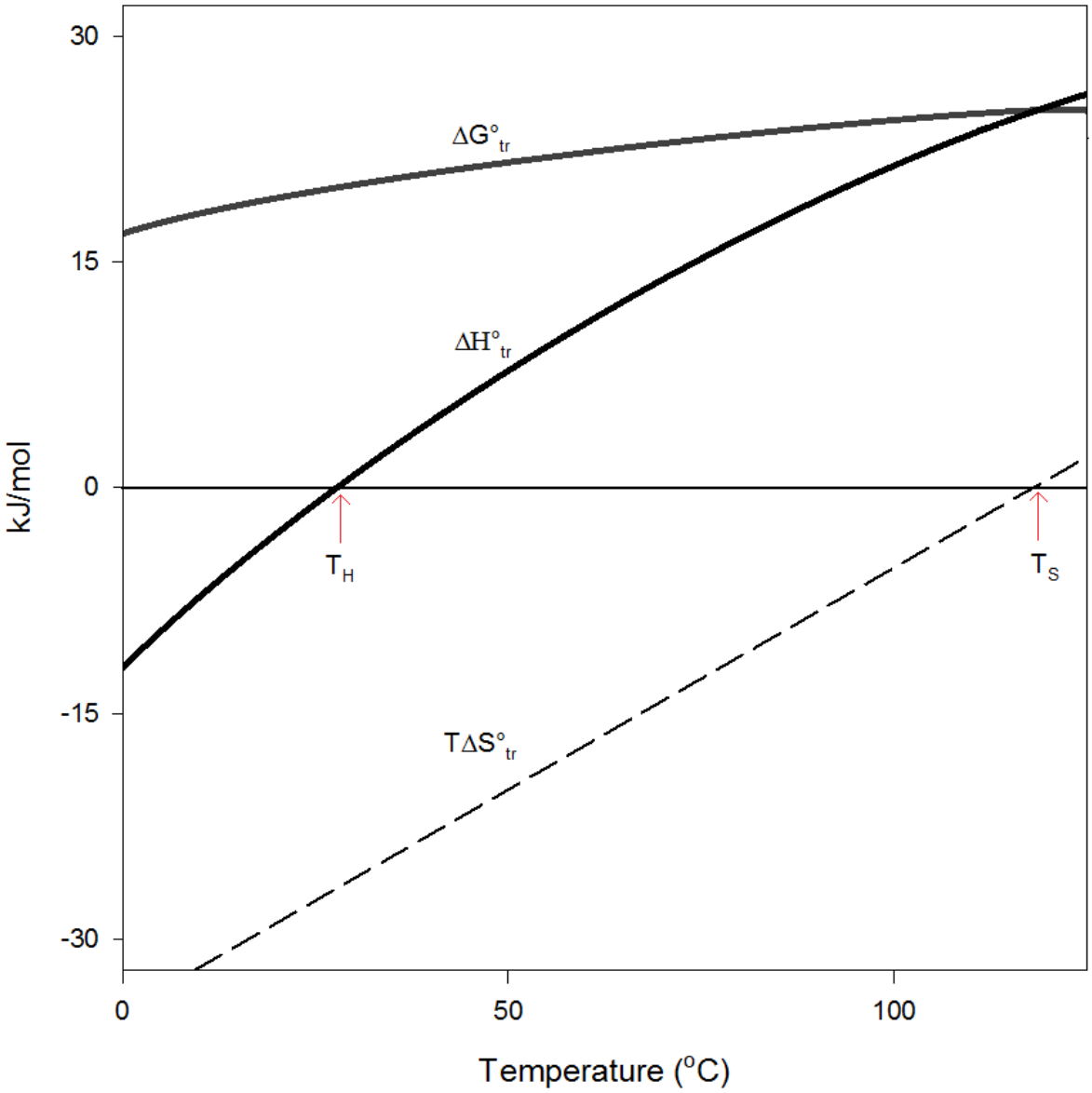

Figure 1-7. Rough graphical representation of the relationship between thermodynamic parameters of a hydrophobic molecule being transferred into a water solvent as a function of temperature. Thermodynamic parameters are defined by equation 1-2. T_H is the temperature where the standard enthalpy of transfer is zero and T_S is the temperature where the standard entropy of transfer is zero. Values based on data from Gill and Privalov [31].

effect.

An alternate way to model the hydrophobic effect is by the utilization of scaled particle theory (SPT). The basis of SPT is that the energy of solute partitioning can be represented by a cavity formation energy term and an interaction energy term [35]. An advantage in the use of SPT is that cavity formation energy in a particular solvent can be calculated with only a few experimental parameters, which include size and solvent density [35]. Sternberg and Jackson show interaction free energy of an alkane in water vs n-hexane is very small, which suggests that cavity formation energetics dominate and this promotes hydrophobes to appear to not 'like' water in the presence of a non-polar solvent [35]. However , this is still a fairly simple explanation of SPT and complex factors such as macroscopic vs microscopic surface tension, surface curvatures, molecular surface area vs accessible surface area, and more are needed for a complete understanding on how SPT can represent the hydrophobic effect [35].

Other than the cage model and scaled particle theory the hydrophobic effect is described by a multitude of models, each with their own advantages and disadvantages. A large group of models falls under the general BIPSE model [45-48], which means "Break Into Pieces, Sum the Energies". In BIPSE models, the free energy term of interest is broken down into smaller free energy terms, which are additive in nature [36]. For example, if the free energy of folding of a protein was of interest than it would be broken down into transfer free energies of single amino acids. However, Haymet et al. [36] have found that the assumptions that these terms are additive has limitations, in that the properties of solvent medium, surface area dependence, and polarity are much more complex than taken into account.

There are also models which, like the iceberg model, use the structure of surrounding water to represent the hydrophobic effect. These include models such as: the Muller model [49], small-size model [50, 51], information theory [52], MB model [53], and pairwise hydrophobic interactions [54]. The pairwise model assumes that cavity formation free energy only depends on the cavity surface area [36]. This model measures the potential mean force (pmf) between two hydrophobes in water, indicating energy minima and maxima. For instance, the pmf between two methane molecules in water is at a minimum when in contact (contact pair) with each other. The pmf is also in a local minimum when they are separated by single solvent layer; known as the solvent-separated pair [36]. As can be seen by the various models and thermodynamic terms, the hydrophobic effect is a very complex phenomenon and no one model is a perfectly accurate representation.

1.3 Organic Osmolytes

Protein structure and folding is overall very complex and is extremely difficult to fully predict the overall fold of a large protein. However, there have been computations where small proteins have been folded [55]. All proteins have optimal conditions in which they can perform best; in the case of enzymes they will catalyze reactions at an optimal rate [56]. For an example, in humans most enzymes have an optimal temperature where they function best; for some this is at body temperature. Other factors such as pH, ion concentrations, osmotic pressure, cofactor availability, etc. all play a big part not only in protein structure but also its function. Another case is that of the enzyme pepsin, which is secreted in the stomach to break down digested proteins, which functions optimally at a pH of 2 [57]. Most organisms can regulate their internal environment through certain mechanisms to maintain these optimal conditions for protein function, i.e., they maintain homeostasis. For instance humans utilize their kidneys, which help

maintain the balance of osmotic pressure and ion concentrations in the body [58]. The kidneys of mammals and other organisms without such organs use molecules called organic osmolytes to regulate osmotic pressure and ion concentrations.

Organic osmolytes are small solutes, such as: urea, methylamines, sugars, polyols, amino acids, and others. They are found in many organisms, mostly those in water-stressed environments, and are mainly used to maintain osmotic pressure to prevent osmotic swelling or shrinkage by matching the internal osmotic pressure with that of the external osmotic pressure [58]. Additionally, they are involved in the transport of ions across membranes to maintain internal osmotic pressure. Other than urea, organic osmolytes are 'compatible', meaning they do not disrupt protein function (or other macromolecules), even at higher concentrations [58]. Interestingly, urea is a strong protein denaturant with the ability to disrupt the fold of a protein, but it is still utilized by the kidneys in mammals as an osmolyte and it also is an abundant waste product. Compatible osmolytes have other functions (either direct or indirect action) than just that of osmoregulation, which include: antioxidation, redox balancing, sulphide/sulphate detoxifications, energy reserves, predator repellent, calcium modulation, thermostability, counteracting inorganic ion inhibition and hydrostatic pressure, and even counteracting the effects of urea [58]. Many thermodynamic insights of the folding of proteins has come from studying the effects of osmolytes on proteins [59-66].

1.3.1 Trimethylamine-N-Oxide

The ability of some organic osmolytes to counteract the effects of the protein denaturant urea is very interesting with regards to biophysical studies. One of the classes of osmolytes that are well known for their stabilizing abilities are the methylamines, which include glycine

betaine, glycerophosphorylcholine (GPC), and trimethylamine-N-oxide (TMAO) [58]. Since urea is a natural protein denaturant, these methylamines are able to counteract its effects by stabilizing the folded state of the protein. From those osmolytes listed above, TMAO is the best methylamine at stabilizing protein structure, and is even able to enhance protein activity as well. Interestingly, TMAO works ideally (at stabilizing proteins) when urea is present as well, which has been shown to be at a two to one ratio of urea to TMAO [58]. This two to one ratio of urea to TMAO is of physiological relevance because this ratio is present in cells (of shallow-water elasmobranch fishes) at approximate concentrations of 400 mM urea and 200 mM TMAO [58].

The stabilizing effects of TMAO on the protein folded-state are perhaps the most well studied, out of all osmolytes, experimentally [62, 66-85]. The addition of TMAO to an aqueous solution containing protein has not only been shown to protect various proteins against urea denaturation but it can also protect against additional denaturants such as guanidinium chloride. Additionally, TMAO has been demonstrated to induce structure in disordered proteins that are normally unfolded under dilute in-vitro conditions [86, 87]. Bolen and co-workers carried out thermodynamic investigations of TMAO's effect on the RCAM-T1 (reduced and carboxyamidated RNase T1) protein, which show that the addition of TMAO induces the protein to fold, driven by the burial of the polypeptide backbone [88, 89]. Further analysis by Bolen et al. demonstrated that addition of TMAO to water converts the aqueous solvent into a "poorer" solvent of the polypeptide backbone [59, 62-66, 75, 82-85, 89-98]. In other words, TMAO causes the disordered state of a protein to become more unstable relative to the folded state and it also protects the protein against the effects of urea and GdmCl (as well as other denaturants), which convert aqueous solution into a "better" solvent of the polypeptide backbone. That being said, interactions between hydrophobic portions of proteins in the presence of TMAO are less

well understood. For instance, the few theoretical calculations on the effect of TMAO on hydrophobic contact-pairs are not in agreement with each other. Garde and co-workers calculated that the addition of TMAO has a minimal effect on the thermodynamics of hydration of methane-like solutes [99, 100], while the findings of Paul and Patey show that TMAO can disrupt the interactions between hydrophobic solutes [101]. On the contrary, Graziano [102] and Daggett [103] calculated that the addition of TMAO strengthens hydrophobic interactions between hydrophobic solutes. Experimentally, Bolen found that hydrophobic amino acid side chains interact favourably with TMAO [104]. Bolen specifically looked at the hydrophobic side chains of the Nank4-7 protein and showed that transfer free energies were negative when the side chains were transferred from water into 1 M TMAO solutions.

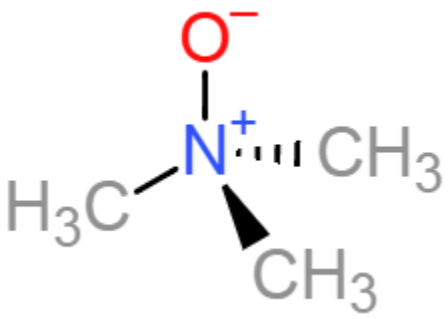

Figure 1-8. Structure of Trimethylamine-N-Oxide.

This work's experimental findings will be able to quantify the effects of TMAO addition on interactions between hydrophobic moieties in solution, which is vital to resolve the discrepancies in predictions previously brought forward. This work provides experimental insight into how TMAO specifically affects interactions between hydrophobic contact-pairs, formed between phenol and a variety of alkyl-carboxylates in aqueous solution. Phenol fluorescence is quenched by the addition of the alkyl-carboxylates, and we have previously developed a methodology for isolating the hydrophobic interactions between the contact-pairs to

the data obtained from fluorescence quenching [105, 106]. The same methodology will be applied in these experiments, due to the fact that the same simple model system of a phenol-carboxylate contact-pair, which was first introduced by Scheraga and co-workers [107, 108], is utilized. The analysis of our fluorescence data shows that the addition of TMAO to aqueous solution containing a phenol-carboxylate contact-pair causes a destabilization between said contact-pair. The findings of this work indicate a destabilization for all alkyl-carboxylates studied and there does not seem to be a size dependence on the carboxylate used. Thus, we conclude that TMAO acts as a "denaturant" toward interactions that are stabilized by the hydrophobic effect and that TMAO does not protect proteins by altering hydrophobic interactions.

1.4 Protein Denaturants

On the other end of the spectrum from compatible osmolytes, like TMAO, there are molecules called denaturants, which have the ability to disrupt the overall fold and structure of a protein. A protein that is folded is said to be in its native state, while a protein that is not in its folded state is said to be denatured [109, 110]. Proteins can be denatured by a variety of methods, such as temperature change, pH change, enzyme exposure (trypsin/chymotrypsin), and exposure to chemical denaturants. An example of a chemical denaturant is the detergent sodium dodecyl sulfate (SDS), which is very efficient at denaturing proteins. Simply speaking, SDS coats protein amino acids in a constant ratio of detergent:amino acid, which causes the intramolecular forces holding the folded structure together to be disrupted [111]. This process of denaturing is great for separating different sized proteins from one another, such as in the popular SDS-PAGE, but it is difficult to achieve back the native state by a refolding process [112]. For unfolding/folding studies of proteins other chemical denaturants are more commonly used. The

non-compatible organic osmolyte urea is one of these denaturants, as well as the salt guanidinium chloride (GdmCl).

1.4.1 Urea

As previously mentioned, urea is known as a non-compatible osmolyte, which is due to the fact that high concentrations of the osmolyte disrupt macromolecules such as proteins. Urea is more commonly referred to as a protein denaturant and it is an often used chemical in biophysical studies regarding protein denaturation and protein folding [62, 113-122]. However, even though urea is extensively used the determination of its mode of action on protein denaturation has long been sought after. Many scientists agree that there are two main modes of protein denaturation by urea known as the direct and indirect mechanisms. The indirect mechanism occurs due to urea disrupting the local water hydrogen bonding network [103, 123, 124], which in turn alters the hydrophobic effect occurring between the solvent and protein, causing the hydrophobic core of the protein to be exposed to the solvent molecules. On the other hand, the direct mechanism is thought to occur through urea directly interacting with the protein, either by interactions with the peptide backbone or amino acid side chains. These interactions may be electrostatic, hydrogen bonding or they may be hydrophobic in nature [104, 125-127]. Although there are some findings that urea denatures protein by indirect means most recent studies support the idea that urea denatures protein through the direct mechanism [128, 129], in fact studies done by the two separate groups of Sharp et al. and Rezus and Bakker found evidence that urea does not significantly alter water hydrogen bonding structure [130, 131].

Of specific interest is the effect of urea on hydrophobic interactions. Recent molecular simulations done by van Gunsteren and Oostenbrink suggest urea has an enhancing effect on

methane clusters of specific size, indicating that urea seems to have no direct effect on hydrophobic interactions [132]. These findings suggest that urea has a direct effect on the polar parts of protein, favouring electrostatic and hydrogen bonding interactions. Additional molecular dynamic simulations of proteins in urea, performed by Daggett et al. [103] and Smith et al. [133], support these conclusions. Thirumalai et al. have shown that urea preferentially adsorbs onto charged polar amino acid side chains of proteins, which results in a disruption of surface amino acids causing a swelling of the protein [134]. This mechanism allows for the hydrophobic core to be exposed to the solvent, which leads to a reduction of hydrophobic interactions in the protein. Thirumalai's findings with regards to the reduced strength of hydrophobic interactions are in agreement with the molecular simulations of Berne et al. [135], who studied the unfolding of a hydrophobic polymer by exposure to urea.

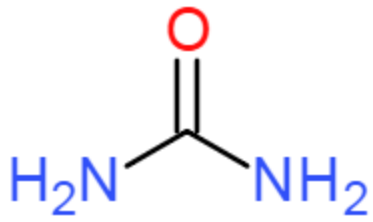

Figure 1-9. Structure of Urea.

Most studies on urea concerning its effects on hydrophobic interactions are carried out through the use of molecular dynamic simulations. Experimental evidence is somewhat more difficult to obtain. However, studies carried out by Shpiruk and Khajehpour give experimental insight on the effect of urea on hydrophobic contact-pairs interactions [106]. They found that hydrophobic pairs between phenol and small alkyl chains, such as acetate, are enhanced by urea, which seems to agree with the findings of van Gunsteren and Oostenbrink [132]. On the other hand they also found that urea disrupts interactions between phenol and large alkyl chains

(hexanoate and larger). These findings are explained by scaled particle theory [35, 136]. It is shown that urea increases the solvent packing density, which increases the energetic cost of cavity formation in the solvent as well as the solvent-solute van der Waals interactions with hydrophobes. In the former case the hydrophobic effect is promoted, while in the latter the hydrophobic effect is decreased. Both these effects working together explains how small hydrophobes are enhanced by urea but large hydrophobes are disrupted. In the case of small hydrophobes cavity formation energetics must dominate, but on the other hand in the case of large hydrophobes van der Waals interactions dominate the energetics.

1.4.2 Guanidinium Chloride

Guanidinium chloride is one of the most widely used protein denaturants in biochemistry. Surprisingly, the mechanism by which it denatures proteins is still not completely understood [103, 118, 132, 137-147]. There are two methods by which GdmCl denaturation is thought to occur: indirectly through alteration of the local water hydrogen bonding network and directly through direct interaction (hydrogen bonds and stacking interactions) between the protein and denaturant. GdmCl is one of the main focuses in this research as there have been few experimental data that look at the effect of GdmCl on hydrophobic interactions between two hydrophobic molecules.

Perhaps one of the simplest hydrophobic interactions is that between two hydrophobes. This simple system lends itself well to investigations of co-solute effects on hydrophobicity [105-108, 148] and there have been quite a few theoretical studies done with regards to studying denaturant effects on pairwise hydrophobic interactions [139, 142, 149-151]. O'Brien et al. looked at the influence of GdmCl on methane (Me) pairs as well as M^+-M^- ion pairs, where M^+ and M^- are methane molecules covered in positive and negative charges respectively, using MD

simulations [151]. They found that Me-Me pairs are stabilized by the addition of GdmCl to the aqueous solution, while the M^+-M^- ion pairs were greatly destabilized. Based on these results O'Brien et al. suggest that the guanidinium ion has strong electrostatic interactions with the ion pair, which leads to their destabilization [151].

The hypothesis that electrostatic interactions contribute to the denaturation properties of GdmCl has also been suggested by Godawat et al. Their calculations confirm that small hydrophobic pairs are stabilized by the addition of GdmCl to the aqueous solution; interestingly, the same work also shows that large hydrophobic pairs are destabilized by adding the denaturant

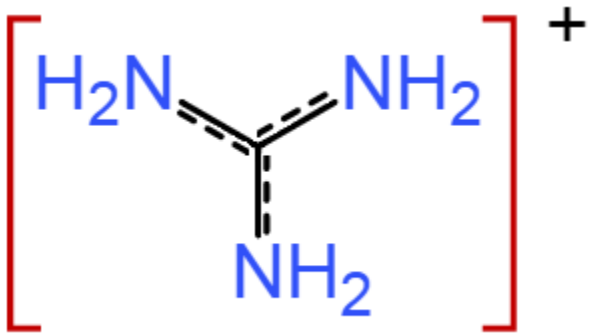

Figure 1-10. Structure of the guanidinium ion.

[149]. These results were attributed by Godawat et al. to be the result of: (a) the guanidinium ion is "multisite" which promotes van der Waals interactions with large hydrophobes, (b) guanidinium ions are much more concentrated at surfaces of large hydrophobes than in the bulk solution [149, 151], and (c) the guanidinium ion's planar shape promotes stacking interactions with protein side chains [152]. Thus, factors other than hydrogen bonding to the polypeptide backbone may contribute significantly to protein denaturation. In fact, hydrogen-deuterium exchange (1D NMR) experiments [153] and neutron diffraction studies [154] indicate that

mechanisms other than direct hydrogen bonding to the polypeptide backbone [151, 155, 156] are involved in guanidinium ion denaturation.

Since interactions other than direct hydrogen bonding play a role in the guanidinium denaturation process, we need to understand how this ion affects hydrophobic interactions. However, most analyses of GdmCl effects are from MD simulations. Therefore, it is vital to also obtain experimental evidence of how this denaturant influences hydrophobicity. This work examines how GdmCl affects interactions between hydrophobic phenyl and alkyl groups in aqueous solution by examining the quenching of phenol fluorescence by a variety of aliphatic carboxylate ions. Previously, we have developed a methodology for isolating the contribution of phenol-carboxylate interactions to fluorescence quenching data [105, 106, 148]. Using the same methodology the hydrophobic interactions between phenol and carboxylate ions, in the presence of GdmCl, are quantified. This is discussed in detail in the results and discussion sections. Our results show that addition of GdmCl to aqueous solution containing small hydrophobic pairs, acetate-phenyl and propionate-phenyl, are energetically favored (stabilized) while hydrophobic pairs containing phenyl and large hydrophobes such as butyrate, heptanoate, and octanoate, are destabilized.

1.5 Fluorescence

The utilization of fluorescence to study biological/biophysical systems is a very powerful method. Fluorescence measurements are very sensitive to the surrounding environment of the fluorescing molecule, the fluorophore [157]. Since fluorescence measurements are very sensitive it is an excellent method for probing and characterizing events such as: protein

folding/unfolding, ligand binding, enzyme kinetics, the three dimensional tumbling of macromolecules, DNA sequencing techniques, and various others.

Fluorescence is a subset of the phenomenon known as luminescence, which is simply the emission of light from a substance. The other category of luminescence is known as phosphorescence, which occurs over a much longer time frame than that of fluorescence [157].

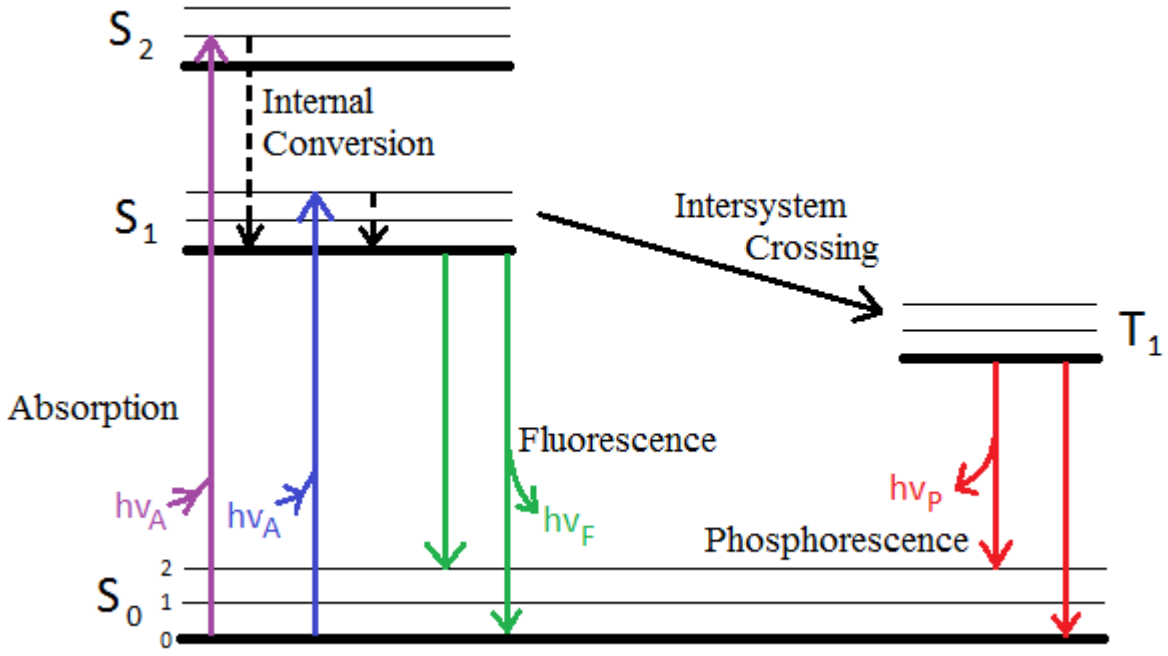

Figure 1-11. Typical form of a Jablonski diagram.

Fluorescence occurs when an electron absorbs energy (a photon) and is excited to an electronic singlet state, where it rapidly relaxes to the ground state by releasing energy in the form of a photon. The time frame for this process is in the nanosecond range; this is also known as the fluorescence life time [157]. Schematically fluorescence is represented by a diagram known as the Jablonski diagram, which can be seen in Figure 1-11.

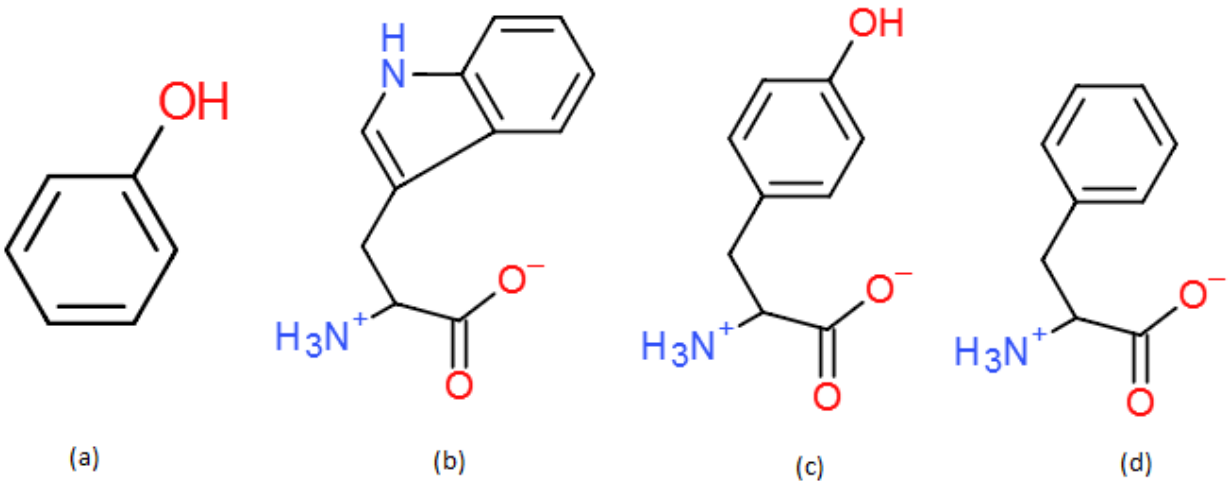

Figure 1-12. Examples of fluorescent molecules, which all contain an aromatic benzene ring. The structures are: (a) phenol, (b) tryptophan, (c) tyrosine, (d) phenylalanine.

Molecules that display fluorescence usually have structural similarities, i.e., they contain a conjugated double bond system and are aromatic. Conveniently, the amino acids phenylalanine, tyrosine, and tryptophan all contain a conjugated double bond system, which allows for proteins containing these residues to be studied using fluorescence spectroscopy. The strength of this method largely depends on the environment of the fluorescent residues, where a buried residue usually gives a much weaker signal than that of an exposed one [157]. If proteins contain these amino acids they are said to have intrinsic protein fluorescence, where tryptophans are the major contributor, tyrosines contributing less, and phenylalanines contributing very little to the overall fluorescence [157].

Fluorescence is measured via an instrument called a spectrofluorometer, where the fluorescence intensity of a solution (typically held in a quartz cuvette) is quantified. A typical fluorescence spectrum is a plot of the measured fluorescence intensity vs either wavelength (nm) or wavenumber (cm^{-}) on the x-axis, which can be observed in Figure 1-13. Changes in the solution environment can alter the spectrum, which include a blue shift of the maximum (smaller

wavelengths), a red shift of the maximum (longer wavelengths), fluoresce intensity can increase, and fluorescence intensity can decrease (fluorescence quenching) [157].

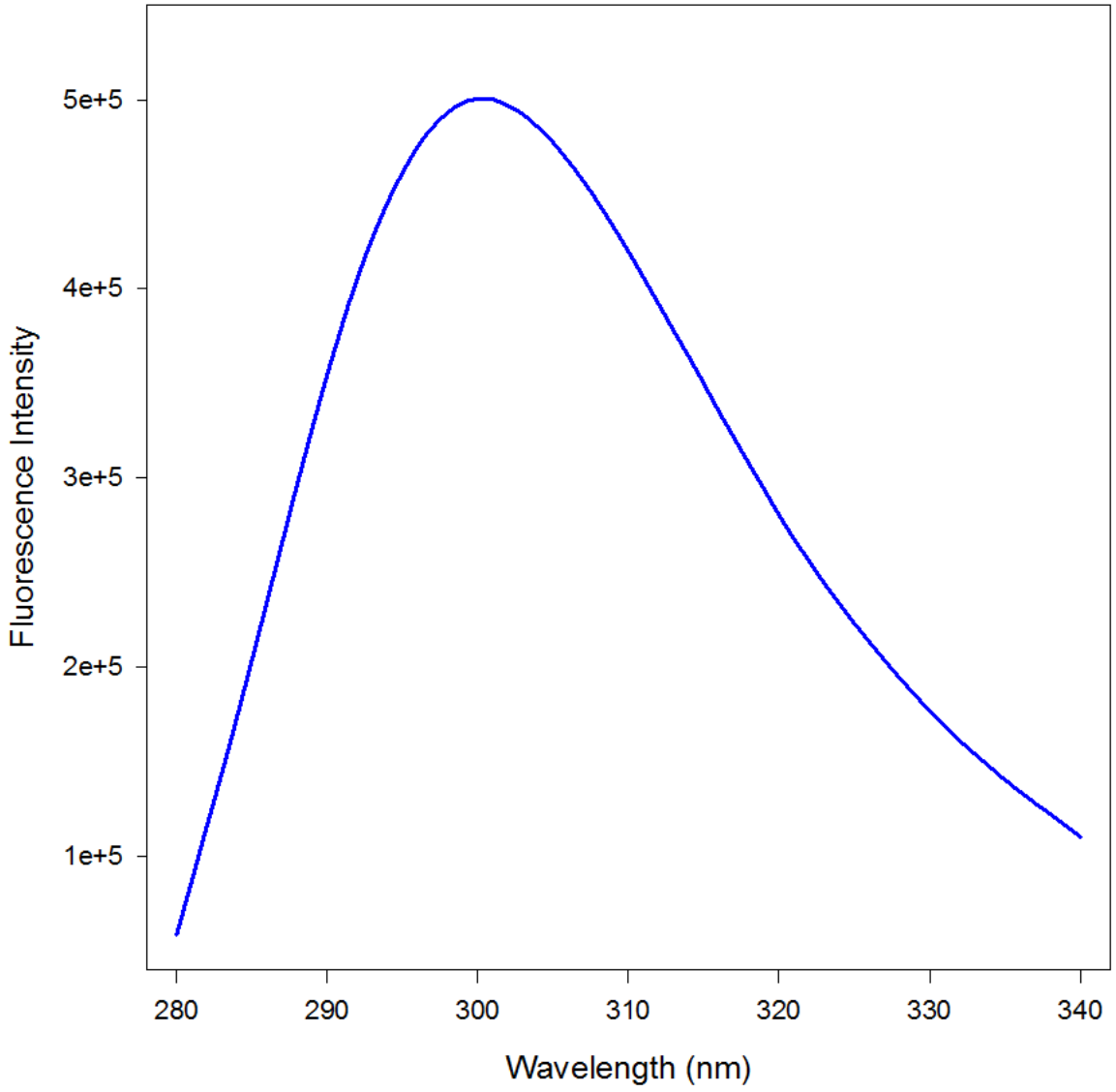

Figure 1-13. Example of a typical fluorescence spectrum, generated by a spectrofluorometer. Spectrum of 200 μM phenol in the presence of octanoate.

1.6 Fluorescence Spectroscopy

As previously mentioned, fluorescence spectra are collected with the use of a spectrofluorometer. A typical spectrofluorometer consists of multiple parts, but the main components are the light source (usually a xenon arc lamp, because it emits high intensity light over most wavelengths), an excitation monochromator, an emission monochromator, and a photo detector, which contains a photomultiplier tube [157]. The xenon arc lamp is the source of energy, which excites electrons in the fluorophore to the excited singlet state, thus causing fluorescence. The job of the excitation and emission monochromators is to split white light (polychromatic light) into its separate colours or wavelengths, which is usually achieved by the use of diffraction gratings, but prisms may also be used. The photomultiplier tube, in simple terms, detects photons emitted by fluorescence and converts the light signal into an electrical signal, which can be read by the attached computer. Since there are more photons present in higher intensity light a stronger current is generated, which gives a different reading [157].

Fluorescence is measured at a 90 degree angle from that of the excitation light source, which prevents improper measurements by the photo bleaching of the detector caused by the light source. A very simple schematic of a spectrofluorometer can be visualized in Figure 1-14. The sample cell is usually a quartz cuvette, which holds the solution of interest. All of the separate components are connected to a computer, which generates the fluorescence spectra. The control of these components, via the computer, allows for the adjustment of excitation and emission slit widths, excitation or emission wavelengths, as well as other parameters. The steady-state spectrofluorometer used in this research is the Fluorolog-3 Horiba Jobin Yvon spectrofluorometer, which can be seen below.

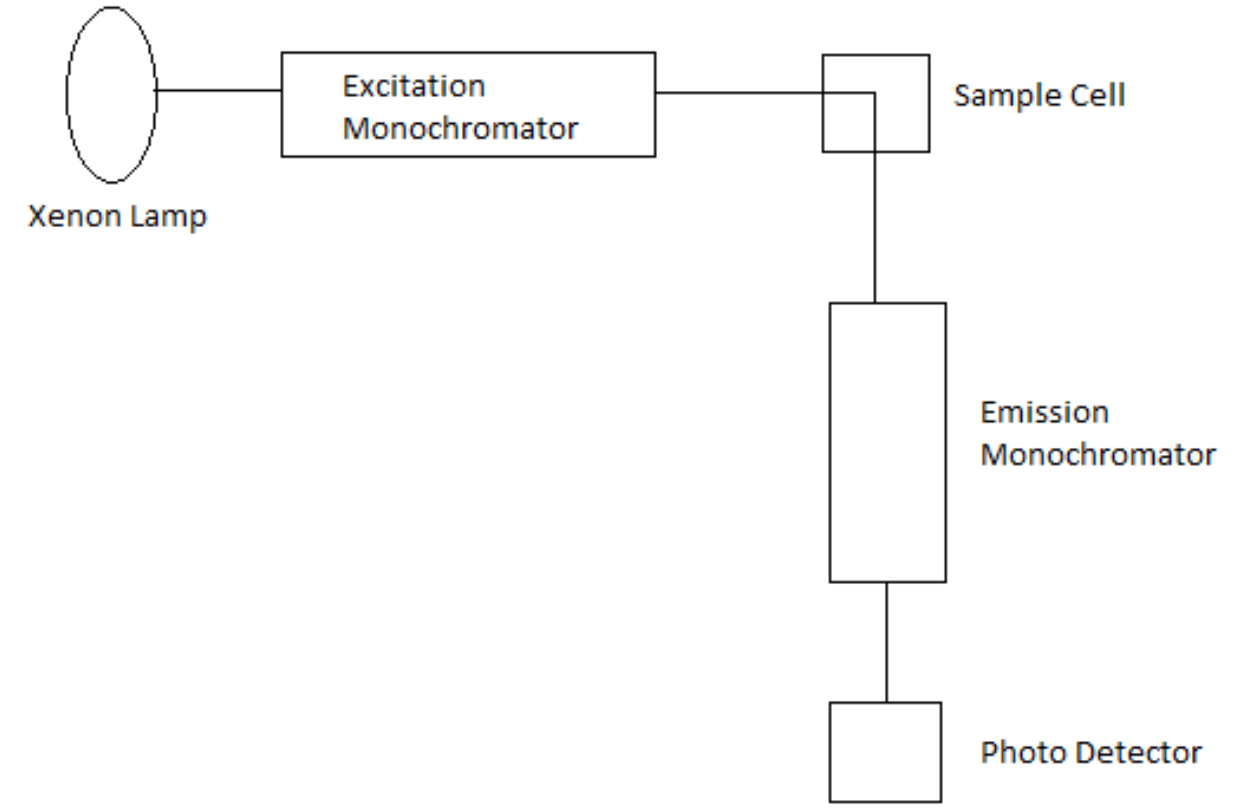

Figure 1-14. Schematic of a simple spectrofluorometer (top half). Picture of a Fluorolog-3 Horiba Jobin Yvon spectrofluorometer (bottom half)

1.7 Fluorescence Quenching

Fluorescence quenching is the non-radiative transfer of excited state energy from the fluorophore to another molecule, which causes a decrease in fluorescence intensity [157]. Molecules that quench fluorescence are referred to as quenchers. Theoretically fluorescence quenching can occur via two ideal processes; static quenching and collisional quenching (also known as dynamic quenching). Static quenching occurs when a non-fluorescent ground-state complex is formed between a fluorophore and a quencher [157]. In this case light absorbed returns to the ground-state immediately with no photon emission.

On the other hand, dynamic quenching occurs when the excited-state fluorophore is returned to the ground-state via an energy transfer with the quencher in solution [157]. The quenching of a fluorophore by a quencher can be represented by the following scheme:

$$F^* + Q \underset{k_{off}}{\overset{k_{on}}{\rightleftharpoons}} [F^* \bullet Q] \xrightarrow{k_{pt}} F + Q$$

Scheme1. Suggested mechanism for the quenching of excited state flourophore (F *) by quencher molecules Q.

Here, F* is the excited fluorophore, Q is the quencher, $[F^* \bullet Q]$ is the encounter complex formed between the quencher and fluorophore, k_{pt} is the rate of energy transfer between the quencher and excited fluorophore within the encounter complex, and F is the fluorophore in the ground state. If k_{pt} is fast, dynamic quenching can be represented by an ideal collision, where the fluorophore is instantly relaxed to its ground state when it contacts the quencher. This diffusive quenching is represented by the widely known Stern-Volmer equation [157]:

$$\frac{F_0}{F} = 1 + k_q \tau_0 |Q| = 1 + K_{SV} |Q| \qquad (1\text{-}4)$$

where F_0 is fluorescence intensity in the absence of quencher, F is the fluoresce intensity at any given quencher concentration Q, k_q is the bimolecular quenching constant, τ_0 is the fluorescence lifetime of the fluorophore in the absence of quencher, and K_{SV} is the Stern-Volmer quenching constant. A typical Stern-Volmer plot is the plot of $\frac{F_0}{F}$ vs Q, the quencher concentration, where the slope is equal to the Stern-Volmer quenching constant K_{SV}. Qualitatively, a larger K_{SV} represents the occurrence of more fluorescence quenching. In the case of a single class of fluorophore, which are all equally available to a quencher, a Stern-Volmer plot should be represented by a linear correlation fit [157]. As an example, the quenching of phenol fluorescence by either carboxylate ions (formate, acetate, etc.) or TMAO can be represent by simple linear Stern-Volmer behavior; as seen in Figure 1-15. Deviations from linear Stern-Volmer plots usually indicate a more complex quenching mechanism, where the type of quenching occurs between the two ideal mechanisms of static and dynamic quenching.

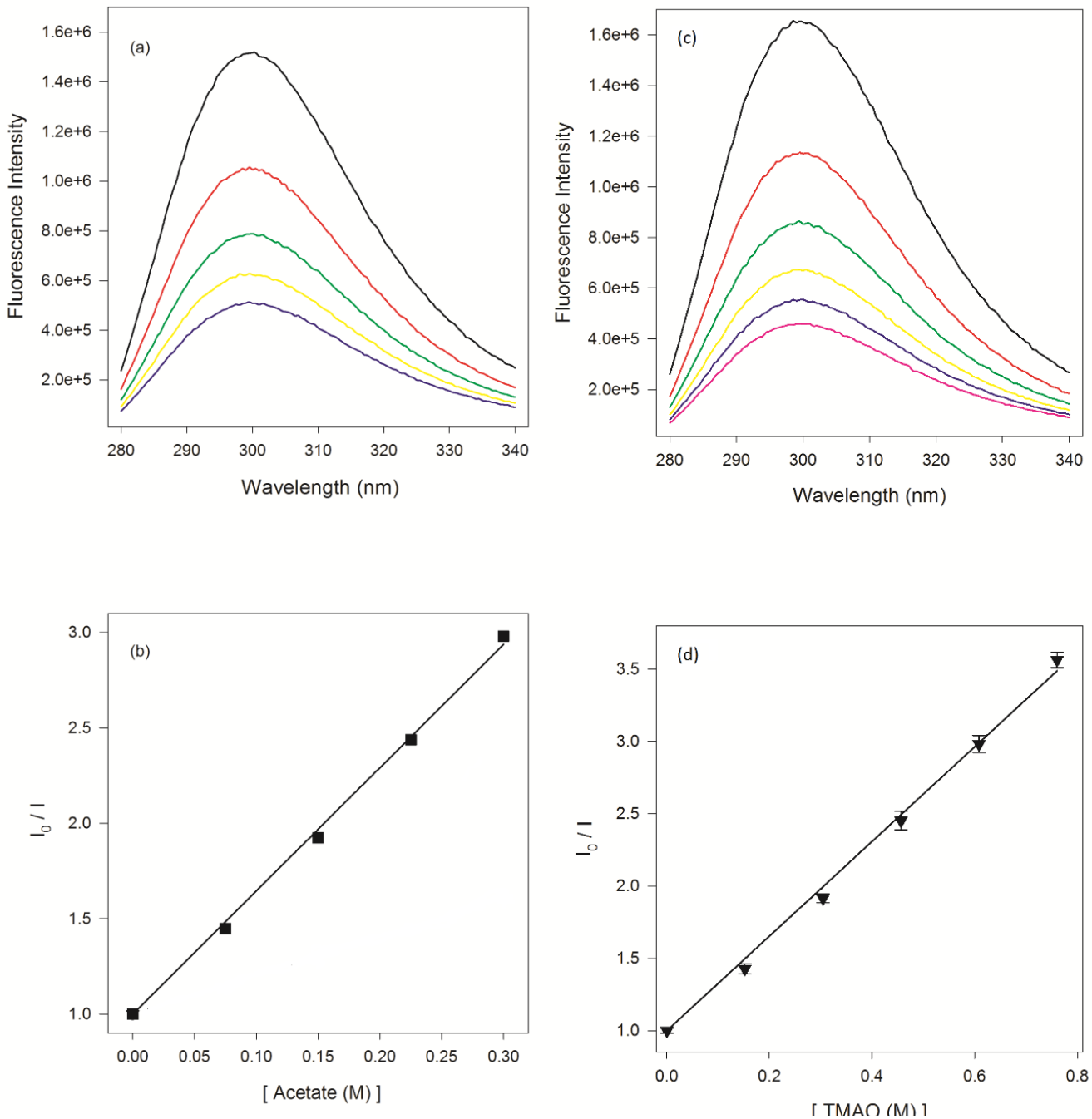

Figure 1-15. Linear Stern-Volmer quenching of phenol fluorescence by acetate (a, b) and TMAO (c, d). (a) Phenol fluorescence spectra in increasing amounts of acetate ion (0→0.3 M), where the black spectrum line contains zero quencher. (b) Stern-Volmer plot of phenol fluorescence quenching by acetate. (c) Phenol fluorescence spectra in increasing amounts of TMAO (0→0.76 M), where the black spectrum line contains zero quencher. (d) Stern-Volmer plot of phenol fluorescence quenching by TMAO. Phenol concentration of 200 µM was used for these fluorescence spectra.

1.8 Phenol Fluorescence and the Model System

To help obtain a better understanding of the method of action of both TMAO and GdmCl the use of phenol as an extrinsic fluorophore was utilized. As seen in the above figure (Figure 1-12), phenol is a simple molecule, consisting of a benzene ring and a substituted hydroxyl group. Additionally, the comparison of the structures of phenol with that of the amino acid tyrosine shows that phenol is simply a derivative of the tyrosine R group. One of the main advantages in the use of phenol, as a fluorophore, is the fact that it is able to fluoresce strongly at the micro-molar concentrations used in this work. Statistically speaking, we can assume that the low micro-molar concentration of phenol used in these experiments does not allow phenol to self-associate and quench its own fluorescence.

Interestingly, phenol's ground state and its excited state have quite different properties regarding the hydroxyl hydrogen. In the ground state the hydroxyl hydrogen has a pk_a of approximately 10, but in the excited state the hydroxyl hydrogen's pk_a drops significantly to approximately 4, which results in a much more acidic excited state compared to that of the ground state [158]. Although it is not completely clear what is causing the change between ground state phenol and excited state phenol acidity the studies of Ratzer and co-workers may resolve this [158]. They specifically studied the structure of the S_1 excited state of phenol by the use of high resolution UV-spectroscopy and were able to determine changes in bond lengths with respect to ground state phenol, demonstrating that the C-O bond length is shortened, while the O-H bond is longer is the S_1 excited state. These bond length changes are consistent with the higher acidity of excited state phenol, and if thought about in simple terms one could imagine that a longer O-H bond is weaker and therefore more likely to undergo dissociation, resulting in the phenolic anion.

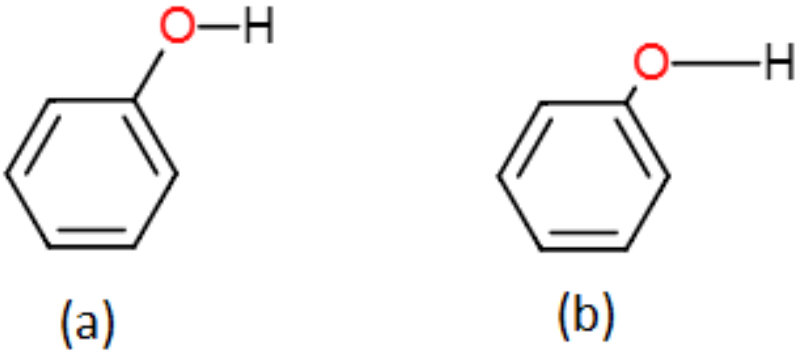

Figure 1-16. Simple representation of the C-O and O-H bond lengths in (a) ground state phenol and (b) the S_1 excited state phenol.

The other practical reason in the use of phenol is that it is involved in the simple model system consisting of the hydrophobic contact-pair formed between phenol and acetate, which has been studied extensively by Scheraga et al. [107, 108] . The quenching of phenol fluorescence by carboxylate ion was first shown in experiments performed by White [159], who showed that the quenching was well represented by a collisional quenching mechanism, and therefore followed Stern-Volmer behaviour (equation 1-4). Scheraga's group studied the system of phenol-acetate specifically, and they were able to show that the complex formed between phenol and acetate consists of more than one interaction. One of the two interactions making up the phenol-acetate complex is a hydrophilic one, which involves the hydrogen bond formed between the phenol hydroxyl hydrogen and the carboxylate group's oxygen. It is this hydrogen bonding interaction which is thought to instantaneously de-excite phenol and cause the quenching of fluorescence.

The second interaction proposed by Scheraga and co-workers is a hydrophobic one, which occurs between the benzene ring portion of phenol and the methyl group of acetate [107, 108]. They determined that the free energy of interaction of the hydrophobic portion could be

isolated by looking at the interaction of the phenol-formate complex as opposed to a phenol-acetate complex. Since formate is essentially a free carboxyl group, the interaction between it and phenol is only made up of the hydrogen bond interaction. If the hydrogen bond portion of the interaction between straight chain carboxylate ions and phenol is approximately equal in all cases, then the hydrophobic interaction free energy can be easily obtained by subtracting out the contribution of the hydrogen bond. Since the complex of phenol-formate is composed of just the hydrogen bond interaction we can subtract this interaction from the acetate-phenol complex interaction to obtain just the contribution of the hydrophobic interaction free energy. This can be applied to any straight chained carboxylate ion and phenol complex. Therefore, the hydrophobic interaction isolated is of that between the tail group of a given carboxylate and the benzene ring of phenol. Thus, the hydrophobic free energy of interaction for any straight chained carboxylate-phenol system can be represented by the following equation:

$$\Delta G_{Hydrophobic} = \Delta G_{Carboxylate} - \Delta G_{Formate} \quad (1\text{-}5)$$

Where $\Delta G_{Hydrophobic}$ is the hydrophobic free energy of the interaction between any given straight chain carboxylate and phenol, $\Delta G_{Carboxylate}$ is the interaction free energy between any straight chain carboxylate and phenol, consisting of a hydrogen bonding and a hydrophobic interaction, and $\Delta G_{Formate}$ is the interaction free energy between formate and phenol, which consists entirely of a hydrogen bonding interaction.

This model-system is a very simple one and was chosen because of this. The additive nature of the two interactions between phenol and carboxylate ion lends itself to the study of the hydrophobic interactions. Additionally, carboxylate ions do not self-aggregate either because of the negative charge repulsive forces between the carboxyl groups. As previously mentioned,

phenol is a derivative of tyrosine, while acetate can be thought of as a derivative of the R group of the amino acid glutamate. Therefore, the interactions involved in the phenol-acetate contact-pair can be related to real interactions that might occur within a folded protein.

1.9 Thesis Objectives

The purpose of this work was to gain a clear understanding of the effects of both TMAO and GdmCl on hydrophobic interactions. To do this we used a very simple model system of a phenol-carboxylate ion pair, where the hydrophobic interaction energy was isolated from the electrostatic interaction energy portion of the contact-pair. The main interest in this particular subject is that there are very few experimental data examining TMAO and GdmCl's effects on hydrophobic interactions. The most prevalent data available is based on molecular dynamic simulations and we hope this work provides experimental evidence that supports these simulations. As GdmCl and TMAO are both highly used to study the unfolding and folding process of proteins it is vital to fully understand how these compounds are interacting with the protein. We hope that our data on hydrophobic interactions can provide insight into the complex mode of action of GdmCl and TMAO on protein denaturation and stabilization, respectively.

References

[1] U. Stelzl, U. Worm, M. Lalowski, C. Haenig, F.H. Brembeck, H. Goehler, M. Stroedicke, M. Zenkner, A. Schoenherr, S. Koeppen, J. Timm, S. Mintzlaff, C. Abraham, N. Bock, S. Kietzmann, A. Goedde, E. Toksoz, A. Droege, S. Krobitsch, B. Korn, W. Birchmeier, H. Lehrach, E.E. Wanker, A Human Protein-Protein Interaction Network: A Resource for Annotating the Proteome, Cell, 122 (2005) 957-968.

[2] T. Kiyono, A. Hiraiwa, M. Fujita, Y. Hayashi, T. Akiyama, M. Ishibashi, Binding of high-risk human papillomavirus E6 oncoproteins to the human homologue of the Drosophila discs large tumor suppressor protein, Proceedings of the National Academy of Sciences, 94 (1997) 11612-11616.

[3] W. Mohler, A.C. Millard, P.J. Campagnola, Second harmonic generation imaging of endogenous structural proteins, Methods, 29 (2003) 97-109.

[4] A.E. Johnson, M.A. van Waes, THE TRANSLOCON: A Dynamic Gateway at the ER Membrane, Annual Review of Cell and Developmental Biology, 15 (1999) 799-842.

[5] C.A. Grimes, R.S. Jope, The multifaceted roles of glycogen synthase kinase 3-Beta in cellular signaling, Progress in Neurobiology, 65 (2001) 391-426.

[6] L. Osborn, S. Kunkel, G.J. Nabel, Tumor necrosis factor alpha and interleukin 1 stimulate the human immunodeficiency virus enhancer by activation of the nuclear factor kappa B, Proceedings of the National Academy of Sciences, 86 (1989) 2336-2340.

[7] H.J. Dyson, P.E. Wright, Intrinsically unstructured proteins and their functions, Nature Reviews Molecular Cell Biology, 6 (2005) 197-208.

[8] J.M. Berg, J.L. Tymoczko, L. Stryer, Biochemistry, 5 ed., W. H. Freeman and Company, New York, 2002.

[9] F. Sanger, The arrangement of amino acids in proteins Advances in Protein Chemistry, 7 (1952) 1-67.

[10] H. Sigel, R.B. Martin, Coordinating properties of the amide bond. Stability and structure of metal ion complexes of peptides and related ligands, Chemical Reviews, 82 (1982) 385-426.

[11] L. Pauling, R.B. Corey, Configurations of Polypeptide Chains With Favored Orientations Around Single Bonds: Two New Pleated Sheets, Proceedings of the National Academy of Sciences, 37 (1951) 729-740.

[12] L. Pauling, R.B. Corey, H.R. Branson, The Structure of Proteins: Two Hydrogen-Bonded Helical Configurations of the Polypeptide Chain, Proceedings of the National Academy of Sciences of the United States of America, 37 (1951) 205-211.

[13] C.M. Roth, B.L. Neal, A.M. Lenhoff, Van der Waals interactions involving proteins, Biophysical Journal, 70 (1996) 977-987.

[14] P.C. Jocelyn, Biochemistry of the SH group; the occurrence, chemical properties, metabolism and biological function of thiols and disulphides, Academic Press, London, New York, 1972.

[15] E. Chanat, U. Weiss, W.B. Huttner, S.A. Tooze, Reduction of the disulfide bond of chromogranin B (secretogranin I) in the trans-Golgi network causes its missorting to the constitutive secretory pathway, EMBO Journal, 12 (1993) 2159-2168.

[16] S.K. Burley, G.A. Petsko, J.T.E.F.M.R. C.B. Anfinsen, S.E. David, Weakly Polar Interactions In Proteins, Advances in Protein Chemistry, Academic Press1988, pp. 125-189.

[17] N.M. Luscombe, R.A. Laskowski, J.M. Thornton, Amino acid-base interactions: a three-dimensional analysis of protein-DNA interactions at an atomic level, Nucleic Acids Research, 29 (2001) 2860-2874.

[18] W.G.J. Hol, The role of the alpha-helix dipole in protein function and structure, Progress in Biophysics and Molecular Biology, 45 (1985) 149-195.

[19] Z.S. Hendsch, B. Tidor, Do salt bridges stabilize proteins? A continuum electrostatic analysis, Protein Science, 3 (1994) 211-226.

[20] C.N. Pace, D.V. Laurents, J.A. Thomson, pH dependence of the urea and guanidine hydrochloride denaturation of ribonuclease A and ribonuclease T1, Biochemistry, 29 (1990) 2564-2572.

[21] C. Tanford, The hydrophobic effect: Formation of micelles and biological membranes, Journal of Polymer Science: Polymer Letters Edition, 18 (1980) 687-687.

[22] C. Tanford, The Hydrophobic Effect and the Organization of Living Matter, Science, 200 (1978) 1012-1018.

[23] W. Kauzmann, M.L.A.K.B. C.B. Anfinsen, T.E. John, Some Factors in the Interpretation of Protein Denaturation, Advances in Protein Chemistry, Academic Press1959, pp. 1-63.

[24] T.E. Creighton, Proteins: Structures and molecular properties, 2 ed., W. H. Freeman and Company, New York, 1992.

[25] R. Breslow, Hydrophobic effects on simple organic reactions in water, Accounts of Chemical Research, 24 (1991) 159-164.

[26] A. Nicholls, K.A. Sharp, B. Honig, Protein folding and association: Insights from the interfacial and thermodynamic properties of hydrocarbons, Proteins: Structure, Function, and Bioinformatics, 11 (1991) 281-296.

[27] C.N. Pace, B.A. Shirley, M. McNutt, K. Gajiwala, Forces contributing to the conformational stability of proteins, The FASEB Journal, 10 (1996) 75-83.

[28] L.R. Pratt, D. Chandler, Theory of the hydrophobic effect, The Journal of Chemical Physics, 67 (1977) 3683-3704.

[29] C. Tanford, Interfacial Free Energy and the Hydrophobic Effect, Proceedings of the National Academy of Sciences of the United States of America, 76 (1979) 4175-4176.

[30] P.L. Privalov, S.J. Gill, The hydrophobic effect: a reappraisal, Pure and Applied Chemistry, 61 (1989) 1097-1104.

[31] P.L. Privalov, S.J. Gill, Stability of protein structure and hydrophobic interaction, Advances in Protein Chemistry, 39 (1988) 191-234.

[32] R.L. Baldwin, Temperature Dependence of the Hydrophobic Interaction in Protein Folding, Proceedings of the National Academy of Sciences of the United States of America, 83 (1986) 8069-8072.

[33] K. Shinoda, "Iceberg" formation and solubility, The Journal of Physical Chemistry, 81 (1977) 1300-1302.

[34] D. Chandler, Interfaces and the driving force of hydrophobic assembly, Nature, 437 (2005) 640.

[35] R.M. Jackson, M.J.E. Sternberg, Application of scaled particle theory to model the hydrophobic effect: implications for molecular association and protein stability, Protein Engineering, 7 (1994) 371-383.

[36] N.T. Southall, K.A. Dill, A.D.J. Haymet, A View of the Hydrophobic Effect, The Journal of Physical Chemistry B, 106 (2001) 521-533.

[37] J.H. Hildebrand, An Improvement in the Theory of Regular Solutions, Proceedings of the National Academy of Sciences of the United States of America, 76 (1979) 6040-6041.

[38] J.A.V. Butler, The energy and entropy of hydration of organic compounds, Transactions of the Faraday Society, 33 (1937) 229-236.

[39] J.A.V. Butler, W.S. Reid, The solubility of non-electrolytes. Part III. The entropy of hydration, Journal of the Chemical Society (Resumed), (1936) 1171-1173.

[40] S.J. Gill, N.F. Nichols, I. Wadso, Calorimetric determination of enthalpies of solution of slightly soluble liquids II. Enthalpy of solution of some hydrocarbons in water and their use in establishing the temperature dependence of their solubilities, The Journal of Chemical Thermodynamics, 8 (1976) 445-452.

[41] H.S. Frank, M.W. Evans, Free Volume and Entropy in Condensed Systems III. Entropy in Binary Liquid Mixtures; Partial Molal Entropy in Dilute Solutions; Structure and Thermodynamics in Aqueous Electrolytes, The Journal of Chemical Physics, 13 (1945) 507-532.

[42] H.S. Ashbaugh, E.W. Kaler, M.E. Paulaitis, A "Universal" Surface Area Correlation for Molecular Hydrophobic Phenomena, Journal of the American Chemical Society, 121 (1999) 9243-9244.

[43] H.A. Scheraga, Theory of Hydrophobic Interactions, Journal of Biomolecular Structure and Dynamics, 16 (1998) 447-460.

[44] K. Shinoda, M. Fujihira, The Analysis of the Solubilty of Hydrocarbons in Water, Bulletin of the Chemical Society of Japan, 41 (1968) 2612-2615.

[45] T. Ooi, M. Oobatake, G. Nemethy, H.A. Scheraga, Accessible Surface Areas as a Measure of the Thermodynamic Parameters of Hydration of Peptides, Proceedings of the National Academy of Sciences of the United States of America, 84 (1987) 3086-3090.

[46] D. Eisenberg, A.D. McLachlan, Solvation energy in protein folding and binding, Nature, 319 (1986) 199-203.

[47] C. Hansch, Quantitative approach to biochemical structure-activity relationships, Accounts of Chemical Research, 2 (1969) 232-239.

[48] P.J. Flory, Principles of Polymer Chemistry, Cornell University Press, Ithaca, NY, 1953.

[49] N. Muller, Search for a realistic view of hydrophobic effects, Accounts of Chemical Research, 23 (1990) 23-28.

[50] B. Lee, The physical origin of the low solubility of nonpolar solutes in water, Biopolymers, 24 (1985) 813-823.

[51] M. Lucas, Size effect in transfer of nonpolar solutes from gas or solvent to another solvent with a view on hydrophobic behavior, The Journal of Physical Chemistry, 80 (1976) 359-362.

[52] G. Hummer, S. Garde, A.E. Garcia, M.E. Paulaitis, L.R. Pratt, Hydrophobic Effects on a Molecular Scale, The Journal of Physical Chemistry B, 102 (1998) 10469-10482.

[53] N.T. Southall, K.A. Dill, The Mechanism of Hydrophobic Solvation Depends on Solute Radius, The Journal of Physical Chemistry B, 104 (2000) 1326-1331.

[54] R.H. Wood, P.T. Thompson, Differences Between Pair and Bulk Hydrophobic Interactions, Proceedings of the National Academy of Sciences of the United States of America, 87 (1990) 946-949.

[55] H. Gelman, M. Gruebele, Fast protein folding kinetics, Quarterly Reviews of Biophysics, 47 (2014) 95-142

[56] A. Zaks, A.M. Klibanov, Enzyme-catalyzed processes in organic solvents, Proceedings of the National Academy of Sciences, 82 (1985) 3192-3196.

[57] B.S. Hartley, Proteolytic Enzymes, Annual Review of Biochemistry, 29 (1960) 45-72.

[58] P.H. Yancey, Organic osmolytes as compatible, metabolic and counteracting cytoprotectants in high osmolarity and other stresses, J Exp Biol, 208 (2005) 2819-2830.

[59] L.M.F. Holthauzen, D.W. Bolen, Mixed osmolytes: The degree to which one osmolyte affects the protein stabilizing ability of another, Protein Science, 16 (2007) 293-298.

[60] F. Guo, J.M. Friedman, Osmolyte-Induced Perturbations of Hydrogen Bonding between Hydration Layer Waters: Correlation with Protein Conformational Changes, The Journal of Physical Chemistry B, 113 (2009) 16632-16642.

[61] D.K. Eggers, J.S. Valentine, Crowding and hydration effects on protein conformation: a study with sol-gel encapsulated proteins, Journal of Molecular Biology, 314 (2001) 911-922.

[62] D.W. Bolen, G.D. Rose, Structure and Energetics of the Hydrogen-Bonded Backbone in Protein Folding, Annual Review of Biochemistry, 77 (2008) 339-362.

[63] M. Auton, A.C.M. Ferreon, D.W. Bolen, Metrics that Differentiate the Origins of Osmolyte Effects on Protein Stability: A Test of the Surface Tension Proposal, Journal of Molecular Biology, 361 (2006) 983-992.

[64] M. Auton, D.W. Bolen, J. Rösgen, Structural thermodynamics of protein preferential solvation: Osmolyte solvation of proteins, aminoacids, and peptides, Proteins: Structure, Function, and Bioinformatics, 73 (2008) 802-813.

[65] M. Auton, D.W. Bolen, Predicting the energetics of osmolyte-induced protein folding/unfolding, Proceedings of the National Academy of Sciences of the United States of America, 102 (2005) 15065-15068.

[66] A. Wang, D.W. Bolen, A Naturally Occurring Protective System in Urea-Rich Cells: Mechanism of Osmolyte Protection of Proteins against Urea Denaturation, Biochemistry, 36 (1997) 9101-9108.

[67] V.N. Uversky, J. Li, A.L. Fink, Trimethylamine-N-oxide-induced folding of alpha-synuclein, FEBS Letters, 509 (2001) 31-35.

[68] J. Tulla-Puche, I.V. Getun, C. Woodward, G. Barany, Native-like Conformations Are Sampled by Partially Folded and Disordered Variants of Bovine Pancreatic Trypsin Inhibitor, Biochemistry, 43 (2004) 1591-1598.

[69] S. Tranier, C. Iobbi-Nivol, C. Birck, M. Ilbert, I. Mortier-Barriere, V. Mejean, J.-P. Samama, A Novel Protein Fold and Extreme Domain Swapping in the Dimeric TorD Chaperone from Shewanella massilia, Structure, 11 (2003) 165-174.

[70] S.L. Lin, A. Zarrine-Afsar, A.R. Davidson, The osmolyte trimethylamine-N-oxide stabilizes the Fyn SH3 domain without altering the structure of its folding transition state, Protein Science, 18 (2009) 526-536.

[71] C. Lendel, V. Dincbas-Renqvist, A. Flores, E. Wahlberg, J. Dogan, P.-Å. Nygren, T. Härd, Biophysical characterization of ZSPA-1—A phage-display selected binder to protein A, Protein Science, 13 (2004) 2078-2088.

[72] R. Kumar, J.M. Serrette, E.B. Thompson, Osmolyte-induced folding enhances tryptic enzyme activity, Archives of Biochemistry and Biophysics, 436 (2005) 78-82.

[73] C.H. Henkels, J.C. Kurz, C.A. Fierke, T.G. Oas, Linked Folding and Anion Binding of the Bacillus subtilis Ribonuclease P Proteinâ€ Biochemistry, 40 (2001) 2777-2789.

[74] O. Gursky, Probing the conformation of a human apolipoprotein C-1 by amino acid substitutions and trimethylamine-N-oxide, Protein Science, 8 (1999) 2055-2064.

[75] M. Gulotta, L. Qiu, R. Desamero, J. Rosgen, D.W. Bolen, R. Callender, Effects of Cell Volume Regulating Osmolytes on Glycerol 3-Phosphate Binding to Triosephosphate Isomerase Biochemistry, 46 (2007) 10055-10062.

[76] M. Gonnelli, G.B. Strambini, No effect of trimethylamine N-oxide on the internal dynamics of the protein native fold, Biophysical Chemistry, 89 (2001) 77-85.

[77] T.C. Gluick, S. Yadav, Trimethylamine N-Oxide Stabilizes RNA Tertiary Structure and Attenuates the Denaturating Effects of Urea, Journal of the American Chemical Society, 125 (2003) 4418-4419.

[78] R.F. Gahl, M. Narayan, G. Xu, H.A. Scheraga, Trimethylamine-N-oxide modulates the reductive unfolding of onconase, Biochemical and Biophysical Research Communications, 325 (2004) 707-710.

[79] Y. Feng, D. Liu, J. Wang, Native-like Partially Folded Conformations and Folding Process Revealed in the N-terminal Large Fragments of Staphylococcal Nuclease: A Study by NMR Spectroscopy, Journal of Molecular Biology, 330 (2003) 821-837.

[80] S.A. Celinski, J.M. Scholtz, Osmolyte effects on helix formation in peptides and the stability of coiled-coils, Protein Science, 11 (2002) 2048-2051.

[81] D.D. Banks, L.M. Gloss, Equilibrium Folding of the Core Histones: the H3-H4 Tetramer Is Less Stable than the H2A-H2B Dimer Biochemistry, 42 (2003) 6827-6839.

[82] M. Auton, D.W. Bolen, Additive Transfer Free Energies of the Peptide Backbone Unit That Are Independent of the Model Compound and the Choice of Concentration Scale, Biochemistry, 43 (2004) 1329-1342.

[83] A.T. Russo, J. Rosgen, D.W. Bolen, Osmolyte Effects on Kinetics of FKBP12 C22A Folding Coupled with Prolyl Isomerization, Journal of Molecular Biology, 330 (2003) 851-866.

[84] L. Rajagopalan, J. Rosgen, D.W. Bolen, K. Rajarathnam, Novel Use of an Osmolyte To Dissect Multiple Thermodynamic Linkages in a Chemokine Ligand-Receptor System, Biochemistry, 44 (2005) 12932-12939.

[85] R. Kumar, J.C. Lee, D.W. Bolen, E.B. Thompson, The Conformation of the Glucocorticoid Receptor AF1/tau1 Domain Induced by Osmolyte Binds Co-regulatory Proteins, Journal of Biological Chemistry, 276 (2001) 18146-18152.

[86] M. Howard, H. Fischer, J. Roux, B.C. Santos, S.R. Gullans, P.H. Yancey, W.J. Welch, Mammalian Osmolytes and S-Nitrosoglutathione Promote F508 Cystic Fibrosis Transmembrane Conductance Regulator (CFTR) Protein Maturation and Function, Journal of Biological Chemistry, 278 (2003) 35159-35167.

[87] B.J. Bennion, M.L. DeMarco, V. Daggett, Preventing Misfolding of the Prion Protein by Trimethylamine N-Oxide Biochemistry, 43 (2004) 12955-12963.

[88] Y. Qu, C.L. Bolen, D.W. Bolen, Osmolyte-driven contraction of a random coil protein, Proceedings of the National Academy of Sciences, 95 (1998) 9268-9273.

[89] P. Wu, D.W. Bolen, Osmolyte-induced protein folding free energy changes, Proteins: Structure, Function, and Bioinformatics, 63 (2006) 290-296.

[90] A. Wang, A.D. Robertson, D.W. Bolen, Effects of a Naturally Occurring Compatible Osmolyte on the Internal Dynamics of Ribonuclease A, Biochemistry, 34 (1995) 15096-15104.

[91] S.N. Timasheff, G. Xie, Preferential interactions of urea with lysozyme and their linkage to protein denaturation, Biophysical Chemistry, 105 (2003) 421-448.

[92] T.O. Street, D.W. Bolen, G.D. Rose, A molecular mechanism for osmolyte-induced protein stability, Proceedings of the National Academy of Sciences, 103 (2006) 13997-14002.

[93] J. Rösgen, B.M. Pettitt, D.W. Bolen, An analysis of the molecular origin of osmolyte-dependent protein stability, Protein Science, 16 (2007) 733-743.

[94] J. Rosgen, B.M. Pettitt, D.W. Bolen, Protein Folding, Stability, and Solvation Structure in Osmolyte Solutions, Biophysical Journal, 89 (2005) 2988-2997.

[95] C.Y. Hu, H. Kokubo, G.C. Lynch, D.W. Bolen, B.M. Pettitt, Backbone additivity in the transfer model of protein solvation, Protein Science, 19 (2010) 1011-1022.

[96] I.V. Baskakov, R. Kumar, G. Srinivasan, Y.-s. Ji, D.W. Bolen, E.B. Thompson, Trimethylamine N-Oxide-induced Cooperative Folding of an Intrinsically Unfolded Transcription-activating Fragment of Human Glucocorticoid Receptor, Journal of Biological Chemistry, 274 (1999) 10693-10696.

[97] I. Baskakov, D.W. Bolen, Forcing Thermodynamically Unfolded Proteins to Fold, Journal of Biological Chemistry, 273 (1998) 4831-4834.

[98] M. Auton, D.W. Bolen, H.u. Dieter, S. Helmut, Chapter Twenty-Three - Application of the Transfer Model to Understand How Naturally Occurring Osmolytes Affect Protein Stability, Methods in Enzymology, Academic Press2007, pp. 397-418.

[99] M.V. Athawale, J.S. Dordick, S. Garde, Osmolyte Trimethylamine-N-Oxide Does Not Affect the Strength of Hydrophobic Interactions: Origin of Osmolyte Compatibility, Biophysical Journal, 89 (2005) 858-866.

[100] M.V. Athawale, S. Sarupria, S. Garde, Enthalpy-Entropy Contributions to Salt and Osmolyte Effects on Molecular-Scale Hydrophobic Hydration and Interactions, The Journal of Physical Chemistry B, 112 (2008) 5661-5670.

[101] S. Paul, G.N. Patey, The Influence of Urea and Trimethylamine-N-oxide on Hydrophobic Interactions, The Journal of Physical Chemistry B, 111 (2007) 7932-7933.

[102] G. Graziano, How does trimethylamine N-oxide counteract the denaturing activity of urea?, Physical Chemistry Chemical Physics, 13 (2011) 17689-17695.

[103] B.J. Bennion, V. Daggett, The Molecular Basis for the Chemical Denaturation of Proteins by Urea, Proceedings of the National Academy of Sciences of the United States of America, 100 (2003) 5142-5147.

[104] L.M.F. Holthauzen, J. Rosgen, D.W. Bolen, Hydrogen Bonding Progressively Strengthens upon Transfer of the Protein Urea-Denatured State to Water and Protecting Osmolytes, Biochemistry, 49 (2010) 1310-1318.

[105] D.L. Beauchamp, M. Khajehpour, The effect of lithium ions on the hydrophobic effect: does lithium affect hydrophobicity differently than other ions?, Biophysical Chemistry, 163-164 (2012) 35-43.

[106] T.A. Shpiruk, M. Khajehpour, The effect of urea on aqueous hydrophobic contact-pair interactions, Physical Chemistry Chemical Physics, 15 (2013) 213-222.

[107] D.K. Kunimitsu, A.Y. Woody, E.R. Stimson, H.A. Scheraga, Thermodynamic data from fluorescence spectra. II. Hydrophobic bond formation in binary complexes, The Journal of Physical Chemistry, 72 (1968) 856-866.

[108] A.Y. Moon, D.C. Poland, H.A. Scheraga, Thermodynamic Data from Fluorescence Spectra. I. The System Phenol-Acetate, The Journal of Physical Chemistry, 69 (1965) 2960-2966.

[109] C. Tanford, J.T.E. C.B. Anfinsen, M.R. Frederic, Protein Denaturation: Part C. Theoretical Models for The Mechanism of Denaturation, Advances in Protein Chemistry, Academic Press1970, pp. 1-95.

[110] C. Tanford, M.L.A.J.T.E. C.B. Anfinsen, M.R. Frederic, Protein Denaturation, Advances in Protein Chemistry, Academic Press1968, pp. 121-282.

[111] A.K. Bhuyan, On the mechanism of SDS-induced protein denaturation, Biopolymers, 93 (2009) 186-199.

[112] A.L. Shapiro, E. Vinuela, J. V. Maizel Jr, Molecular weight estimation of polypeptide chains by electrophoresis in SDS-polyacrylamide gels, Biochemical and Biophysical Research Communications, 28 (1967) 815-820.

[113] N.C. Pace, B.M.P. Huyghues-Despointes, H. Fu, K. Takano, J.M. Scholtz, G.R. Grimsley, Urea denatured state ensembles contain extensive secondary structure that is increased in hydrophobic proteins, Protein Science, 19 (2010) 929-943.

[114] D.R. Canchi, D. Paschek, A.E. Garcia, Equilibrium Study of Protein Denaturation by Urea, Journal of the American Chemical Society, 132 (2010) 2338-2344.

[115] L. Ma, L. Pegram, M.T. Record, Q. Cui, Preferential Interactions between Small Solutes and the Protein Backbone: A Computational Analysis, Biochemistry, 49 (2010) 1954-1962.

[116] S. Lee, Y.L. Shek, T.V. Chalikian, Urea interactions with protein groups: A volumetric study, Biopolymers, 93 (2010) 866-879.

[117] A.C. Miklos, C. Li, N.G. Sharaf, G.J. Pielak, Volume Exclusion and Soft Interaction Effects on Protein Stability under Crowded Conditions, Biochemistry, 49 (2010) 6984-6991.

[118] J. Heyda, M. Kozisek, L. Bednarova, G. Thompson, J. Konvalinka, J. Vondrasek, P. Jungwirth, Urea and Guanidinium Induced Denaturation of a Trp-Cage Miniprotein, The Journal of Physical Chemistry B, 115 (2011) 8910-8924.

[119] E.J. Guinn, L.M. Pegram, M.W. Capp, M.N. Pollock, M.T. Record, Quantifying why urea is a protein denaturant, whereas glycine betaine is a protein stabilizer, Proceedings of the National Academy of Sciences, 108 (2011) 16932-16937.

[120] W. Li, R. Zhou, Y. Mu, Salting Effects on Protein Components in Aqueous NaCl and Urea Solutions: Toward Understanding of Urea-Induced Protein Denaturation, The Journal of Physical Chemistry B, 116 (2012) 1446-1451.

[121] A. Das, C. Mukhopadhyay, Urea-Mediated Protein Denaturation: A Consensus View, The Journal of Physical Chemistry B, 113 (2009) 12816-12824.

[122] Y. Zhang, P.S. Cremer, Chemistry of Hofmeister Anions and Osmolytes, Annual Review of Physical Chemistry, 61 (2010) 63-83.

[123] X. Chen, L.B. Sagle, P.S. Cremer, Urea Orientation at Protein Surfaces, Journal of the American Chemical Society, 129 (2007) 15104-15105.

[124] F. Vanzi, B. Madan, K. Sharp, Effect of the Protein Denaturants Urea and Guanidinium on Water Structure: A Structural and Thermodynamic Study, Journal of the American Chemical Society, 120 (1998) 10748-10753.

[125] O.D. Bonner, J.M. Bednarek, R.K. Arisman, Heat capacities of ureas and water in water and dimethylformamide, Journal of the American Chemical Society, 99 (1977) 2898-2902.

[126] H. Schönert, L. Stroth, Thermodynamic interaction between urea and the peptide group in aqueous solutions at 25°C, Biopolymers, 20 (1981) 817-831.

[127] M.M. Thayer, R.C. Haltiwanger, V.S. Allured, S.C. Gill, S.J. Gill, Peptide-urea interactions as observed in diketopiperazine-urea cocrystal, Biophysical Chemistry, 46 (1993) 165-169.

[128] J.D. Batchelor, A. Olteanu, A. Tripathy, G.J. Pielak, Impact of Protein Denaturants and Stabilizers on Water Structure, Journal of the American Chemical Society, 126 (2004) 1958-1961.

[129] D. Horinek, R.R. Netz, Can Simulations Quantitatively Predict Peptide Transfer Free Energies to Urea Solutions? Thermodynamic Concepts and Force Field Limitations, The Journal of Physical Chemistry A, 115 (2011) 6125-6136.

[130] Y.L.A. Rezus, H.J. Bakker, Effect of urea on the structural dynamics of water, Proceedings of the National Academy of Sciences, 103 (2006) 18417-18420.

[131] K.A. Sharp, B. Madan, E. Manas, J.M. Vanderkooi, Water structure changes induced by hydrophobic and polar solutes revealed by simulations and infrared spectroscopy, The Journal of Chemical Physics, 114 (2001) 1791-1796.

[132] C. Oostenbrink, W.F. van Gunsteren, Methane clustering in explicit water: effect of urea on hydrophobic interactions, Physical Chemistry Chemical Physics, 7 (2005) 53-58.

[133] L.J. Smith, R.M. Jones, W.F. van Gunsteren, Characterization of the denaturation of human α-lactalbumin in urea by molecular dynamics simulations, Proteins: Structure, Function, and Bioinformatics, 58 (2005) 439-449.

[134] A. Wallqvist, D.G. Covell, D. Thirumalai, Hydrophobic Interactions in Aqueous Urea Solutions with Implications for the Mechanism of Protein Denaturation, Journal of the American Chemical Society, 120 (1998) 427-428.

[135] R. Zangi, R. Zhou, B.J. Berne, Urea's Action on Hydrophobic Interactions, Journal of the American Chemical Society, 131 (2009) 1535-1541.

[136] G. Graziano, On the Solubility of Aliphatic Hydrocarbons in 7 M Aqueous Urea, The Journal of Physical Chemistry B, 105 (2001) 2632-2637.

[137] K.C. Aune, C. Tanford, Thermodynamics of the denaturation of lysozyme by guanidine hydrochloride. II. Dependence on denaturant concentration at 25°C, Biochemistry, 8 (1969) 4586-4590.

[138] A. Caballero-Herrera, K. Nordstrand, K.D. Berndt, L. Nilsson, Effect of Urea on Peptide Conformation in Water: Molecular Dynamics and Experimental Characterization, Biophysical Journal, 89 (2005) 842-857.

[139] C. Camilloni, A. Guerini Rocco, I. Eberini, E. Gianazza, R.A. Broglia, G. Tiana, Urea and Guanidinium Chloride Denature Protein L in Different Ways in Molecular Dynamics Simulations, Biophysical Journal, 94 (2008) 4654-4661.

[140] J.L. England, V.S. Pande, G. Haran, Chemical Denaturants Inhibit the Onset of Dewetting, Journal of the American Chemical Society, 130 (2008) 11854-11855.

[141] A. Huerta-Viga, S. Woutersen, Protein Denaturation with Guanidinium: A 2D-IR Study, The Journal of Physical Chemistry Letters, 4 (2013) 3397-3401.

[142] T. Koishi, K. Yasuoka, S.Y. Willow, S. Fujikawa, X.C. Zeng, Molecular Insight into Different Denaturing Efficiency of Urea, Guanidinium, and Methanol: A Comparative Simulation Study, Journal of Chemical Theory and Computation, 9 (2013) 2540-2551.

[143] F. Mehrnejad, M. Khadem-Maaref, M. Ghahremanpour, F. Doustdar, Mechanisms of amphipathic helical peptide denaturation by guanidinium chloride and urea: a molecular dynamics simulation study, Journal of Computer-Aided Molecular Design, 24 (2010) 829-841.

[144] J.K. Myers, C. Nick Pace, J. Martin Scholtz, Denaturant m values and heat capacity changes: Relation to changes in accessible surface areas of protein unfolding, Protein Science, 4 (1995) 2138-2148.

[145] D. Trzesniak, N.F.A. van der Vegt, W.F. van Gunsteren, Computer simulation studies on the solvation of aliphatic hydrocarbons in 6.9 M aqueous urea solution, Physical Chemistry Chemical Physics, 6 (2004) 697-702.

[146] D.B. Watlaufer, S.K. Malik, L. Stoller, R.L. Coffin, Nonpolar Group Participation in the Denaturation of Proteins by Urea and Guanidinium Salts. Model Compound Studies, Journal of the American Chemical Society, 86 (1964) 508-514.

[147] Z. Xia, P. Das, E.I. Shakhnovich, R. Zhou, Collapse of Unfolded Proteins in a Mixture of Denaturants, Journal of the American Chemical Society, 134 (2012) 18266-18274.

[148] R.D. Macdonald, M. Khajehpour, Effects of the osmolyte TMAO (Trimethylamine-N-oxide) on aqueous hydrophobic contact-pair interactions, Biophysical Chemistry, 184 (2013) 101-107.

[149] R. Godawat, S.N. Jamadagni, S. Garde, Unfolding of Hydrophobic Polymers in Guanidinium Chloride Solutions, The Journal of Physical Chemistry B, 114 (2010) 2246-2254.

[150] P.E. Mason, J.W. Brady, G.W. Neilson, C.E. Dempsey, The Interaction of Guanidinium Ions with a Model Peptide, Biophysical Journal, 93 (2007) L04-L06.

[151] E.P. O'Brien, R.I. Dima, B. Brooks, D. Thirumalai, Interactions between Hydrophobic and Ionic Solutes in Aqueous Guanidinium Chloride and Urea Solutions: Lessons for Protein Denaturation Mechanism, Journal of the American Chemical Society, 129 (2007) 7346-7353.

[152] W. Li, Y. Mu, Dissociation of hydrophobic and charged nano particles in aqueous guanidinium chloride and urea solutions: A molecular dynamics study, Nanoscale, 4 (2012) 1154-1159.

[153] W.K. Lim, J. Rosgen, S.W. Englander, Urea, but Not Guanidinium, Destabilizes Proteins by Forming Hydrogen Bonds to the Peptide Group, Proceedings of the National Academy of Sciences of the United States of America, 106 (2009) 2595-2600.

[154] P.E. Mason, G.W. Neilson, C.E. Dempsey, A.C. Barnes, J.M. Cruickshank, The Hydration Structure of Guanidinium and Thiocyanate Ions: Implications for Protein Stability in Aqueous Solution, Proceedings of the National Academy of Sciences of the United States of America, 100 (2003) 4557-4561.

[155] G.I. Makhatadze, P.L. Privalov, Protein interactions with urea and guanidinium chloride: A calorimetric study, Journal of Molecular Biology, 226 (1992) 491-505.

[156] D.R. Robinson, W.P. Jencks, The Effect of Compounds of the Urea-Guanidinium Class on the Activity Coefficient of Acetyltetraglycine Ethyl Ester and Related Compounds, Journal of the American Chemical Society, 87 (1965) 2462-2470.

[157] J.R. Lakowicz, Principles of fluorescence spectroscopy, 3rd Edition, Analytical and Bioanalytical Chemistry, 390 (2008) 1223-1224.

[158] C. Ratzer, J. Kupper, D. Spangenberg, M. Schmitt, The structure of phenol in the S1-state determined by high resolution UV-spectroscopy, Chemical Physics, 283 (2002) 153-169.

[159] A. White, Effect of pH on fluorescence of tryosine, tryptophan and related compounds, Biochemical Journal, 71 (1959) 217-220.

Chapter 2

Experimental

2.1 Materials for GdmCl Quenching Assays

Sodium formate, sodium propionate, and taurine were purchased from Sigma-Aldrich (St. Louis, MO). Sodium Acetate, hydrochloric acid solution, and sodium hydroxide were purchased from Fisher Scientific (Hampton, NH). Sodium heptanoate and sodium octanoate were purchased from TCI America (Portland, OR). The phenol was purchased from J.T Baker Chemical Co. (Phillipsburg, NJ) and guanidinium chloride was purchased from Chem-Impex International Inc. (Wood Dale, IL).

2.2 Methods for GdmCl Quenching Assays

Phenol fluorescence was measured in the presence of five quencher (carboxylate ion) concentrations, at each of five different GdmCl concentrations (1.50, 1.88, 2.25, 2.63, and 3.00 M). The addition of quencher would therefore contribute less than 20 percent to the ionic strength. All samples had 10 mM taurine buffer and 200 μM phenol present. All samples were adjusted to pH 8.5 (carboxylate ions essentially deprotanated) with concentrated HCl/NaOH. All samples were prepared in triplicate. Steady-state fluorescence spectra were collected using a Fluorolog-3 Horiba Jobin Yvon spectrofluorometer (Edison, NJ). Fluorescence spectra were collected using an excitation wavelength set to 270 nm; excitation and emission slits were set to 5 nm band pass resolution. All samples were measured at room temperature (20°C) and held in a 10 x 3 mm^2 quartz cuvette. The molar extinction coefficient of phenol in water is 1373 $M^{-1}cm^{-1}$ [1], therefore, no appreciable inner-filter effect corrections need to be applied to the measured phenol fluorescence values. The quenching assays were monitored by changes in fluorescence intensity at the emission maximum of 297 nm as a function of quencher concentration. All data were analyzed by the use of Sigma Plot 12 software (Point Richmond, CA).

2.3 Materials for TMAO Quenching Assays

TMAO, sodium formate, sodium acetate, sodium propionate and sodium hexanoate were purchased from Sigma (St-Louis, MO). The phenol was purchased from J.T.Baker Chemical Co. (Phillipsburg, NJ). Hydrochloric acid solution, sodium hydroxide, and sodium chloride were purchased from Fisher Scientific (Hampton, NH).

2.4 Methods for TMAO Quenching Assays

Phenol fluorescence was measured in the presence of five quencher (carboxylate ion) concentrations, at each of six different TMAO concentrations (0.00, 0.15, 0.30, 0.45, 0.60 and 0.75 M). All samples contained 200 μM phenol. All samples were adjusted to pH 8.5 (carboxylate ions essentially deprotanated) with concentrated HCl/NaOH. As well, all samples were adjusted to an ionic strength of 0.3 M, using NaCl. All samples were prepared in triplicate. Steady-state fluorescence spectra were measured on a Fluorolog-3 Horiba Jobin Yvon spectrofluorometer (Edison, NJ). All samples were measured at room temperature (20°C) and were held in a 10 × 3 mm^2 quartz cuvette. Fluorescence spectra were collected using an excitation wavelength set to 270 nm; excitation and emission slits were set to 5 nm band pass resolution. Quenching studies were performed by monitoring changes in the fluorescence intensity at the maximum emission of 297 nm as a function of quencher concentration. All statistical data analyses including linear and nonlinear regressions were performed using Sigma Plot 10 software (Point Richmond, CA).

References

[1] C.H. Chan, J.C. Escalante-Semerena, ArsAB, a novel enzyme from Sporomusa ovata activates phenolic bases for adenosylcobamide biosynthesis, Molecular Microbiology, 81 (2011) 952-967.

Chapter 3

Results

3.1 Data Analysis Overview

Similar experiments were performed using both TMAO and GdmCl. Although the methodologies are similar, the results lead to much different discussions and interpretations. Therefore, the experiments will be discussed separate from one another. That said, the data analysis of each experiment was similar and follow these steps: 1) Collection of fluorescence quenching data by various carboxylate ions, 2) the generation of Stern-Volmer plots for each TMAO/GdmCl concentration studied, as well for each carboxylate used, 3) the Stern-Volmer quenching constants are adjusted for varying fluorescent lifetimes, 4) the adjusted Stern-Volmer quenching constants are plotted as a function of TMAO/GdmCl concentration and are fitted to a linear correlation line (done for every carboxylate used), 5) the equation of the linear correlation line was used to generate K_{SV} for all TMAO/GdmCl concentrations, ranging from minimum TMAO/GdmCl concentrations used to maximum, 6) the generated K_{SV} for a given carboxylate are divided by the K_{SV} for formate and are normalized, and 7) finally interaction free energy is calculated using the values generated in step 6 and are plotted as a function of TMAO/GdmCl concentration. These steps and more will be discussed in much more depth in the upcoming sections of this chapter.

3.2 Guanidinium Chloride

Phenol fluorescence quenching assays were performed to study the effect of GdmCl on the phenol-carboxylate ion hydrophobic contact pair model system. The model system is a simple one in nature, representing the interaction between just two molecules, which allows for the ease of studying the additional effects of guanidinium chloride as it is introduced to the system. We are specifically interested in the effect GdmCl has on hydrophobic interactions

between that of the phenol ring and the aliphatic tail of carboxylate ions. Phenol fluorescence has been shown to be quenched, by carboxylate ions, through a dynamic and collisional quenching mechanism [1-4]. These previous findings mean that the quenching of phenol fluorescence by carboxylate ions follows linear Stern-Volmer behavior, represented by the equation [5]:

$$\frac{F_0}{F} = 1 + K_{SV}[Q] = 1 + k_q\tau[Q] \quad (3.2\text{-}1)$$

Here, F_0 is the fluorescence of phenol in the absence of quencher, F is the fluorescence of phenol in the presence of Q molar of quencher; the parameter K_{SV} is the Stern-Volmer constant, which is composed of two components: k_q the quenching rate constant and τ the fluorescence lifetime of phenol in the absence of a quencher. Linear Stern-Volmer behavior implies that the plot of $\frac{F_0}{F}$ vs [Q], also known as a Stern-Volmer plot, will be linearly correlated having a y-intercept of one and a slope of K_{SV}.

These experiments study the interactions between phenol with a range of straight chain carboxylate ions in the presence of varying concentrations of GdmCl. Figure 3-1 displays the effect of the acetate ion of phenol fluorescence spectra in the absence of GdmCl. The specific carboxylate ions used to quench phenol fluorescence were formate, acetate, propionate, butyrate, heptanoate, and octanoate. In all of the experiments performed we found that all of the carboxylate ions used did in fact quench phenol fluorescence by linear Stern-Volmer behavior, even in the presence of GdmCl; these results are demonstrated in the following figures: Figure 3-2 - Figure 3-7. Although GdmCl has no effect on the linearity of Stern-Volmer plots, it does have a pronounced effect on the K_{SV} (the slope), which shows a decline as GdmCl concentration is increased (pictured in Figure 3-8). As viewed in Figure 3-8, the correlation of K_{SV} with respect to GdmCl concentrations appears to be roughly linear, but one can observe that the data also has

some minor deviations from linearity. This may be attributed to GdmCl affecting the lifetime of phenol fluorescence.

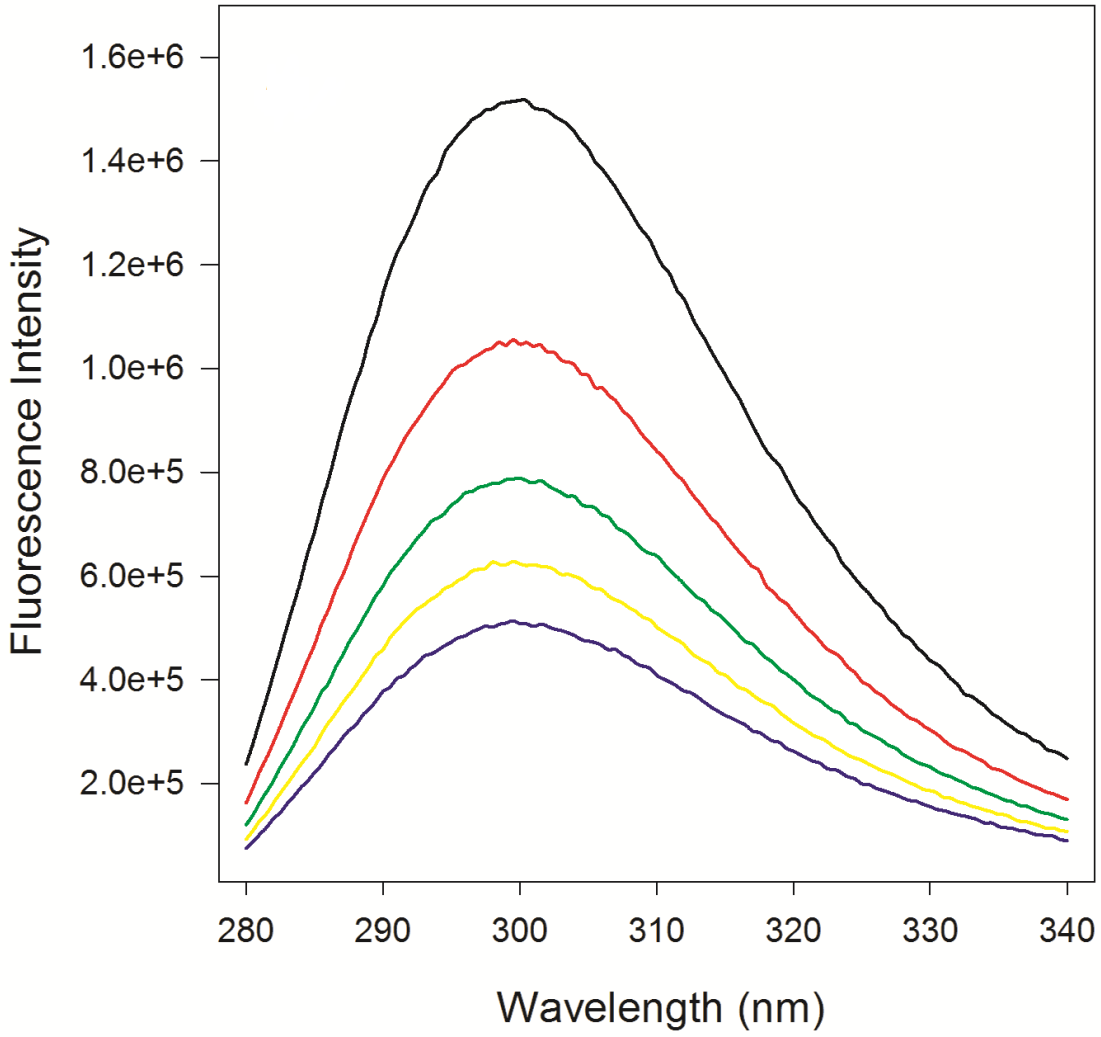

Figure 3-1. Fluorescence spectra of 200 µM phenol in presence of increasing amounts of acetate ion. Acetate ion concentration was steadily increased from 0 M (black line) to a final concentration of 0.3 M (purple line).

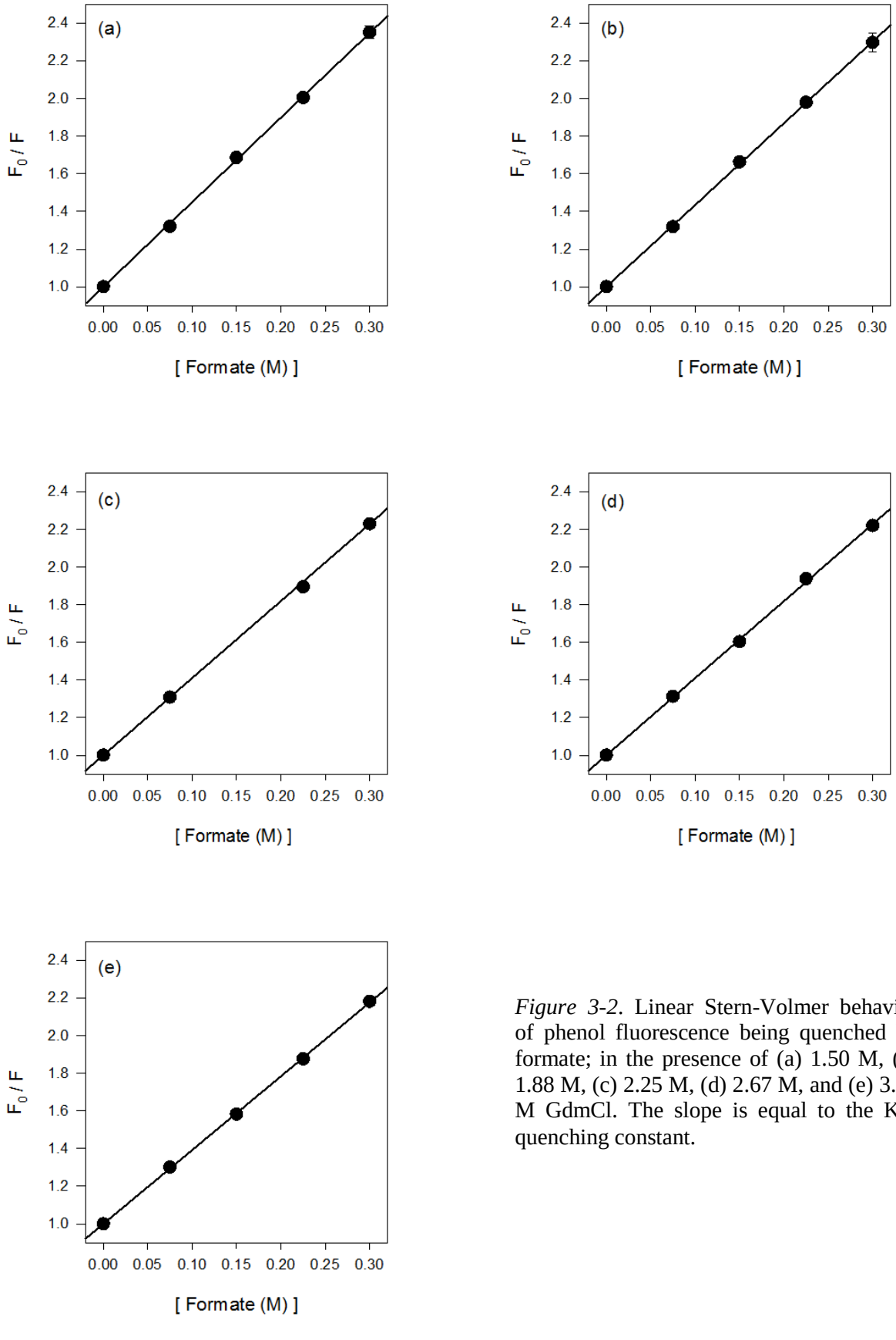

Figure 3-2. Linear Stern-Volmer behavior of phenol fluorescence being quenched by formate; in the presence of (a) 1.50 M, (b) 1.88 M, (c) 2.25 M, (d) 2.67 M, and (e) 3.00 M GdmCl. The slope is equal to the K_{SV} quenching constant.

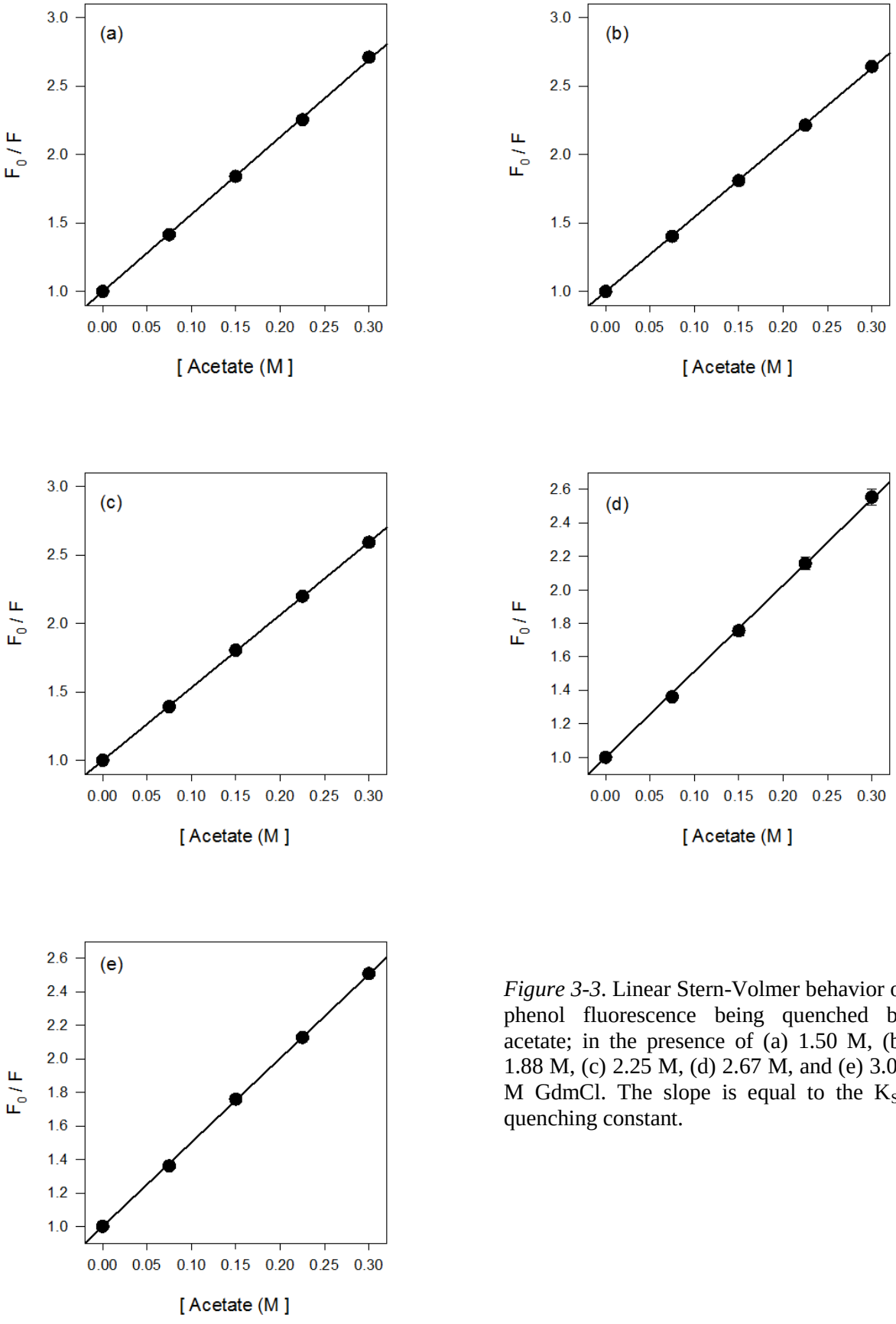

Figure 3-3. Linear Stern-Volmer behavior of phenol fluorescence being quenched by acetate; in the presence of (a) 1.50 M, (b) 1.88 M, (c) 2.25 M, (d) 2.67 M, and (e) 3.00 M GdmCl. The slope is equal to the K_{SV} quenching constant.

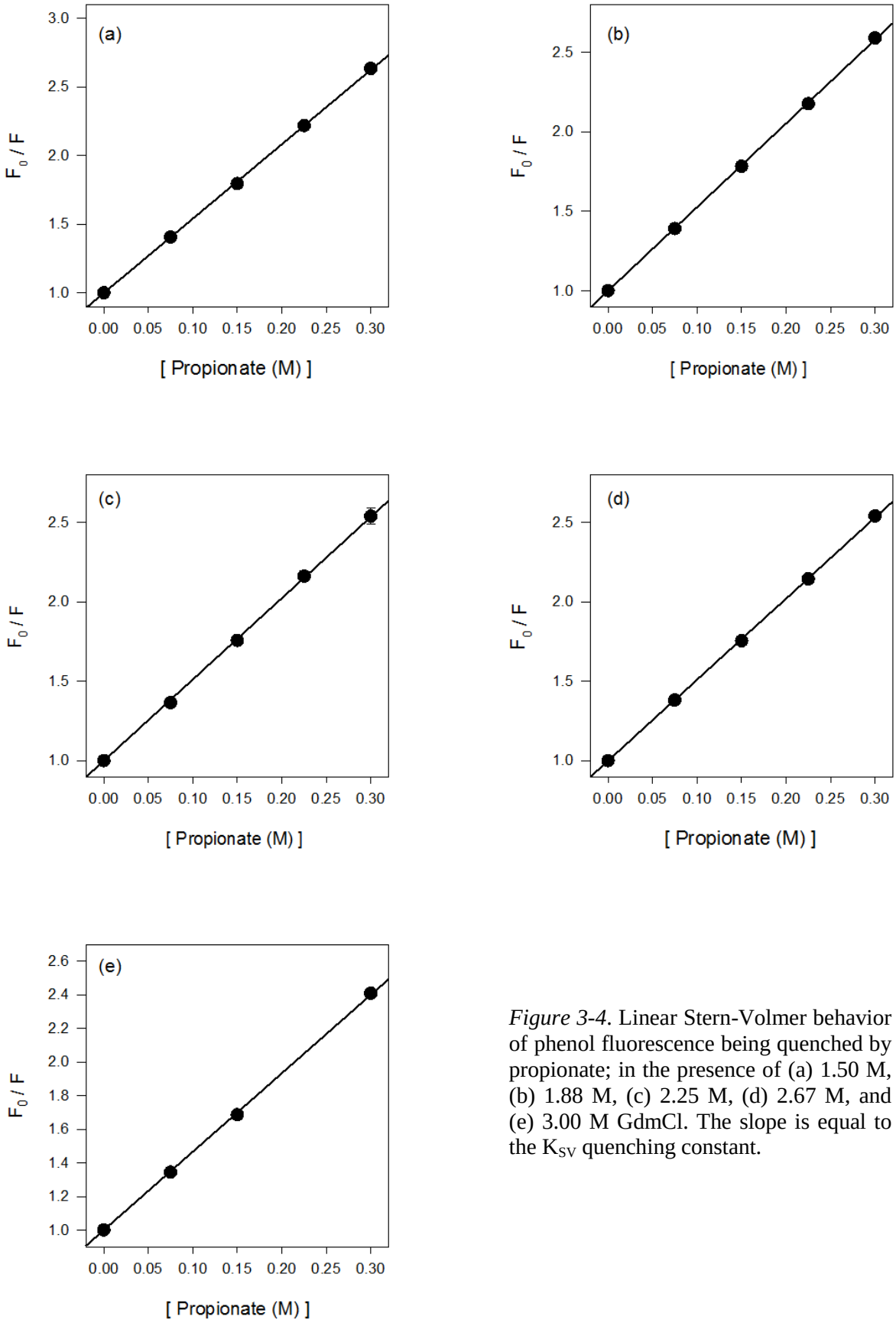

Figure 3-4. Linear Stern-Volmer behavior of phenol fluorescence being quenched by propionate; in the presence of (a) 1.50 M, (b) 1.88 M, (c) 2.25 M, (d) 2.67 M, and (e) 3.00 M GdmCl. The slope is equal to the K_{SV} quenching constant.

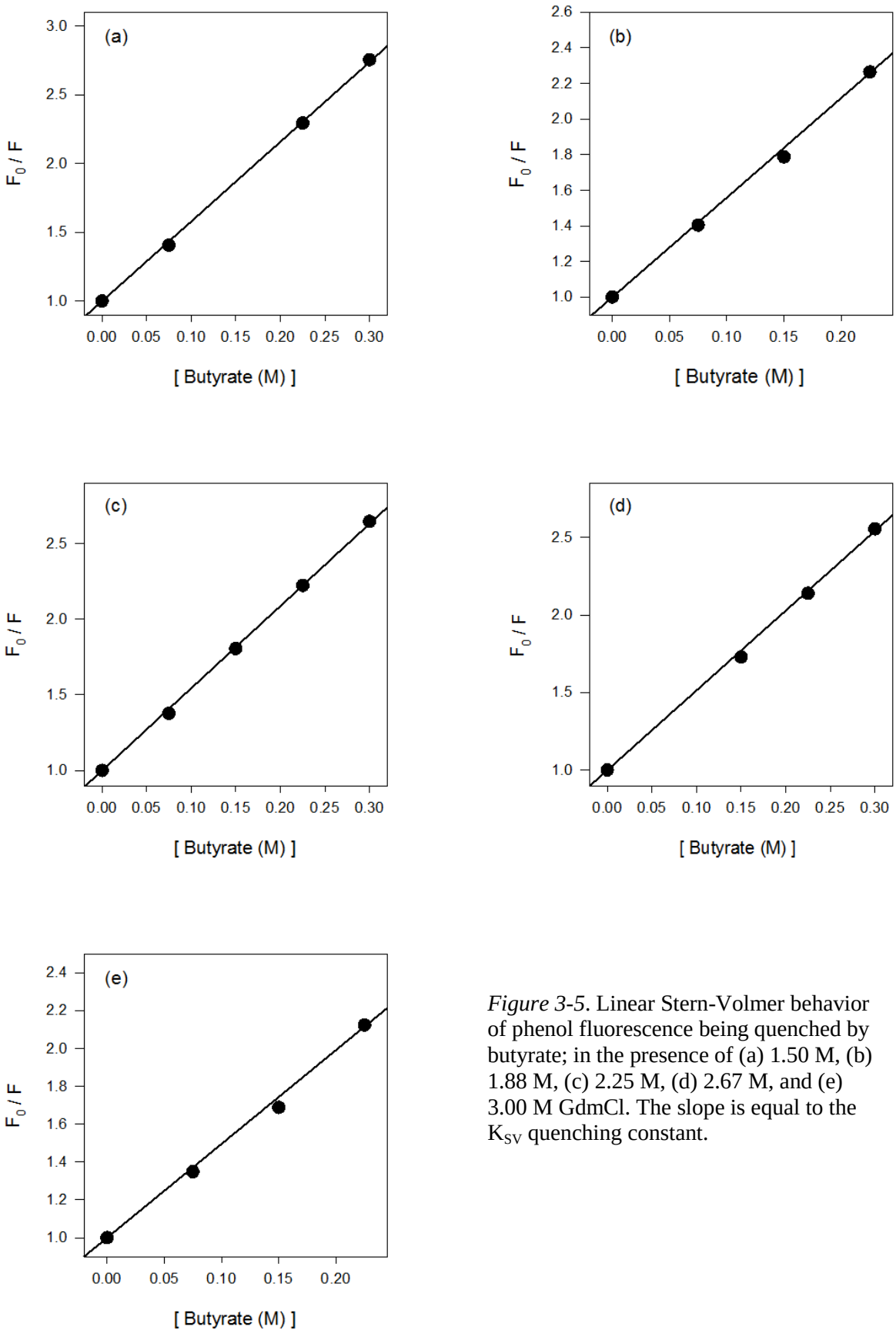

Figure 3-5. Linear Stern-Volmer behavior of phenol fluorescence being quenched by butyrate; in the presence of (a) 1.50 M, (b) 1.88 M, (c) 2.25 M, (d) 2.67 M, and (e) 3.00 M GdmCl. The slope is equal to the K_{SV} quenching constant.

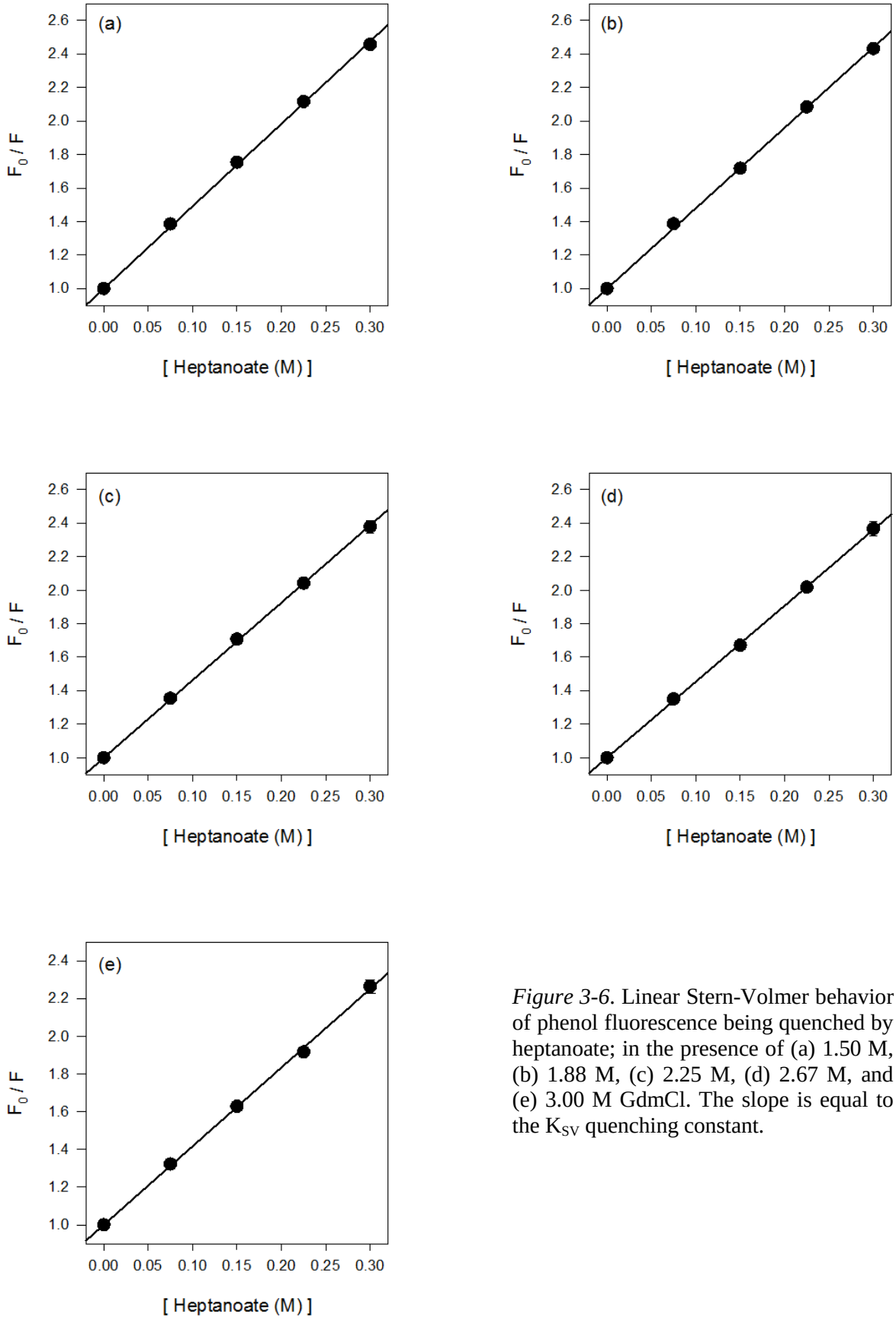

Figure 3-6. Linear Stern-Volmer behavior of phenol fluorescence being quenched by heptanoate; in the presence of (a) 1.50 M, (b) 1.88 M, (c) 2.25 M, (d) 2.67 M, and (e) 3.00 M GdmCl. The slope is equal to the K_{SV} quenching constant.

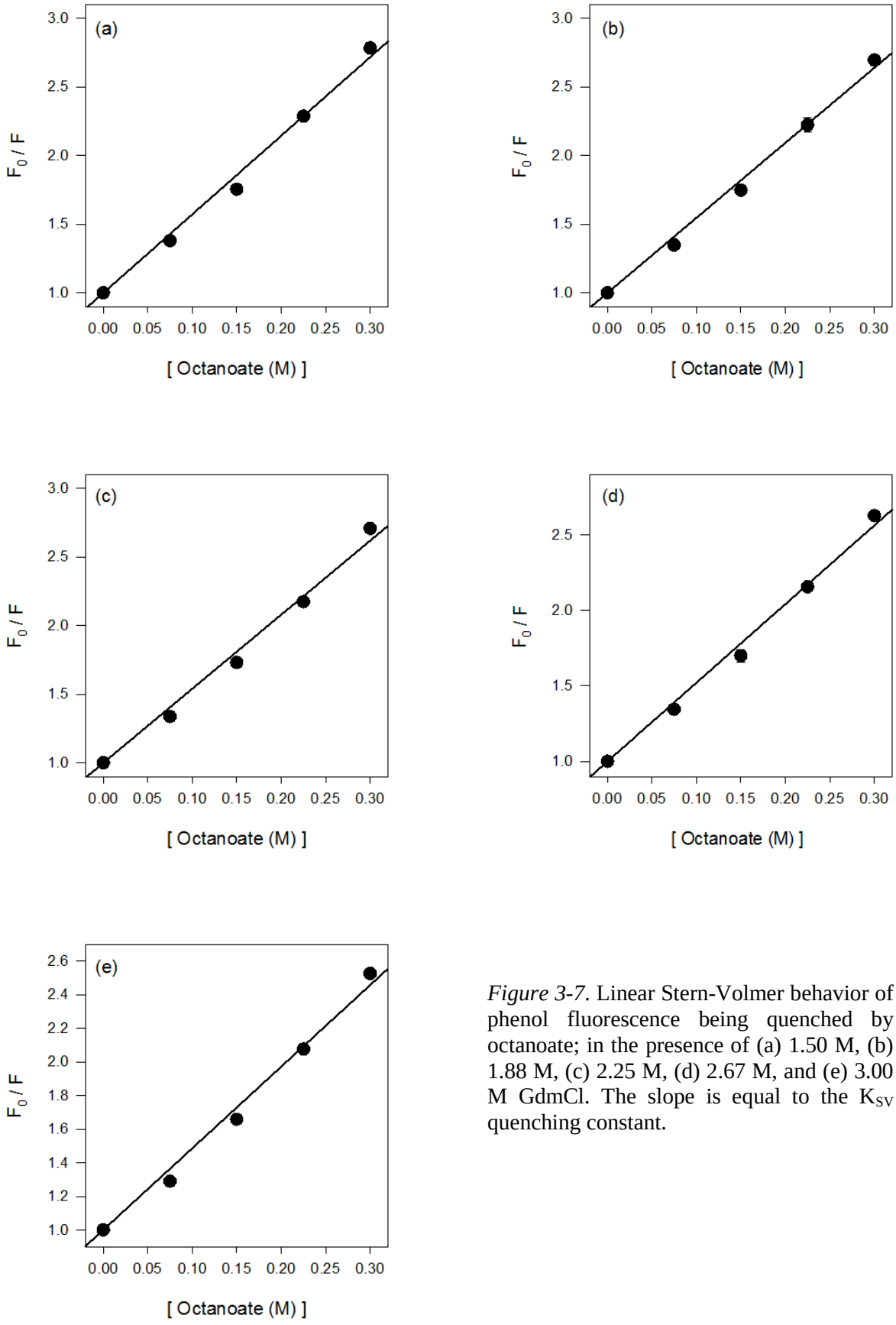

Figure 3-7. Linear Stern-Volmer behavior of phenol fluorescence being quenched by octanoate; in the presence of (a) 1.50 M, (b) 1.88 M, (c) 2.25 M, (d) 2.67 M, and (e) 3.00 M GdmCl. The slope is equal to the K_{SV} quenching constant.

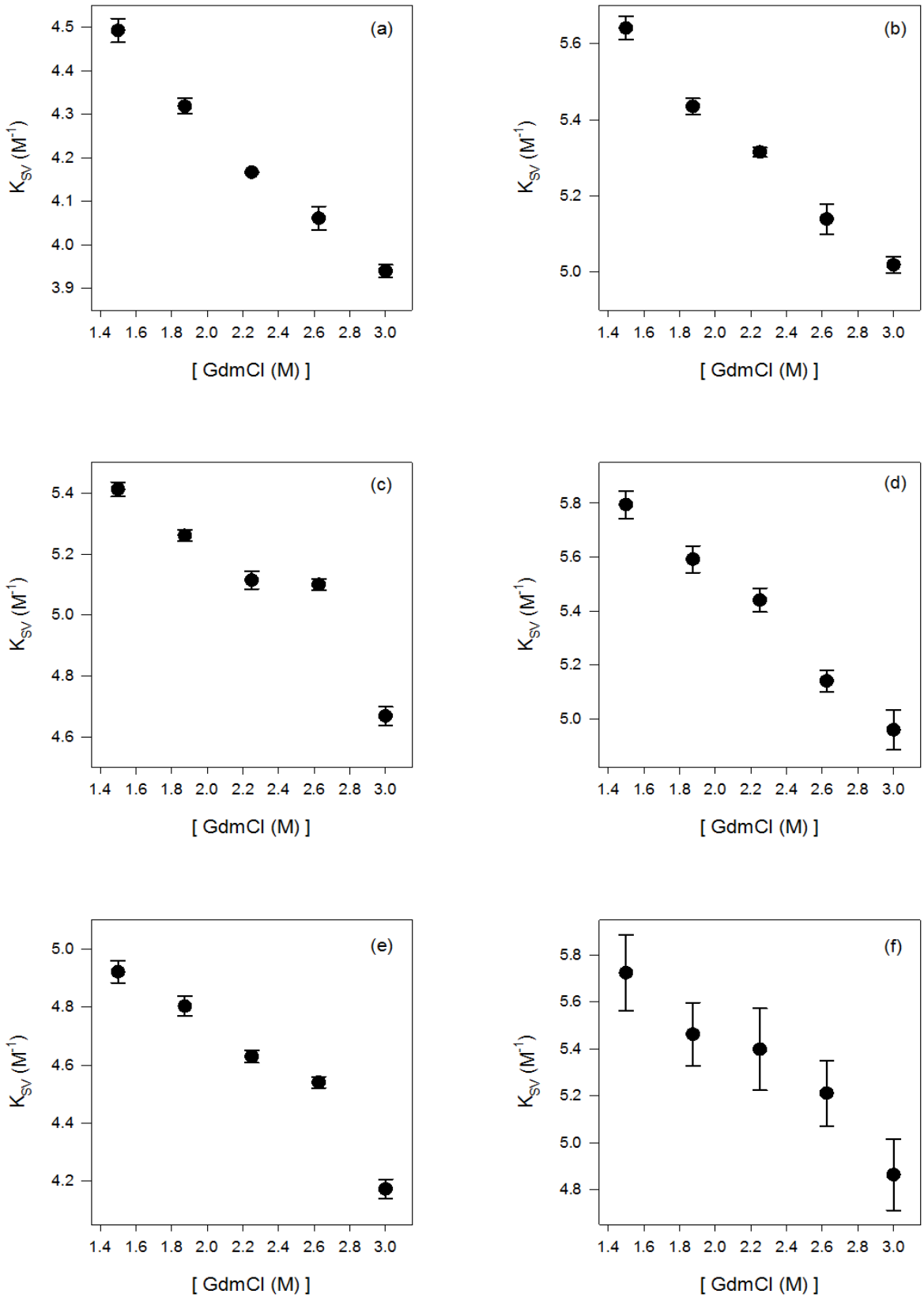

Figure 3-8. The effects of GdmCl on the measured Stern-Volmer constant K_{SV} of phenol fluorescence, quenched by: (a) formate, (b) acetate, (c) propionate, (d) butyrate, (e) heptanoate, (f) octanoate.

Therefore, we specifically looked at the effect of GdmCl on phenol fluorescence in the absence of carboxylate ions and found that GdmCl has a very small (~5%) enhancing effect on phenol fluorescence (Figure 3-9).

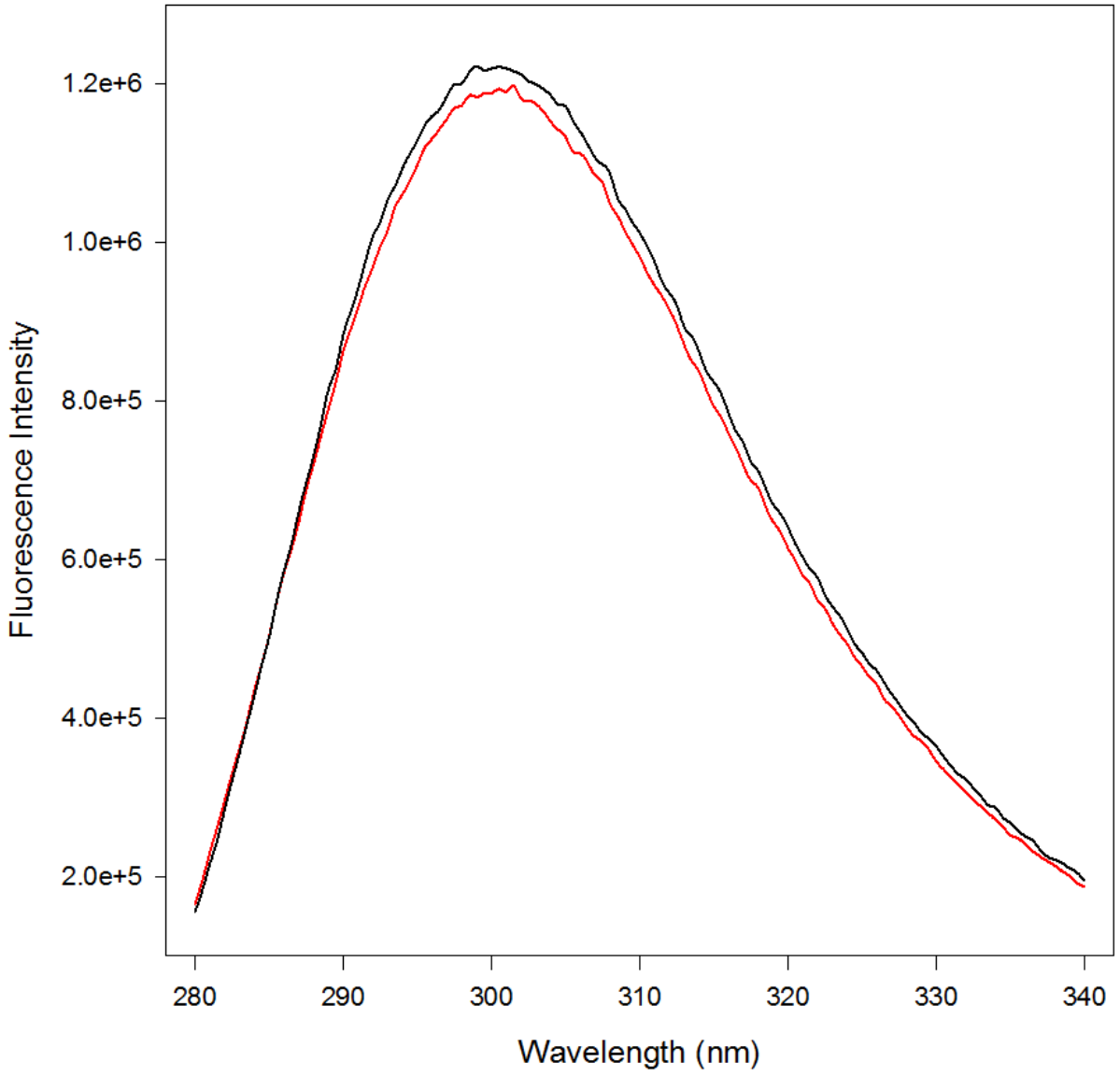

Figure 3-9. Fluorescence spectra of 200 µM Phenol in the presence of 1.5 M GdmCl (red line) and 3.0 M GdmCl (black line). Spectra taken in the absence of any carboxylate ion

Thus, we have applied a correction to the measured K_{SV} values, by a factor of $\frac{I_0}{I(C)}$, to account for the small fluctuations in the data [2]. The equation used for this correction is the following:

$$K'_{SV}(C) = K_{SV} \times \frac{I_0}{I(C)} \quad (3.2\text{-}2)$$

In this equation, $K'_{SV}(C)$ is the "corrected" Stern-Volmer constant, K_{SV} is the measured Stern-Volmer constant, I_0 is the fluorescence intensity of phenol at 1.5 M GdmCl, and I(C) is the fluorescence intensity of the same amount of phenol measured at a given guanidinium concentration of C when there is no quencher present. The visualization of the correction, by Eq.(3.2-2), can be viewed in Figure 3-10, where the "corrected" Stern-Volmer constants plotted against GdmCl concentration show a greater trend to be more linearized, due to the fact the data is less scattered. Thus, the more linearized plots supports our notion that the scattering of the data is most likely a result of GdmCl causing variations in phenol fluorescence lifetimes. Measured K_{SV} and "corrected" $K'_{SV}(C)$, along with their coefficients of determination were compiled for every carboxylate ion used and are shown in Table 3-1.

From Figure 3-10, it can be noted that the $K'_{SV}(C)$ are linearly correlated with GdmCl concentration, where there is a decrease in $K'_{SV}(C)$ as GdmCl concentration increases. The plots were fitted to the following equation:

$$K'_{SV}(C) = y_0 + a \times [GdmCl] \quad (3.2\text{-}3)$$

where, $K'_{SV}(C)$ is the "corrected" Stern-Volmer constant, while y_0 and a are the linear fitting parameters. The linear fitting parameters and the coefficients of determination of these plots are tabulated and found in Table 3-2. Equation (3.2-3) was further used to determine the $K'_{SV}(C)$ at more GdmCl concentrations, than those measured experimentally. The $K'_{SV}(C)$ were calculated over a range of 1.5 M to 3.0 M GdmCl, using 0.05 M increments. The appearance of the relative large uncertainties in octanoate data (~3% relative error) in Figure 3-10 can be attributed to the

surfactant-like qualities of octanoate, which creates more viscous solutions. These properties of octanoate decrease pipetting accuracy.

Table 3-1. Compiled measured (K_{SV}) and corrected ($K'_{SV}(C)$) Stern-Volmer constant values of various carboxylate ions, obtained from the quenching of phenol fluorescence. These values are plotted in both Figure 3-8 and Figure 3-10 as a function of GdmCl concentration.

Quencher	[GdmCl] (M)	Measured K_{SV} (M^{-1})	Corrected $K'_{SV}(C)$ (M^{-1})
Formate	1.500	4.49±0.03	4.49±0.03
	1.875	4.34±0.02	4.32±0.02
	2.250	4.10±0.00	4.17±0.00
	2.625	4.09±0.03	4.06±0.03
	3.000	3.92±0.01	3.94±0.01
Acetate	1.500	5.64±0.03	5.64±0.03
	1.875	5.43±0.02	5.39±0.02
	2.250	5.32±0.01	5.33±0.01
	2.625	5.14±0.04	5.09±0.04
	3.000	5.02±0.02	4.96±0.02
Propionate	1.500	5.41±0.02	5.41±0.02
	1.875	5.26±0.02	5.23±0.02
	2.250	5.11±0.03	5.11±0.03
	2.625	5.10±0.02	4.99±0.02
	3.000	4.67±0.03	4.70±0.03
Butyrate	1.500	5.79±0.05	5.79±0.05
	1.875	5.59±0.05	5.47±0.05
	2.250	5.44±0.04	5.41±0.04
	2.625	5.14±0.04	5.14±0.04
	3.000	4.96±0.07	4.98±0.07
Heptanoate	1.500	4.92±0.04	4.92±0.04
	1.875	4.80±0.03	4.70±0.03
	2.250	4.63±0.02	4.52±0.02
	2.625	4.54±0.02	4.45±0.02
	3.000	4.17±0.03	4.13±0.03
Octanoate	1.500	5.72±0.16	5.72±0.16
	1.875	5.46±0.13	5.43±0.13
	2.250	5.40±0.17	5.25±0.17
	2.625	5.21±0.14	5.01±0.13
	3.000	4.86±0.15	4.73±0.15

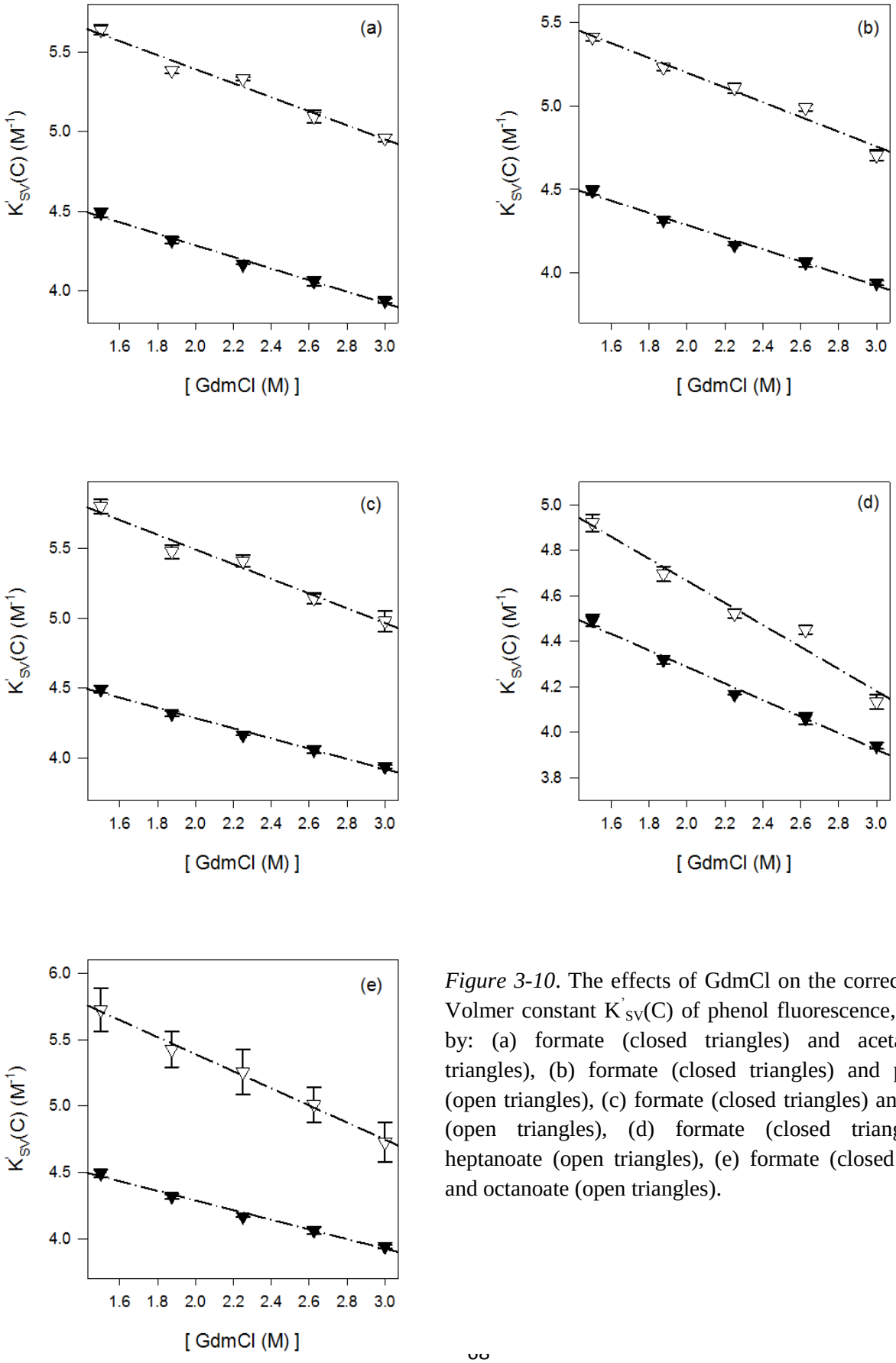

Figure 3-10. The effects of GdmCl on the corrected Stern-Volmer constant $K'_{SV}(C)$ of phenol fluorescence, quenched by: (a) formate (closed triangles) and acetate (open triangles), (b) formate (closed triangles) and propionate (open triangles), (c) formate (closed triangles) and butyrate (open triangles), (d) formate (closed triangles) and heptanoate (open triangles), (e) formate (closed triangles) and octanoate (open triangles).

Table 3-2. Linear regression fitting parameters obtained from correlating the data in Figure 3-10 to Eq. (3.2-3).

Quencher	α (M^{-2})	y0 (M^{-1})	r^2
Formate	-0.36±0.02	5.01±0.05	0.99
Acetate	-0.44±0.04	6.27±0.10	0.97
Propionate	-0.44±0.04	6.08±0.10	0.97
Butyrate	-0.52±0.05	6.54±0.12	0.97
Heptanoate	-0.49±0.05	5.64±0.12	0.97
Octanoate	-0.64±0.03	6.68±0.07	0.99

3.3 Trimethylamine-N-Oxide

As previously mentioned, the data analysis and our developed methodology for our TMAO experiments are very similar to the experiments involving GdmCl. Consequently, this section will be less in depth in the derivation of the methodology.

Phenol fluorescence quenching assays were performed in the absence of TMAO and as well in the presence of five different concentrations of TMAO. Phenol fluorescence is quenched by both carboxylate ions and TMAO by a collisional mechanism that follows Stern-Volmer behavior:

$$\frac{F_0}{F} = 1 + K_{SV}[Q] = 1 + k_q\tau[Q] \tag{3.3-1}$$

The carboxylate ions that were specifically used in these experiments were: formate, acetate, propionate, and hexanoate. Each carboxylate quenched phenol fluorescence following linear Stern-Volmer behavior, both in the absence and in the presence of TMAO, which can be seen in Figure 3-11 - Figure 3-14. Unlike GdmCl, TMAO itself is a strong quencher of phenol fluorescence and it also follows linear Stern-Volmer behaviour, as seen in Figure 3-16. The minimal curvature observed in all the Stern-Volmer plots indicates that there is an absence of any additional ground state fluorophore association that can contribute to the quenching process. The lack of pre-association makes the presence of both carboxylate and TMAO in the near proximity of the excited phenol statistically unlikely, making the contribution of a presumed additional simultaneous quenching mechanism inconceivable. The quenching of phenol fluorescence in a solution containing carboxylate and TMAO molecules can therefore be assumed to be the result of two uncoupled kinetic pathways.

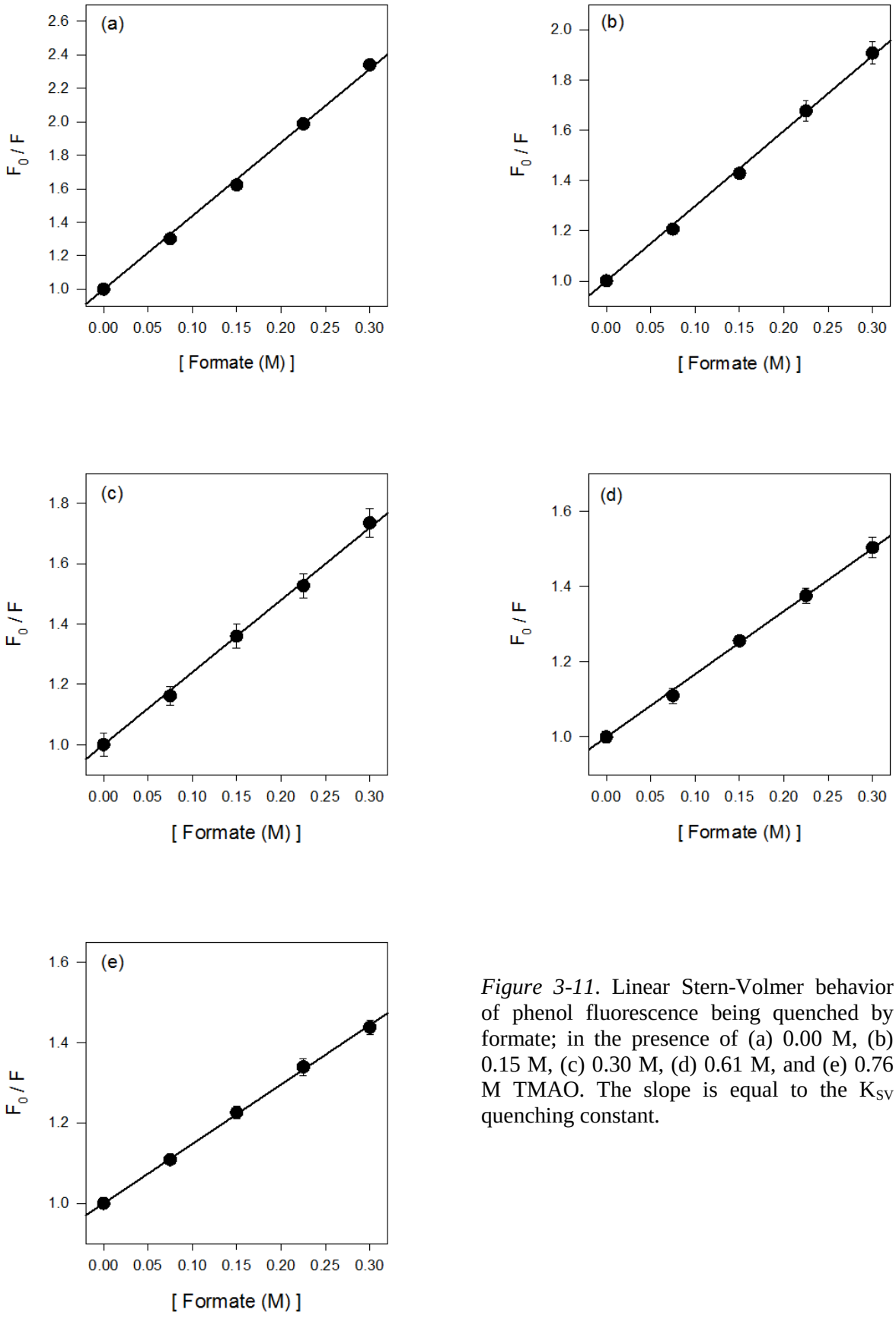

Figure 3-11. Linear Stern-Volmer behavior of phenol fluorescence being quenched by formate; in the presence of (a) 0.00 M, (b) 0.15 M, (c) 0.30 M, (d) 0.61 M, and (e) 0.76 M TMAO. The slope is equal to the K_{SV} quenching constant.

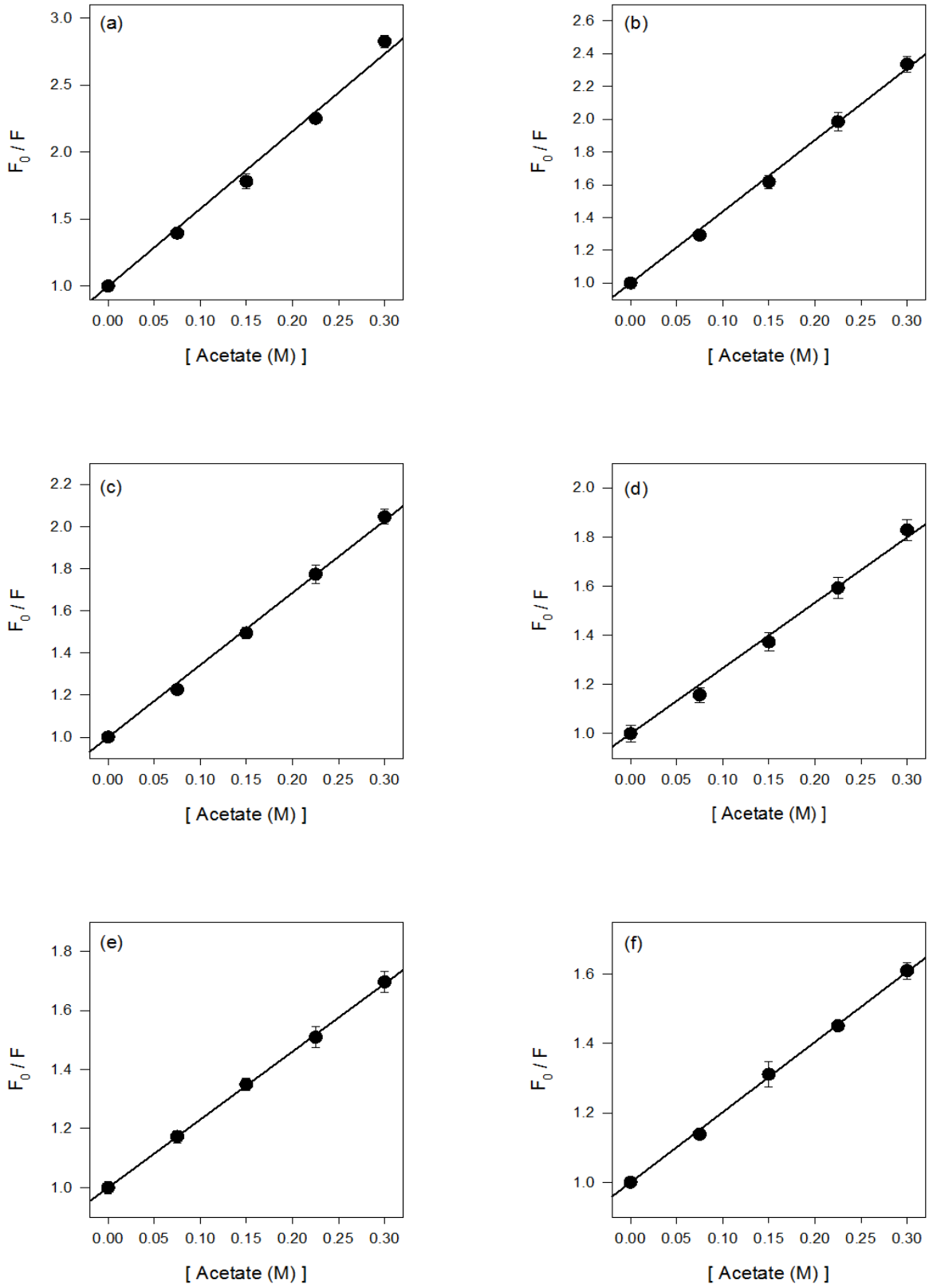

Figure 3-12. Linear Stern-Volmer behavior of phenol fluorescence being quenched by acetate; in the presence of (a) 0.00 M, (b) 0.15 M, (c) 0.30 M, (d) 0.46 M, (e) 0.61 M, and (f) 0.76 M TMAO. The slope is equal to the K_{SV} quenching constant.

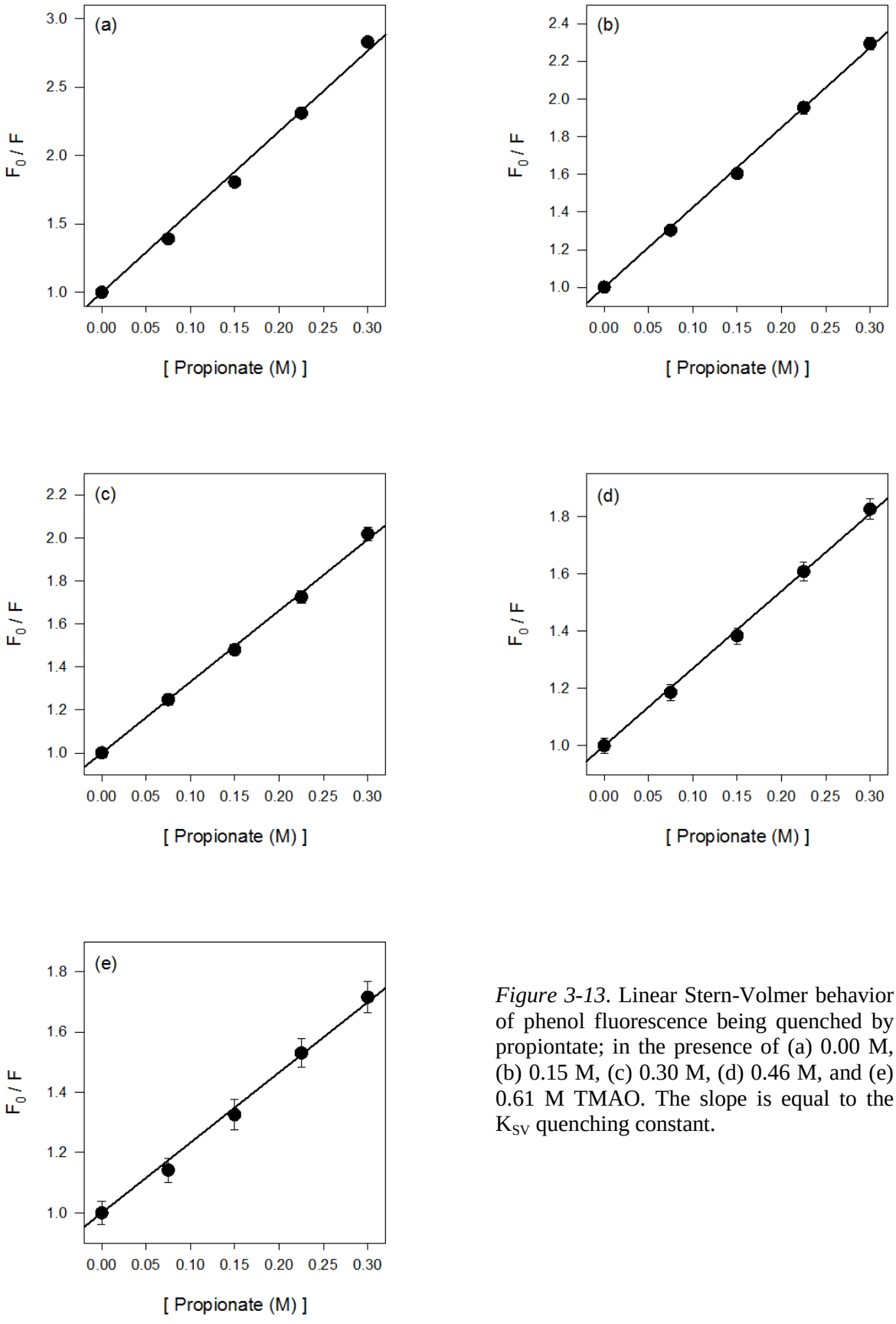

Figure 3-13. Linear Stern-Volmer behavior of phenol fluorescence being quenched by propiontate; in the presence of (a) 0.00 M, (b) 0.15 M, (c) 0.30 M, (d) 0.46 M, and (e) 0.61 M TMAO. The slope is equal to the K_{SV} quenching constant.

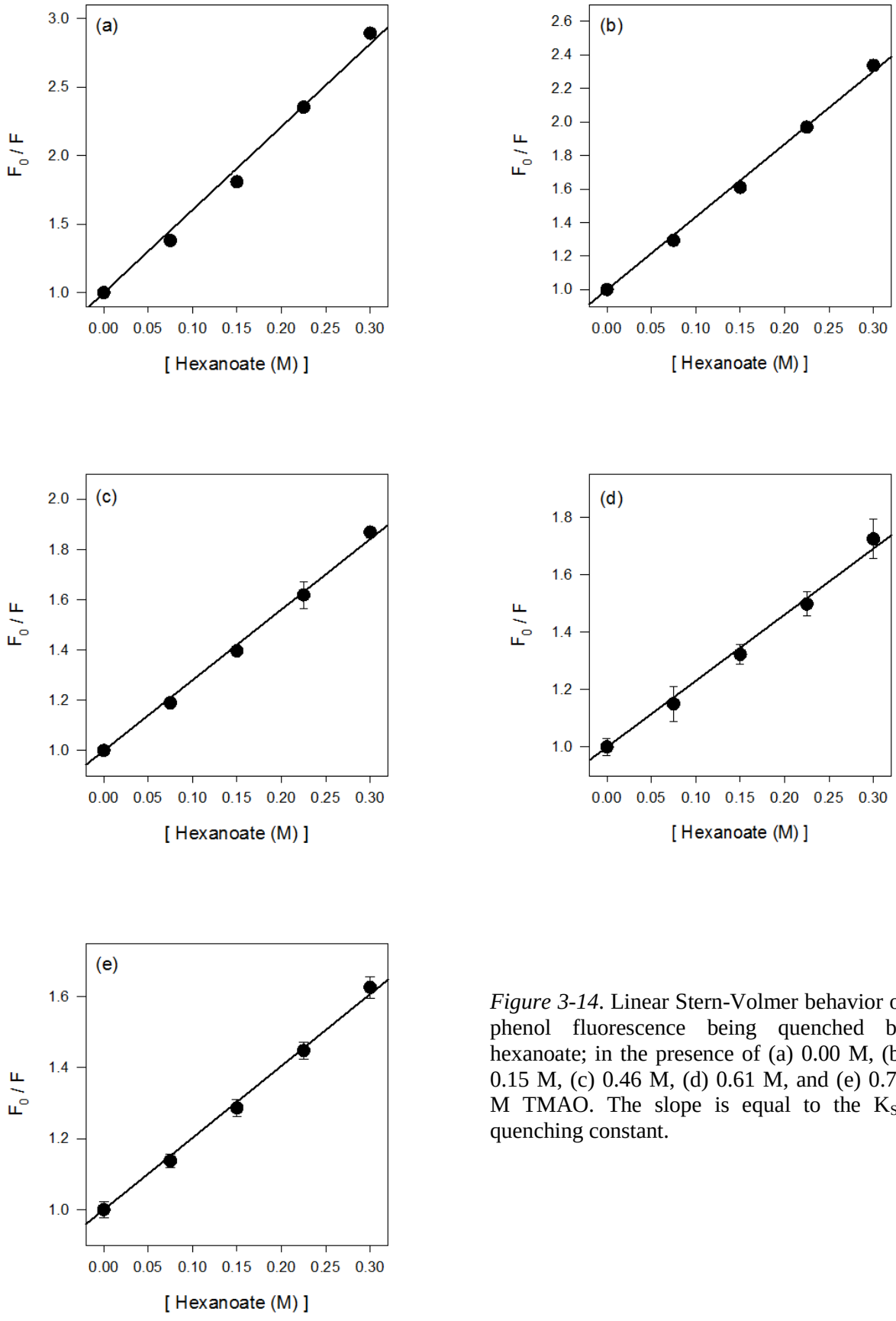

Figure 3-14. Linear Stern-Volmer behavior of phenol fluorescence being quenched by hexanoate; in the presence of (a) 0.00 M, (b) 0.15 M, (c) 0.46 M, (d) 0.61 M, and (e) 0.76 M TMAO. The slope is equal to the K_{SV} quenching constant.

The plots of K_{SV} vs TMAO concentration (Figure 3-15) reveal that there is a slight hyperbolic relationship between the two. Since TMAO is a strong quencher of phenol fluorescence, we attribute this curvature away from linearity to TMAO's effect on phenol fluorescence lifetimes. Therefore, similar to the GdmCl experiments, we have applied the following correction to the measured K_{SV}:

$$K'_{SV}(C) = K_{SV} \times \frac{I_0}{I(C)} \tag{3.3-2}$$

In this equation, I_0 is the fluorescence intensity of phenol at 0.0 M TMAO, and I(C) is the fluorescence intensity of the same amount of phenol measured at a given TMAO concentration of C when there is no quencher present. Measured K_{SV}, corrected $K'_{SV}(C)$, and their linear coefficients of determination are compiled in Table 3-3. Figure 3-17 is a plot of the corrected $K'_{SV}(C)$ vs TMAO concentration and it is apparent that the corrections have indeed corrected for TMAO's effect on phenol fluorescence lifetimes, by the presence of more linearized plots. The plots were fitted to the following equation:

$$K'_{SV}(C) = y_0 + a \times [GdmCl] \tag{3.3-3}$$

The linear fitting parameters y_0 and a are tabulated along with the linear coefficients of determinations in Table 3-4. Using Eq. (3.3-3), $K'_{SV}(C)$ were determined and extrapolated for TMAO concentrations ranging from 0.0 to 1.0 M, using increments of 0.1 M.

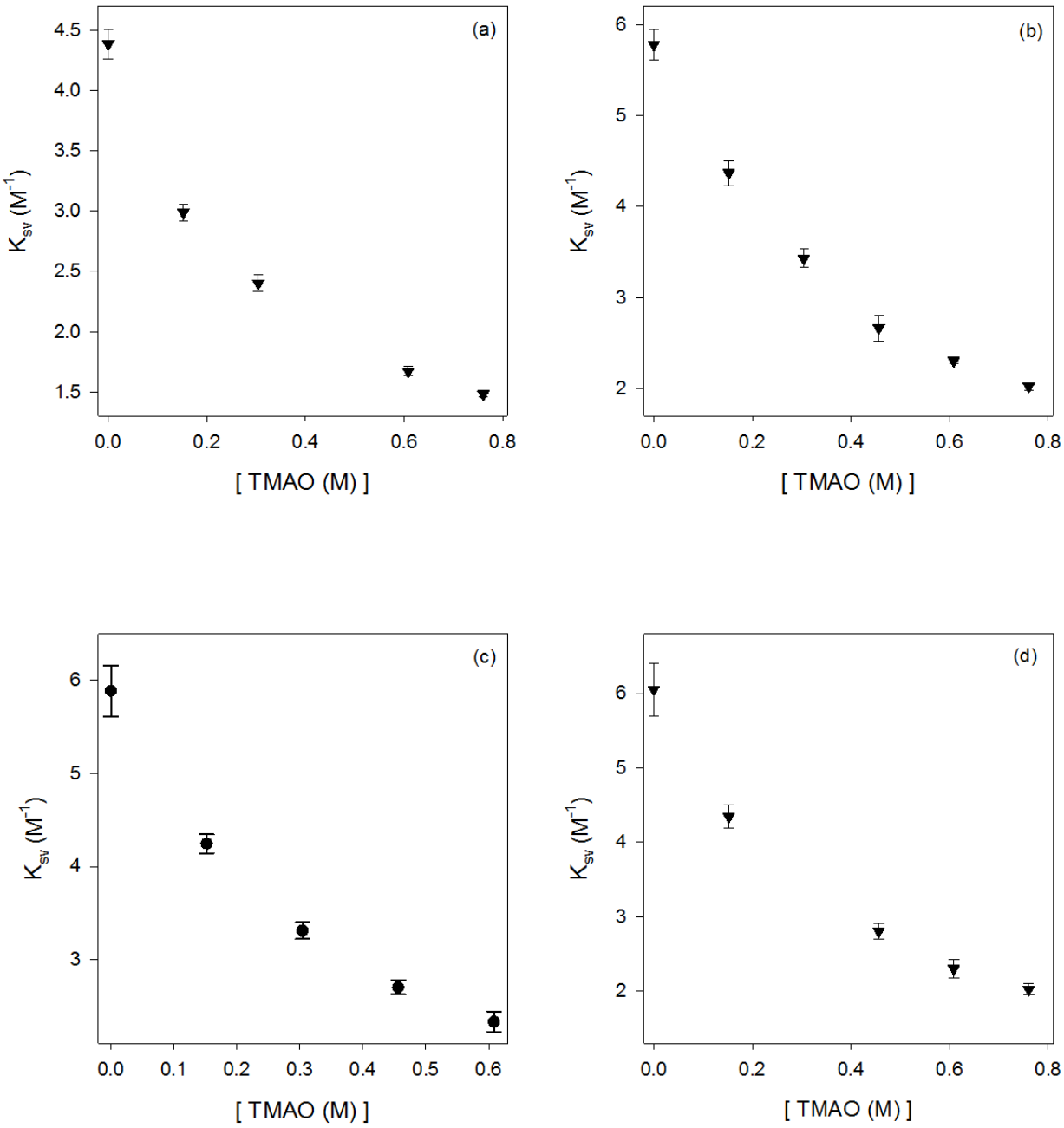

Figure 3-15. The effects of TMAO on the measured Stern-Volmer constant K_{SV} of phenol fluorescence, quenched by: (a) formate, (b) acetate, (c) propionate, and (d) hexanoate

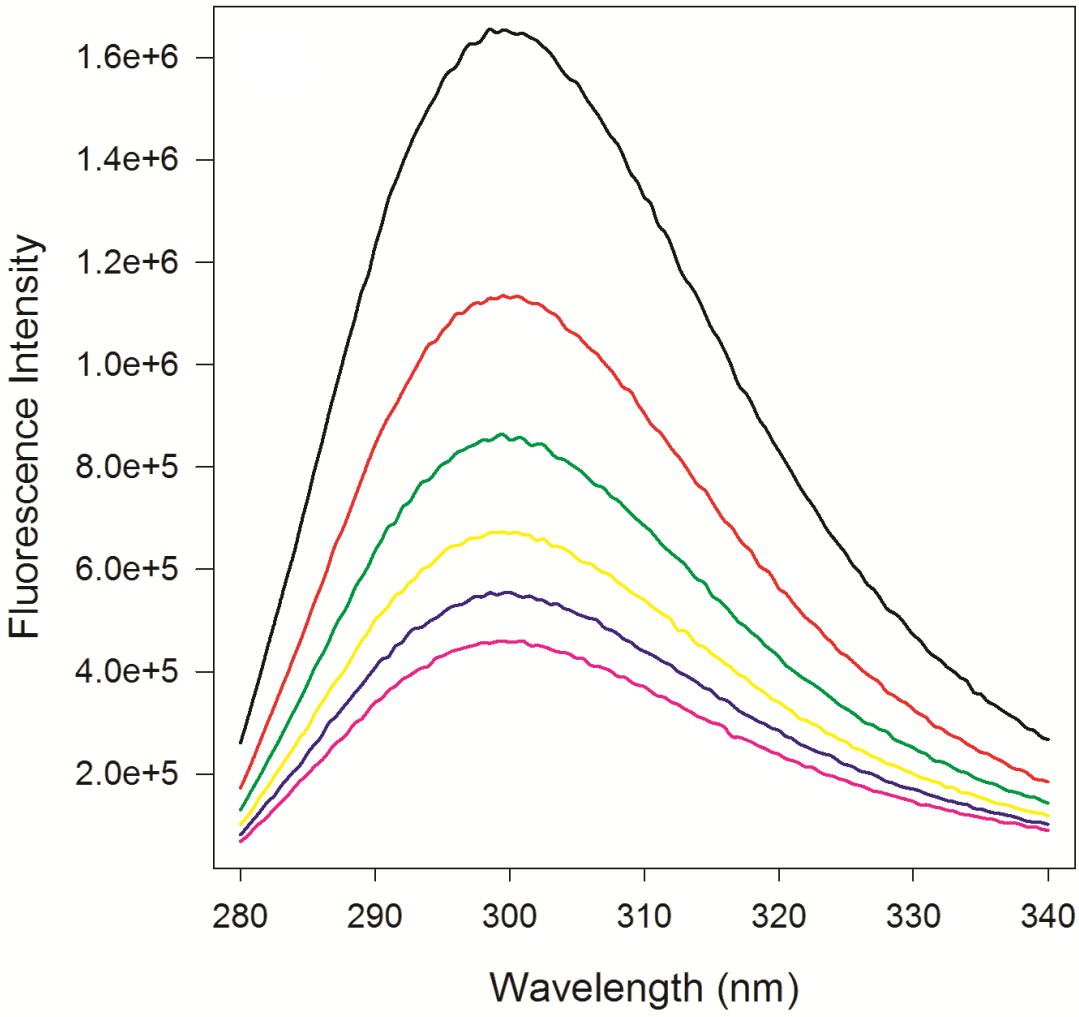

Figure 3-16. Fluorescence spectra of 200 µM Phenol in the presence of 0.0 M TMAO (black line), 0.15 M TMAO (red line), 0.30 M TMAO (green line), 0.46 M TMAO (yellow line), 0.61 M TMAO (purple line), and 0.76 M TMAO (pink line). Spectra taken in the absence of any carboxylate ion

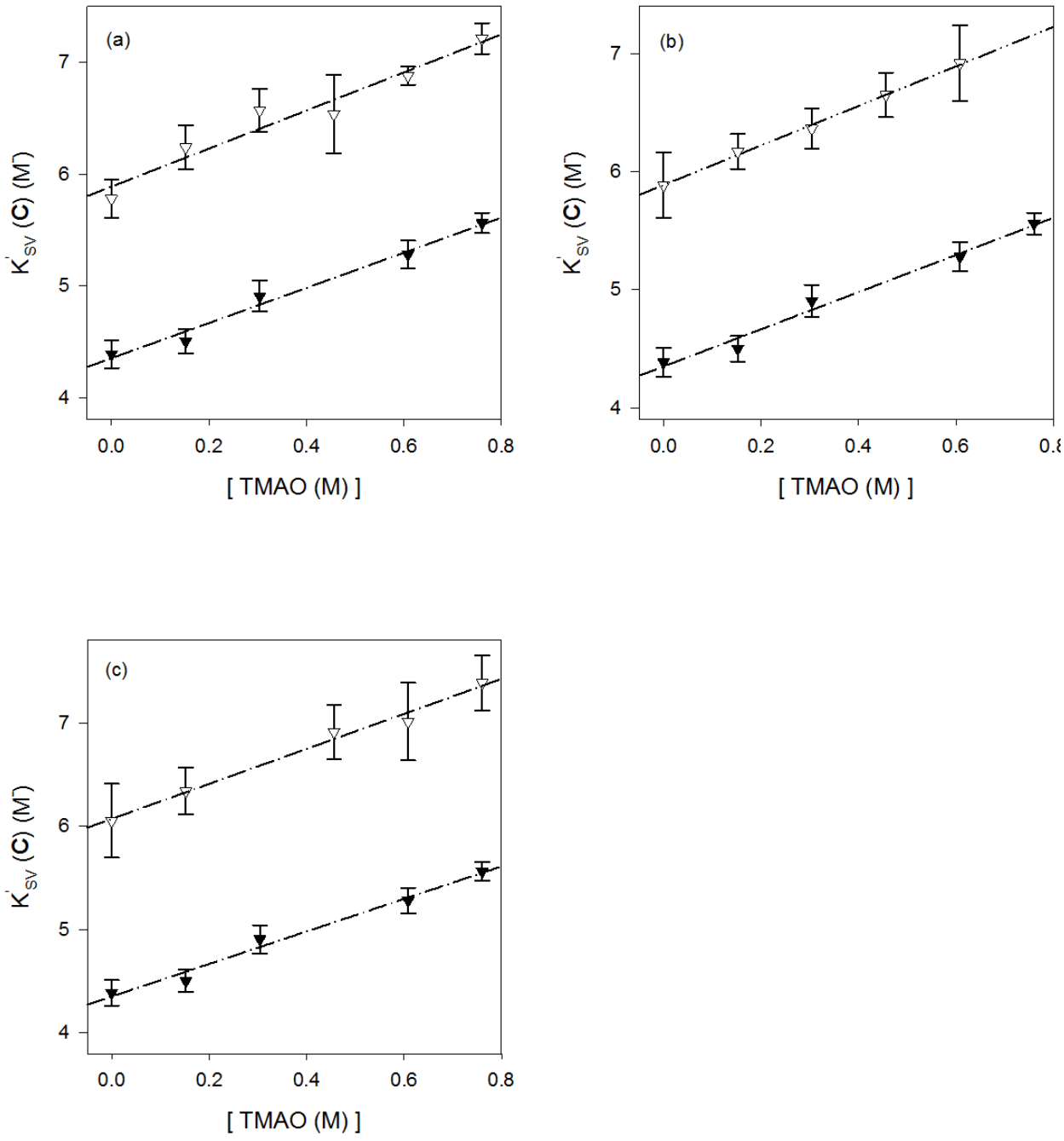

Figure 3-17. The effects of TMAO on the corrected Stern-Volmer constant $K'_{SV}(C)$ of phenol fluorescence, quenched by: (a) formate (closed triangles) and acetate (open triangles), (b) formate (closed triangles) and propionate (open triangles), (c) formate (closed triangles) and hexanoate (open triangles).

Table 3-3. Compiled measured (K_{SV}) and corrected ($K'_{SV}(C)$) Stern-Volmer constant values of various carboxylate ions, obtained from the quenching of phenol fluorescence. These values are plotted in both Figure 3-15 and Figure 3-17 as a function of TMAO concentration.

Quencher	[TMAO] (M)	Measured K_{SV} (M^{-1})	Corrected $K'_{SV}(C)$ (M^{-1})
Formate	0.00	4.39 ± 0.12	4.39 ± 0.12
	0.15	2.99 ± 0.07	4.50 ± 0.11
	0.30	2.40 ± 0.07	4.91 ± 0.14
	0.61	1.67 ± 0.04	5.28 ± 0.12
	0.76	1.48 ± 0.02	5.56 ± 0.09
Acetate	0.00	5.78 ± 0.17	5.78 ± 0.17
	0.15	4.37 ± 0.14	6.24 ± 0.20
	0.30	3.43 ± 0.10	6.57 ± 0.19
	0.46	2.67 ± 0.14	6.54 ± 0.35
	0.61	2.31 ± 0.03	6.88 ± 0.08
	0.76	2.02 ± 0.04	7.21 ± 0.14
Propionate	0.00	5.89 ± 0.27	5.89 ± 0.27
	0.15	4.25 ± 0.10	6.17 ± 0.15
	0.30	3.31 ± 0.09	6.36 ± 0.17
	0.46	2.70 ± 0.08	6.65 ± 0.19
	0.61	2.33 ± 0.11	6.92 ± 0.32
Hexanoate	0.00	6.05 ± 0.36	6.05 ± 0.36
	0.15	4.34 ± 0.15	6.34 ± 0.22
	0.46	2.81 ± 0.11	6.91 ± 0.26
	0.61	2.30 ± 0.12	7.01 ± 0.38
	0.76	2.03 ± 0.07	7.39 ± 0.27

Table 3-4. Linear regression fitting parameters obtained from correlating the data in Figure 3-17 to Eq. (3.33).

Quencher	a (M^{-2})	y0 (M^{-1})	r^2
Formate	1.57 ± 0.12	4.35 ± 0.05	0.98 ± 0.07
Acetate	1.70 ± 0.20	5.89 ± 0.09	0.95 ± 0.13
Propionate	1.67 ± 0.05	5.89 ± 0.02	0.99 ± 0.03
Hexanoate	1.69 ± 0.11	6.07 ± 0.05	0.99 ± 0.07

References

[1] D.L. Beauchamp, M. Khajehpour, The effect of lithium ions on the hydrophobic effect: does lithium affect hydrophobicity differently than other ions?, Biophysical Chemistry, 163-164 (2012) 35-43.

[2] R.D. Macdonald, M. Khajehpour, Effects of the osmolyte TMAO (Trimethylamine-N-oxide) on aqueous hydrophobic contact-pair interactions, Biophysical Chemistry, 184 (2013) 101-107.

[3] A.Y. Moon, D.C. Poland, H.A. Scheraga, Thermodynamic Data from Fluorescence Spectra. I. The System Phenol-Acetate, The Journal of Physical Chemistry, 69 (1965) 2960-2966.

[4] T.A. Shpiruk, M. Khajehpour, The effect of urea on aqueous hydrophobic contact-pair interactions, Physical Chemistry Chemical Physics, 15 (2013) 213-222.

[5] J.R. Lakowicz, Principles of fluorescence spectroscopy, 3rd Edition, Analytical and Bioanalytical Chemistry, 390 (2008) 1223-1224.

Chapter 4

Discussion

4.1 Guanidinium Chloride

4.1.1 Identifying the contribution of contact pair formation to the quenching data

The quenching of phenol fluorescence by carboxylate ions can be represented by the following scheme:

$$F^* + Q \underset{k_{off}}{\overset{k_{on}}{\rightleftarrows}} [F^* \bullet Q] \xrightarrow{k_{pt}} F + Q$$

Scheme1. Suggested mechanism for the quenching of excited state phenol (F *) fluorescence by quencher molecules Q.

where, F* is the excited fluorophore, Q is the quencher, $[F^* \bullet Q]$ is the encounter complex formed between the quencher and fluorophore, k_{pt} is the rate of energy transfer between the quencher and excited fluorophore within the encounter complex, and F is the fluorophore in the ground state. Scheraga and co-workers have shown that phenol fluorescence is quenched, by both acetate and formate, in a "reaction controlled" proton transfer process from the excited phenol hydroxide to the acetate or formate ion [1, 2]. As mentioned earlier, Scheraga et al. also showed the quenching of phenol fluorescence, by carboxylate ion, occurs through a collisional mechanism (dynamic) and not a static mechanism. Thus, the Stern-Volmer quenching constant can be represented with respect to the parameters of Scheme 1:

$$K_{SV} = k_q \tau = K_{ec} \times k_{pt} \times \tau \qquad (4.1\text{-}1)$$

where, K_{SV} is the Stern-Volmer constant, k_q is the rate constant associated with dynamic quenching, τ is the fluorescence lifetime of phenol in the absence of quencher, K_{ec} is the equilibrium constant associated with the formation of the encounter complex, and k_{pt} is the intrinsic rate of proton transfer from the excited state phenol to the carboxylate ion. Bakker and

co-workers have demonstrated that the proton transfer process occurs significantly when the acceptor and donor moieties are separated by 0-5 water molecules [3]. Therefore, in order for the quenching process to compete with the phenol fluorescence the hydroxyl group and carboxylate groups must be within 9 Å in solution. Since this value is smaller than the sum of the van der Waals diameters of the fluorophore and quencher molecules, we can assume that there is a high probability that the encounter complex involves reacting molecules coming into van der Waals contact with one another.

4.1.1 Isolating the contribution of the hydrophobic effect to contact pair formation

Previously, our lab has developed a methodology to isolate the hydrophobic contribution of the phenol-carboxylate ion interaction to K_{SV} [4-6]. The interaction free energy of contact-pair formation between any straight chain carboxylate and phenol, $\Delta G_{ec,}$ is assumed to be comprised of the following two interactions: (a) the hydrophilic, hydrogen bonding interaction between the carboxylate head group and the phenol hydroxide, and (b) the hydrophobic interaction between the phenol benzene ring and the alkyl tail of the carboxylate. This can be represented by:

$$\Delta G_{ec} \approx \Delta G_{head} + \Delta G_{alkyl} \tag{4.1-2}$$

where, ΔG_{ec} is the interaction free energy of the encounter complex formed between phenol and alkyl-carboxylate, ΔG_{head} is the hydrogen bonding interaction free energy, and ΔG_{alkyl} is the hydrophobic interaction free energy. If the formate-phenol contact pair interaction free energy is subtracted from that of any other phenol-carboxylate, we obtain:

$$\psi = \{\Delta G_{ec}\}_{carboxylate} - \{\Delta G_{ec}\}_{formate} \approx \Delta G_{head} + \Delta G_{alkyl} - \Delta G_{formate} \tag{4.1-3}$$

where,ψ is the hydrophobic interaction free energy of contact pair formation.

Any co-solute's effect on contact pair formation can be calculated by subtracting the value of ψ at any given GdmCl concentration S, from that of ψ determined when there is 1.5 M of GdmCl co-solute present:

$$\Delta\psi = \psi_{[S]} - \psi_{[S]=1.5M} =$$

$$(\Delta G_{head} + \Delta G_{alkyl} - \Delta G_{formate})_{[S]} - \left(\Delta G_{head} + \Delta G_{alkyl} - \Delta G_{formate}\right)_{[S]=1.5M} \quad (4.1\text{-}4)$$

The concentration of 1.5 M GdmCl was chosen as our reference point because at lower guanidinium concentrations the quencher species would also contribute significantly to the ionic strength. Rearranging the terms gives the following:

$$\Delta\psi = \left\{(\Delta G_{head})_{[S]} - (\Delta G_{head})_{[S]=1.5M}\right\} - \left\{\left(\Delta G_{formate}\right)_{[S]} - \left(\Delta G_{formate}\right)_{[S]=1.5M}\right\} +$$

$$\left\{\left(\Delta G_{alkyl}\right)_{[S]} - \left(\Delta G_{alkyl}\right)_{[S]=1.5M}\right\} \quad (4.1\text{-}4a)$$

If the effects of GdmCl on ΔG_{head} and $\Delta G_{formate}$ are assumed to be linear, which is valid at values close to 1.5 M:

$$(\Delta G_{head})_{[S]} = (\Delta G_{head})_{[S]=1.5M} + m^*[S] \quad (4.1\text{-}5a)$$

$$\left(\Delta G_{formate}\right)_{[S]} = \left(\Delta G_{formate}\right)_{[S]=1.5M} + n^*[S] \quad (4.1\text{-}5b)$$

where *m* and *n* are constants. Inserting Eqs. (4.1-5a) and (4.1-5b) in Eq. (4.1-4) results in:

$$\Delta\psi = (m-n)^*[S] + \left\{\left(\Delta G_{alkyl}\right)_{[S]} - \left(\Delta G_{alkyl}\right)_{[S]=1.5M}\right\} \quad (4.1\text{-}6)$$

Formate is a carboxylate with a pK_a of 3.8, while the pK_a of acetate is 4.75 and the rest of the carboxylates vary between pK_as of 4.87 and 4.89 [7]. Since the experiments were performed at pH 8.5, all carboxylate groups used are essentially deprotonated. Therefore, the electrostatic

interactions between phenol and the various alkyl-carboxylate head groups (COO^- portion) should be similarly affected by GdmCl, which means the factor of $(m - n)$ is small and similar for all quenchers. Thus, $\Delta\psi$ mostly reflects the difference between the alkyl-phenyl interaction in the presence and absence of additional GdmCl.

We can now introduce the parameter Φ (the calculated parameter from our data analysis of the experimental measurements) and define for any given alkyl-carboxylate quencher:

$$\Phi = -RTln\left(\frac{(K_{SV})_{alkyl-carboxylate}}{(K_{SV})_{formate}}\right) \tag{4.1-7}$$

where, the K_{SV} represent the "corrected" $K'_{SV}(C)$. The values of $K'_{SV}(C)$ are obtained from the linear fits of Table 3-2. We may now define $\Delta\Phi$:

$$\Delta\Phi = \Phi_{[S]} - \Phi_{[S]=1.5M} = -RTln\left(\frac{(K_{SV})_{alkyl-carboxylate}}{(K_{SV})_{formate}}\right)_{[S]} + RTln\left(\frac{(K_{SV})_{alkyl-carboxylate}}{(K_{SV})_{formate}}\right)_{[S]=1.5M} \tag{4.1-8}$$

Substituting Eq. (4.1-1) in Eq. (4.1-8) we obtain:

$$\Delta\Phi = \Delta\psi - RTln\left(\frac{(k_{pt})_{alkyl-carboxylate}}{(k_{pt})_{formate}}\right)_{[S]} + RTln\left(\frac{(k_{pt})_{alkyl-carboxylate}}{(k_{pt})_{formate}}\right)_{[S]=1.5M} \tag{4.1-8a}$$

Addition of salt (GdmCl) to a solution that contains a system involved in the proton transfer process causes changes in activation free energy, which can be described by linear free energy relationships [1, 2]. Therefore, the GdmCl dependence of the activation free energy can be presumed to be represented by:

$$\Delta\Phi = \Delta\psi + (\Delta G^{\ddagger} + \alpha[S])_{alkyl-carboxylate} - (\Delta G^{\ddagger} + \beta[S])_{formate} - (\Delta G^{\ddagger})_{alkyl-carboxylate} +$$

$$(\Delta G^{\ddagger})_{formate} = \Delta\psi + (\alpha - \beta)[S] \quad (4.1\text{-}9)$$

There are no primary salt effects on the rate constants since phenol is a neutral molecule [8], therefore changes in ionic strength will have small effects on the activation free energy. Since the pKa values of all the carboxylates are similar then the factor $(\alpha - \beta)$ should also be small and similar for all alkyl-carboxylate quenchers. Re-writing Eq. (4.1-9) gives:

$$\Delta\Phi = \left\{\left(\Delta G_{alkyl}\right)_{[S]} - \left(\Delta G_{alkyl}\right)_{[S]=1.5M}\right\} + (m - n + \alpha - \beta)[S] \quad (4.1\text{-}9a)$$

where, the first term isolates the contribution that the interaction between hydrophobic phenyl and alkyl moieties makes to $K'_{SV}(C)$ values; while $(m - n + \alpha - \beta)$ is small and should be essentially constant for the longer carboxylates which have practically the same pK_a values. Figure 4-1 plots $\Delta\Phi$ as a function of GdmCl concentration. The values of $\Delta\Phi$ are obtained from the corrected Stern-Volmer constants using Eq. (4.1-8) and at each given GdmCl concentration the value of $K'_{SV}(C)$ is obtained from the linear fitting parameters found in Table 3-2. It can be observed from the $\Delta\Phi$ plots that the phenyl-carboxylate contact pairs are affected by GdmCl in a size-dependent fashion. The derivative $\frac{d(\Delta\Phi)}{d[GdmCl]}$ quantifies how the interactions between the hydrophobic phenyl ring and alkyl moieties are influenced by the addition of GdmCl. When the derivative $\left[\frac{d(\Delta\Phi)}{d[GdmCl]}\right]_{[GdmCl]=1.5\ M}$ is taken and plotted as a function of $(d_v)^2$, the cube of the hard sphere

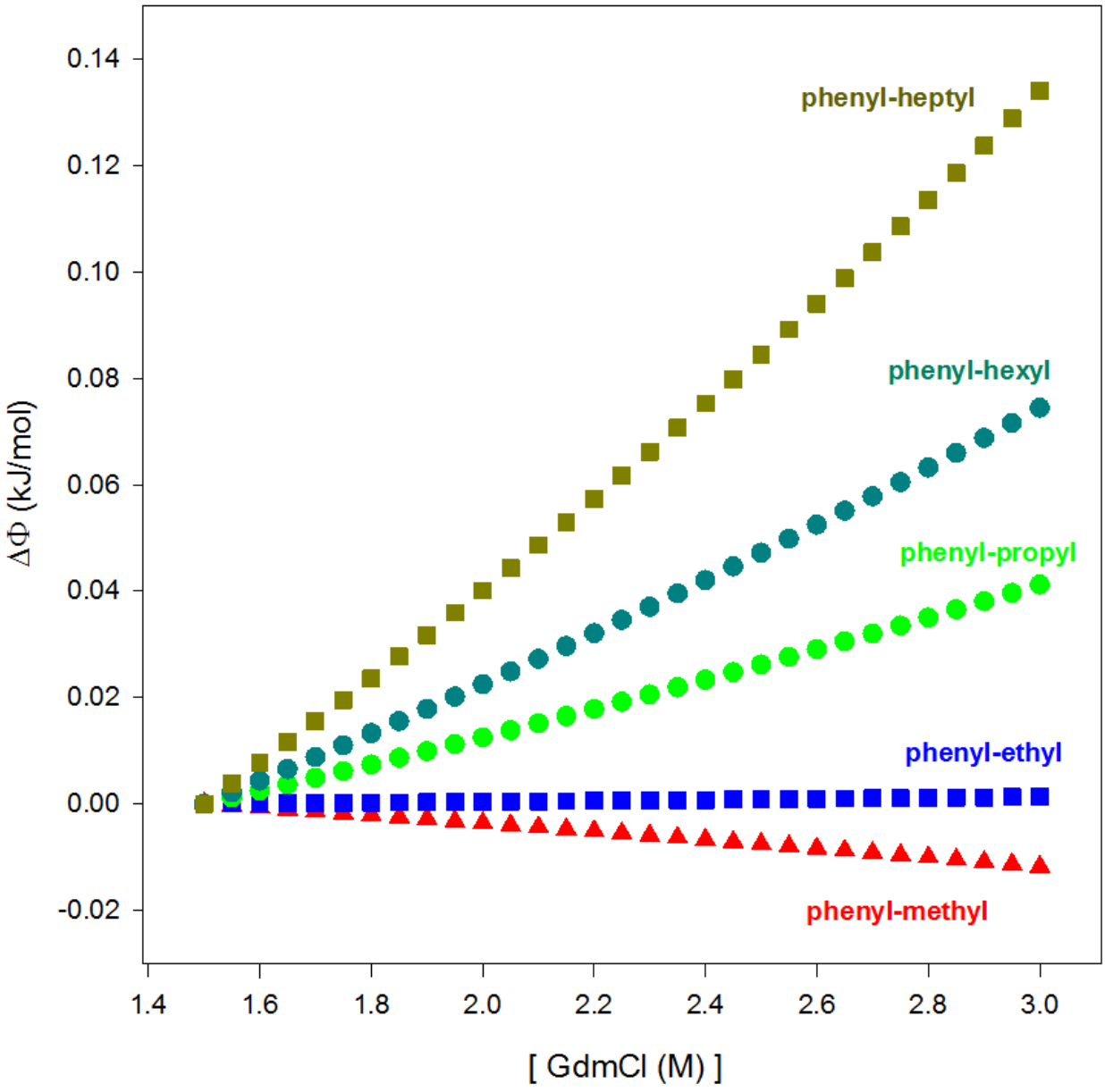

Figure 4-1. GdmCl concentration dependence of $\Delta\Phi$ as defined by Eq. (4.1-8). The initial slopes are: phenyl-methyl = -6.84E-03, phenyl-ethyl = 7.74E-04, phenyl-propyl = 2.36E-02, phenyl-hexyl = 4.23E-02, and phenyl-heptyl = 7.51E-02; the initial slopes have units of $\frac{kJ*L}{mol^2}$.

diameter [9] of the alkyl groups, the observed size-dependent effect of GdmCl on the phenyl-carboxylate contact pairs is further demonstrated, which can be seen by the appearance of a linear correlation dependence in Figure 4-2.

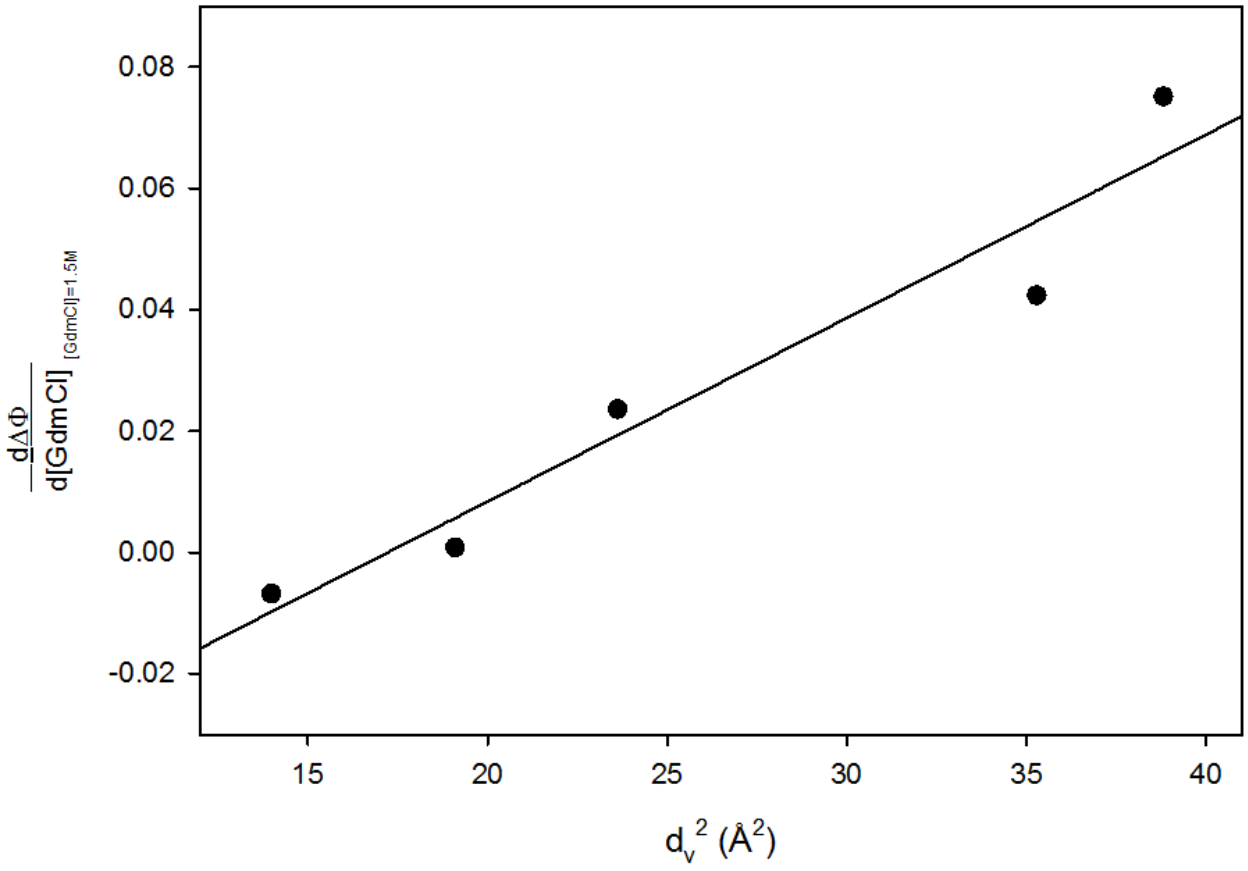

Figure 4-2. Initial slope $\left[\frac{d(\Delta\Phi)}{d[GdmCl]}\right]_{[GdmCl]=1.5\ M}$ values plotted as a function of hard sphere diameters of the alkyl tail groups. The diameters are obtained from Price et al. [8] and the coefficient of determination of this plot is r^2= 0.93.

The work done by Graziano can further advance the understanding of the size-dependent effects of GdmCl on phenyl-alkyl contact pairs. Graziano suggested that the ΔG_{alkyl} term could be further broken down into two separate terms [10]:

$$\Delta G_{alkyl} = \Delta G_{cav} + \Delta G_{att} \tag{4.1-10}$$

In this equation, ΔG_{cav} represents the contribution from the reversible work that is required to make a cavity that will accommodate the alkyl group in the solvent and ΔG_{att} is the contribution

from the reversible work that is required to turn on attractive interactions between the solvent molecules and the alkyl moiety. If we expand the derivative we obtain:

$$\frac{d(\Delta\Phi)}{d[GdmCl]} = \frac{d(\Delta G_{cav})}{d[GdmCl]} + \frac{d(\Delta G_{att})}{d[GdmCl]} + (m - n + \alpha - \beta) \quad (4.1\text{-}11)$$

Further calculations done by Graziano show that the addition of GdmCl makes it more difficult to form a cavity in the aqueous solution and this promotes hydrophobic contact-pair promotion [11-13]. However, he also calculated that the addition of GdmCl increases the magnitude of attractive interactions between the alkyl moiety and the solvent molecules disrupting the hydrophobic contact pair. In other words, adding GdmCl makes ΔG_{cav} more negative while simultaneously making ΔG_{att} more positive. For spherical hydrophobic solutes both ΔG_{cav} and ΔG_{att} depend on the hydrophobic surface area, but the attractive interactions show a much sharper dependence on the cube of the solute diameter. Therefore, beyond a certain solute size, the attractive contributions will dominate the value of $\left[\frac{d(\Delta\Phi)}{d[GdmCl]}\right]_{[GdmCl]=1.5\ M}$ resulting in the observed sign change. Based on these results we can suggest that guanidinium ions affect hydrophobic interactions in a size dependent fashion. The denaturant is either indifferent towards, or slightly stabilizes, the interactions between small hydrophobes; however, as the size of the interacting hydrophobes increases, the denaturant becomes more and more effective in disturbing the stability of contact pairs formed between the molecules.

4.2 Trimethylamine-N-Oxide

4.2.1 Identifying the contribution of contact pair formation to the quenching data

The model system of a phenyl-alkyl contact pair is still utilized, therefore the system can still be accurately represented by scheme 1:

$$F^* + Q \underset{k_{off}}{\overset{k_{on}}{\rightleftarrows}} [F^* \bullet Q] \xrightarrow{k_{pt}} F + Q$$

Scheme1. Suggested mechanism for the quenching of excited state phenol (F *) fluorescence by quencher molecules Q.

Using the same rationale and arguments for the GdmCl experiments, the Stern-Volmer quenching constant can be represented by the parameters of scheme 1, where [1, 2]:

$$K_{SV} = k_q\tau = K_{ec} \times k_{pt} \times \tau \quad (4.2\text{-}1)$$

As we have previously determined, TMAO has an effect on phenol's fluorescence lifetime, thus the correct Stern-Volmer constant $K'_{SV}(C)$ can be equated to these parameters as well.

4.2.2 Isolating the contribution of the hydrophobic effect to contact pair formation

Just as with GdmCl, the hydrophobic contribution of the phenol-carboxylate ion interaction to K_{SV} is isolated.

$$\Delta G_{ec} \approx \Delta G_{head} + \Delta G_{alkyl} \quad (4.2\text{-}2)$$

where, ΔG_{ec} is the interaction free energy of the encounter complex formed between phenol and alkyl-carboxylate, ΔG_{head} is the hydrogen bonding interaction free energy, and ΔG_{alkyl} is the

hydrophobic interaction free energy. If the formate-phenol contact pair interaction free energy is subtracted from that of any other phenol-carboxylate, we obtain:

$$\psi = \{\Delta G_{ec}\}_{carboxylate} - \{\Delta G_{ec}\}_{formate} \approx \Delta G_{head} + \Delta G_{alkyl} - \Delta G_{formate} \quad (4.2\text{-}3)$$

Any co-solute's effect on contact pair formation can be calculated by subtracting the value of ψ at any given TMAO concentration S, from that of ψ determined when there is 0.0 M of TMAO co-solute present:

$$\Delta\psi = \psi_{[S]} - \psi_{[S]=0} =$$

$$(\Delta G_{head} + \Delta G_{alkyl} - \Delta G_{formate})_{[S]} - \left(\Delta G_{head} + \Delta G_{alkyl} - \Delta G_{formate}\right)_{[S]=0} \quad (4.2\text{-}4)$$

Unlike GdmCl, TMAO does not contribute to the overall ionic strength of the aqueous solution, therefore we have chosen 0.0 M TMAO as our reference point. To insure that ionic strength was kept stable we adjusted each sample to an ionic strength of 0.3 M, using a NaCl stock solution. Rearranging the terms gives the following:

$$\Delta\psi = \left\{(\Delta G_{head})_{[S]} - (\Delta G_{head})_{[S]=0}\right\} - \left\{\left(\Delta G_{formate}\right)_{[S]} - \left(\Delta G_{formate}\right)_{[S]=0}\right\} + \left\{\left(\Delta G_{alkyl}\right)_{[S]} - \left(\Delta G_{alkyl}\right)_{[S]=0}\right\} \quad (4.2\text{-}4a)$$

If the effects of TMAO on ΔG_{head} and $\Delta G_{formate}$ are assumed to be linear, which is valid at values close to 0.0 M:

$$(\Delta G_{head})_{[S]} = (\Delta G_{head})_{[S]=0} + m^*[S] \quad (4.2\text{-}5a)$$

$$\left(\Delta G_{formate}\right)_{[S]} = \left(\Delta G_{formate}\right)_{[S]=0} + n^*[S] \quad (4.2\text{-}5b)$$

where *m* and *n* are constants. Inserting Eqs. (4.2-5a) and (4.2 -5b) in Eq. (4.2-4) results in:

$$\Delta\psi = (m-n)^{*}[S] + \left\{\left(\Delta G_{alkyl}\right)_{[S]} - \left(\Delta G_{alkyl}\right)_{[S]=0}\right\} \quad (4.2\text{-}6)$$

Similar to GdmCl, the experiments were performed at pH 8.5, thus all carboxylate groups used are essentially deprotonated. Therefore, the same reasoning that was used with GdmCl can be applied to TMAO, which means the factor of $(m-n)$ is small and similar for all quenchers. Thus, $\Delta\psi$ mostly reflects the difference between the alkyl-phenyl interaction in the presence and absence of additional TMAO.

We can now introduce the familiar parameter Φ and define it for any given alkyl-carboxylate quencher:

$$\Phi = -RTln\left(\frac{(K_{SV})_{alkyl-carboxylate}}{(K_{SV})_{formate}}\right) \quad (4.2\text{-}7)$$

where, the K_{SV} represent the corrected $K'_{SV}(C)$. The values of $K'_{SV}(C)$ are obtained from the linear fits of Table 3-4. We may now define $\Delta\Phi$:

$$\Delta\Phi = \Phi_{[S]} - \Phi_{[S]=0} = -RTln\left(\frac{(K_{SV})_{alkyl-carboxylate}}{(K_{SV})_{formate}}\right)_{[S]} + RTln\left(\frac{(K_{SV})_{alkyl-carboxylate}}{(K_{SV})_{formate}}\right)_{[S]=0} \quad (4.2\text{-}8)$$

Substituting Eq. (4.2-1) in Eq. (4.2-8) we obtain:

$$\Delta\Phi = \Delta\psi - RTln\left(\frac{(k_{pt})_{alkyl-carboxylate}}{(k_{pt})_{formate}}\right)_{[S]} + RTln\left(\frac{(k_{pt})_{alkyl-carboxylate}}{(k_{pt})_{formate}}\right)_{[S]=0} \quad (4.2\text{-}8a)$$

Like GdmCl, TMAO dependence of the activation free energy can be described by linear free energy relationships [1, 2], which can be assumed to be represented by:

$$\Delta\Phi = \Delta\psi + (\Delta G^{\ddagger} + \alpha[S])_{alkyl-carboxylate} - (\Delta G^{\ddagger} + \beta[S])_{formate} - (\Delta G^{\ddagger})_{alkyl-carboxylate} +$$

$$(\Delta G^{\ddagger})_{formate} = \Delta\psi + (\alpha - \beta)[S] \quad (4.2\text{-}9)$$

Since, the pKa values of the carboxylates are close to each other and ionic strength is kept constant in these experiments, then the factor $(\alpha - \beta)$ should also be small and similar for all alkyl-carboxylate quenchers. Re-writing Eq. (3.3-12) gives:

$$\Delta\Phi = \left\{\left(\Delta G_{alkyl}\right)_{[S]} - \left(\Delta G_{alkyl}\right)_{[S]=0}\right\} + (m - n + \alpha - \beta)[S] \quad (4.2\text{-}$$

9a) Where, the first term isolates the contribution that the interaction between hydrophobic phenyl and alkyl moieties makes to $K'_{SV}(C)$ values; while $(m - n + \alpha - \beta)$ is small and should be essentially constant for the longer carboxylates which have essentially the same pK_a values. In Figure 4-3, $\Delta\Phi$ is plotted as a function of TMAO concentration, where $\Delta\Phi$ becomes more positive as TMAO concentration is increased. In contrast to GdmCl $\Delta\Phi$ plots, there appears to be no size-dependence with regards to alkyl-carboxylate length. We can conclude from this figure that TMAO is able to disrupt the hydrophobic interactions between phenol and alkyl-carboxylates in a similar magnitude, without depending on the size of the alkyl chain length.

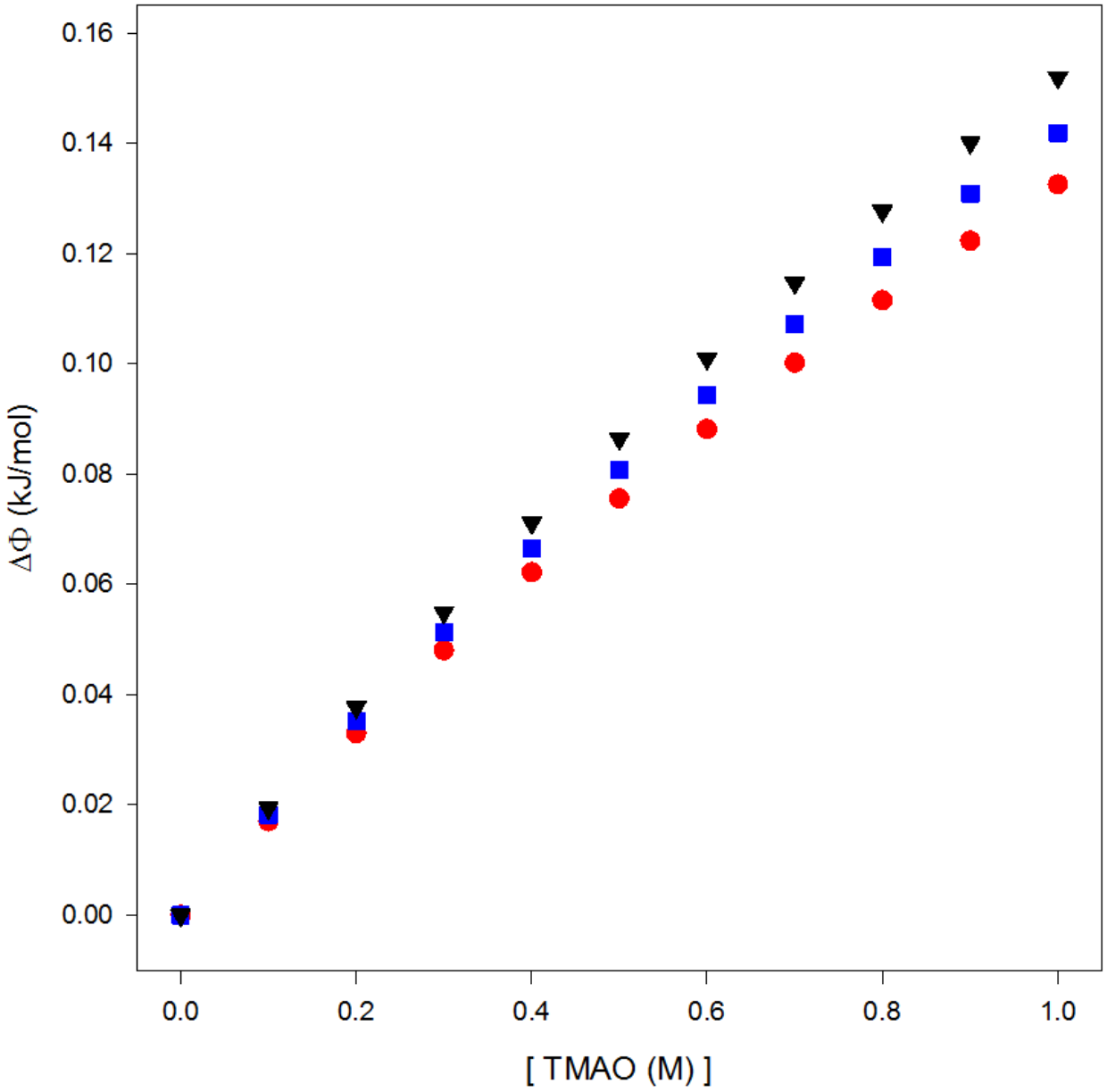

Figure 4-3. TMAO concentration dependence of ΔΦ as defined by Eq. (4.2-8). The hydrophobic interactions between phenyl and the tail groups of our alkyl-carboxylates are as follows: phenyl-methyl (red circles), phenyl-ethyl (blue squares), and phenyl-pentyl (black triangles).

References

[1] D.K. Kunimitsu, A.Y. Woody, E.R. Stimson, H.A. Scheraga, Thermodynamic data from fluorescence spectra. II. Hydrophobic bond formation in binary complexes, The Journal of Physical Chemistry, 72 (1968) 856-866.

[2] A.Y. Moon, D.C. Poland, H.A. Scheraga, Thermodynamic Data from Fluorescence Spectra. I. The System Phenol-Acetate, The Journal of Physical Chemistry, 69 (1965) 2960-2966.

[3] B.J. Siwick, M.J. Cox, H.J. Bakker, Long-Range Proton Transfer in Aqueous Acid-Base Reactions, The Journal of Physical Chemistry B, 112 (2007) 378-389.

[4] D.L. Beauchamp, M. Khajehpour, The effect of lithium ions on the hydrophobic effect: does lithium affect hydrophobicity differently than other ions?, Biophysical Chemistry, 163-164 (2012) 35-43.

[5] T.A. Shpiruk, M. Khajehpour, The effect of urea on aqueous hydrophobic contact-pair interactions, Physical Chemistry Chemical Physics, 15 (2013) 213-222.

[6] R.D. Macdonald, M. Khajehpour, Effects of the osmolyte TMAO (Trimethylamine-N-oxide) on aqueous hydrophobic contact-pair interactions, Biophysical Chemistry, 184 (2013) 101-107.

[7] M. Namazian, S. Halvani, Calculations of pKa values of carboxylic acids in aqueous solution using density functional theory, The Journal of Chemical Thermodynamics, 38 (2006) 1495-1502.

[8] N.C. Price, R.A. Dwek, R.G. Ratcliffe, M.R. Wormald, Principles and Problems in Physical Chemistry for Biochemists, 3rd ed., Oxford University Press, Oxford, 2001.

[9] V. Gogonea, C. Baleanu-Gogonea, E. Osawa, Solvent hard sphere diameter from van der Waals volume A statistical analysis of computed and solubility determined solvent diameters, Journal of Molecular Structure: THEOCHEM, 432 (1998) 177-189.

[10] G. Graziano, Role of salts on the strength of pairwise hydrophobic interaction, Chemical Physics Letters, 483 (2009) 67-71.

[11] G. Graziano, On the size dependence of hydrophobic hydration, Journal of the Chemical Society, Faraday Transactions, 94 (1998) 3345-3352.

[12] G. Graziano, On the Solubility of Aliphatic Hydrocarbons in 7 M Aqueous Urea, The Journal of Physical Chemistry B, 105 (2001) 2632-2637.

[13] G. Graziano, Contrasting the denaturing effect of guanidinium chloride with the stabilizing effect of guanidinium sulfate, Physical Chemistry Chemical Physics, 13 (2011) 12008-12014.

Chapter 5

Conclusions

4.1 Guanidinium Chloride

In our work with the protein denaturant GdmCl we have determined the effects of GdmCl on hydrophobic interactions between phenol and a variety of alkyl-carboxylate ions, which form hydrophobic contact-pairs. The formation of contact-pairs in this work is the basis of our model system, while its simplicity allows us to isolate the effects of GdmCl on hydrophobic interactions. We were able to quantitatively show that the presence of GdmCl may stabilize or be indifferent towards smaller hydrophobic pairs, but on the other hand, GdmCl was shown to destabilize hydrophobic contact pairs formed between phenol and larger hydrophobes. Our results agree with those of Godawat and co-worker's molecular dynamic simulations, which showed that methane pairs are stabilized by the addition of GdmCl, but large hydrophobes are destabilized [1]. Our findings are consistent with other observed experimental results as well. Large hydrophobes, such as micelles and lipid bilayers [2, 3], have been shown to be destabilized in the presence of guanidinium chloride. Studies on protein folding have shown that proteins denatured by GdmCl still contain residual order, which defines a non-random-coil denatured state. The persistence of residual order in proteins may demonstrate that small hydrophobic interactions are being stabilized by the denaturant [4-6].

The three dimensional fold that makes up a protein is very complex and is held together by a variety of different interactions, such as hydrogen bonding, electrostatic interactions, van der Waal's interactions, and the hydrophobic effect. The complexity of these interactions all acting together makes it extremely hard to determine how specific molecules affect them. This is why the mechanism by which guanidinium chloride denatures proteins has been questioned and studied for many years without a definitive answer. Thus, we are intrigued by how these interactions are affected by the presence GdmCl, although it is still not clear which mechanism

the denaturant partakes in to destabilize the folded states of proteins. However, as far as simple hydrophobic interactions are concerned, in this case those between phenyl and alkyl moieties, the linear dependence of $\left[\frac{d(\Delta\Phi)}{d[GdmCl]}\right]_{[GdmCl]=1.5\ M}$ on $(d_v)^2$ indicates that the guanidinium ion interacts with hydrophobic molecules through surface-mediated interactions. Guanidinium can accomplish this by modulating hydrophobic hydration, where guanidinium is able to accumulate at the surface of hydrophobic molecules because: (1) Gdm^+ is a weakly hydrated ion and it breaks few hydrogen bonds while it comes in contact with the hydrophobic surfaces, and (2) the guanidinium ion's planar shape, which is attributed to resonance stabilization, allows it to stack parallel to the hydrophobic surface [1, 7, 8]; the parallel stacking of Gdm^+ also allows for the disruption of hydrophobic interactions between protein side chains through van der Waals interactions between the denaturant and hydrophobic molecules [1]. These two interactions, hydrophobic dehydration and van der Waals interactions, are surface-dependent, therefore van der Waals interactions become more dominant when guanidinium is interacting with hydrophobic molecules having large surfaces. This confirms that non-hydrogen bonding interactions play a role in the denaturation mechanism of the guanidinium ion. Nevertheless, recent spectroscopic data demonstrate that the addition of guanidinium ion to an aqueous solvent changes the hydrogen bonding properties of the aqueous solvent system [9, 10]. Therefore, it is possible that a "unified description" similar to that suggested by Moeser and Horinek for urea, may provide a realistic picture of guanidinium denaturation [11].

4.2 Trimethylamine-N-Oxide

The mode of action by which TMAO stabilizes the protein folded state has been studied extensively, although a clear picture has not been developed yet. In this work we specifically

looked at the effects of TMAO on hydrophobic contact-pair interactions between phenol and a number of alkyl-carboxylates, such as acetate, propionate, and hexanoate. As this work only focuses on hydrophobic interactions a complete picture can still not be formed about its mechanism of stabilizing proteins, thus investigations of TMAO's effects on hydrogen bonding and electrostatic interactions should be looked at as well. Our experimental results show that hydrophobic interactions within a contact-pair are destabilized in the presence of TMAO, in a non-size-dependent manner. These findings are consistent with the predictions of Paul and Patey [12], as well as the thermodynamic analyses performed by Bolen and co-workers [13-33], which suggest that the addition of TMAO to an aqueous solvent increases hydrophobic moiety solubility. In other words, TMAO can act as a "denaturing surfactant" for hydrophobic interactions. The understanding of how TMAO affects hydrophobic interactions can be applied to its practical use in various fields of study, like molecular biology and biotechnology. For example, Bennion et al. have shown that TMAO can prevent misfolding of prion proteins [34], while Yancey and co-workers demonstrated that TMAO can restore function to one form of a mutant protein found in cystic fibrosis [35]. These cases show that determining TMAO's mode of action for stabilizing proteins is important, and determining its effects on hydrophobic interactions is a key part to the complete understanding. Additionally, these results should also be of particular importance to theoreticians using protein unfolding/refolding data for developing algorithms that predict protein structure.

References

[1] R. Godawat, S.N. Jamadagni, S. Garde, Unfolding of Hydrophobic Polymers in Guanidinium Chloride Solutions, The Journal of Physical Chemistry B, 114 (2010) 2246-2254.

[2] J.K. Mahendra, Possible modes of interaction of small molecules with lipid bilayer in biomembrane, Proceedings of the Indian National Science Academy, 45 (1979) 567-577.

[3] R.J. Midura, M. Yanagishita, Chaotropic Solvents Increase the Critical Micellar Concentrations of Detergents, Analytical Biochemistry, 228 (1995) 318-322.

[4] P. Mandal, A.R. Molla, D.K. Mandal, Denaturation of bovine spleen galectin-1 in guanidine hydrochloride and fluoroalcohols: structural characterization and implications for protein folding, Journal of Biochemistry, 154 (2013) 531-540.

[5] R. Meloni, C. Camilloni, G. Tiana, Sampling the Denatured State of Polypeptides in Water, Urea, and Guanidine Chloride to Strict Equilibrium Conditions with the Help of Massively Parallel Computers, Journal of Chemical Theory and Computation, 10 (2014) 846-854.

[6] D.J. Segel, A.L. Fink, K.O. Hodgson, S. Doniach, Protein Denaturation: A Small-Angle X-ray Scattering Study of the Ensemble of Unfolded States of Cytochrome c, Biochemistry, 37 (1998) 12443-12451.

[7] Q. Shao, Y. Fan, L. Yang, Y.Q. Gao, Counterion Effects on the Denaturing Activity of Guanidinium Cation to Protein, Journal of Chemical Theory and Computation, 8 (2012) 4364-4373.

[8] E. Wernersson, J. Heyda, M. Vazdar, M. Lund, P.E. Mason, P. Jungwirth, Orientational Dependence of the Affinity of Guanidinium Ions to the Water Surface, The Journal of Physical Chemistry B, 115 (2011) 12521-12526.

[9] I.M. Pazos, F. Gai, Solute's Perspective on How Trimethylamine Oxide, Urea, and Guanidine Hydrochloride Affect Water's Hydrogen Bonding Ability, The Journal of Physical Chemistry B, 116 (2012) 12473-12478.

[10] J.N. Scott, N.V. Nucci, J.M. Vanderkooi, Changes in Water Structure Induced by the Guanidinium Cation and Implications for Protein Denaturation, The Journal of Physical Chemistry A, 112 (2008) 10939-10948.

[11] B. Moeser, D. Horinek, Unified Description of Urea Denaturation: Backbone and Side Chains Contribute Equally in the Transfer Model, The Journal of Physical Chemistry B, 118 (2014) 107-114.

[12] S. Paul, G.N. Patey, The Influence of Urea and Trimethylamine-N-oxide on Hydrophobic Interactions, The Journal of Physical Chemistry B, 111 (2007) 7932-7933.

[13] M. Auton, A.C.M. Ferreon, D.W. Bolen, Metrics that Differentiate the Origins of Osmolyte Effects on Protein Stability: A Test of the Surface Tension Proposal, Journal of Molecular Biology, 361 (2006) 983-992.

[14] I.V. Baskakov, R. Kumar, G. Srinivasan, Y.-s. Ji, D.W. Bolen, E.B. Thompson, Trimethylamine N-Oxide-induced Cooperative Folding of an Intrinsically Unfolded Transcription-activating Fragment of Human Glucocorticoid Receptor, Journal of Biological Chemistry, 274 (1999) 10693-10696.

[15] L.M.F. Holthauzen, D.W. Bolen, Mixed osmolytes: The degree to which one osmolyte affects the protein stabilizing ability of another, Protein Science, 16 (2007) 293-298.

[16] Y. Qu, C.L. Bolen, D.W. Bolen, Osmolyte-driven contraction of a random coil protein, Proceedings of the National Academy of Sciences, 95 (1998) 9268-9273.

[17] L. Rajagopalan, J. Rosgen, D.W. Bolen, K. Rajarathnam, Novel Use of an Osmolyte To Dissect Multiple Thermodynamic Linkages in a Chemokine Ligand-Receptor System, Biochemistry, 44 (2005) 12932-12939.

[18] J. Rosgen, B.M. Pettitt, D.W. Bolen, Protein Folding, Stability, and Solvation Structure in Osmolyte Solutions, Biophysical Journal, 89 (2005) 2988-2997.

[19] J. Rösgen, B.M. Pettitt, D.W. Bolen, An analysis of the molecular origin of osmolyte-dependent protein stability, Protein Science, 16 (2007) 733-743.

[20] A.T. Russo, J. Rosgen, D.W. Bolen, Osmolyte Effects on Kinetics of FKBP12 C22A Folding Coupled with Prolyl Isomerization, Journal of Molecular Biology, 330 (2003) 851-866.

[21] P. Wu, D.W. Bolen, Osmolyte-induced protein folding free energy changes, Proteins: Structure, Function, and Bioinformatics, 63 (2006) 290-296.

[22] M. Auton, D.W. Bolen, Additive Transfer Free Energies of the Peptide Backbone Unit That Are Independent of the Model Compound and the Choice of Concentration Scale, Biochemistry, 43 (2004) 1329-1342.

[23] M. Auton, D.W. Bolen, Predicting the energetics of osmolyte-induced protein folding/unfolding, Proceedings of the National Academy of Sciences of the United States of America, 102 (2005) 15065-15068.

[24] M. Auton, D.W. Bolen, H.u. Dieter, S. Helmut, Chapter Twenty-Three - Application of the Transfer Model to Understand How Naturally Occurring Osmolytes Affect Protein Stability, Methods in Enzymology, Academic Press2007, pp. 397-418.

[25] M. Auton, D.W. Bolen, J. Rösgen, Structural thermodynamics of protein preferential solvation: Osmolyte solvation of proteins, aminoacids, and peptides, Proteins: Structure, Function, and Bioinformatics, 73 (2008) 802-813.

[26] I. Baskakov, D.W. Bolen, Forcing Thermodynamically Unfolded Proteins to Fold, Journal of Biological Chemistry, 273 (1998) 4831-4834.

[27] D.W. Bolen, G.D. Rose, Structure and Energetics of the Hydrogen-Bonded Backbone in Protein Folding, Annual Review of Biochemistry, 77 (2008) 339-362.

[28] M. Gulotta, L. Qiu, R. Desamero, J. Rosgen, D.W. Bolen, R. Callender, Effects of Cell Volume Regulating Osmolytes on Glycerol 3-Phosphate Binding to Triosephosphate Isomerase Biochemistry, 46 (2007) 10055-10062.

[29] C.Y. Hu, H. Kokubo, G.C. Lynch, D.W. Bolen, B.M. Pettitt, Backbone additivity in the transfer model of protein solvation, Protein Science, 19 (2010) 1011-1022.

[30] R. Kumar, J.C. Lee, D.W. Bolen, E.B. Thompson, The Conformation of the Glucocorticoid Receptor AF1/tau1 Domain Induced by Osmolyte Binds Co-regulatory Proteins, Journal of Biological Chemistry, 276 (2001) 18146-18152.

[31] T.O. Street, D.W. Bolen, G.D. Rose, A molecular mechanism for osmolyte-induced protein stability, Proceedings of the National Academy of Sciences, 103 (2006) 13997-14002.

[32] A. Wang, D.W. Bolen, A Naturally Occurring Protective System in Urea-Rich Cells: Mechanism of Osmolyte Protection of Proteins against Urea Denaturation, Biochemistry, 36 (1997) 9101-9108.

[33] A. Wang, A.D. Robertson, D.W. Bolen, Effects of a Naturally Occurring Compatible Osmolyte on the Internal Dynamics of Ribonuclease A, Biochemistry, 34 (1995) 15096-15104.

[34] B.J. Bennion, M.L. DeMarco, V. Daggett, Preventing Misfolding of the Prion Protein by Trimethylamine N-Oxide Biochemistry, 43 (2004) 12955-12963.

[35] M. Howard, H. Fischer, J. Roux, B.C. Santos, S.R. Gullans, P.H. Yancey, W.J. Welch, Mammalian Osmolytes and S-Nitrosoglutathione Promote F508 Cystic Fibrosis Transmembrane Conductance Regulator (CFTR) Protein Maturation and Function, Journal of Biological Chemistry, 278 (2003) 35159-35167.